FABRICATION AND CHARACTERIZATION OF B_4C AND BN REINFORCED ALUMINIUM MATRIX COMPOSITES BY SQUEEZE CASTING

by

AMIN NEKOUYAN

B.S, Mechanical Engineering, Islamic Azad University (Central Tehran Branch), 2008

Submitted to the Institute of Graduate Studies in
Science and Engineering in partial fulfillment of
the requirements for the degree of
Master of Science

Graduate Program in Mechanical Engineering

Boğaziçi University

2016

dedicated to my family

ACKNOWLEDGEMENTS

First I would like to sincerely thank my graduate advisor Prof. Sabri Altıntaş for his support, patience and encouragement. He taught me the most valuable lesson, by giving me the freedom to plan, schedule and manage the work myself, while supporting me closely to implement this study. I also extend my appreciation to the members of my thesis committee, Assoc. Prof. Nuri Ersoy and Assist. Prof. Mehmet İpekoğlu for allocating their time to evaluate this work. Also I should thank them and Önder Albayrak for their kind helps during the work.

I would like to show the deepest love and appreciation to my wife Sadaf who was a great source of support, encouragement and love which was in the end what made this dissertation possible. Hossein and Mohaddeseh, my parents and my brother Ehsan receive my deepest gratitude and love for their dedication and the many years of support. Their supports always encouraged me to keep on each step of my life.

I would like to thank my labmate Mustafa Şengör and also my friends Farhad Kazemi, Mehdi Montakhab, Fatih Öz, Altay Brusan, Farid Heshmati, Samad Kazemi, Sahand Baghergili and last but not least Saleh Khalesi for their help and friendship. I would also like to appreciate the staff of the mechanical engineering department at Boğaziçi University for their help.

ABSTRACT

FABRICATION AND CHARACTERIZATION OF B_4C AND BN REINFORCED ALUMINIUM MATRIX COMPOSITES BY SQUEEZE CASTING

Aluminium matrix composites (AMC) with different ceramic particle reinforcements gained significant attention due to high demand for materials with versatile properties in the industry. In the present work boron carbide (B_4C) and boron nitride (BN) ceramics in different volume fractions were used as the reinforcement materials to fabricate Al-B_4C and Al-B_4C-BN composite materials which then underwent different squeezing pressures. The processes of this study were conducted in two steps. In the first stage, the effect of various B_4C contents (3 % , 5 % and 10 %) under different squeezing pressures (0, 75 and 150 MPa) were studied for tensile strength, hardness characteristics, machinability, density and the microstructure of fabricated samples. In the second stage, Al-B_4C-BN hybrid AMC samples were manufactured with constant squeezing pressure (75 MPa) and constant B_4C volume fraction of 5 % but with three different BN volume fractions (3 %, 5 % and 10 %). For this purpose, again previously mentioned tests were applied on the samples. Total of 105 samples were manufactured and tested. One of the main challenges in the manufacturing process was low wettability of B_4C and BN particles with aluminium melt which was successfully overcome by addition of K_2TiF_6 flux in the case of B_4C and applying high temperatures in the case of BN. The main objectives of this research are first to evaluate the effect of B_4C reinforcement and squeeze casting on the properties of AMC. Secondly since it is known that Al-B_4C AMC would have low machinability due to the presence of abrasive B_4C particles, it is aimed to evaluate how addition of BN particles with lubricating properties can improve this drawback and thirdly to find out what is the optimum composition of AMC to be used in the industry. Also it was finally aimed to evaluate the effect of K_2TiF_6 on wettability of B_4C particles by aluminium melt.

ÖZET

B_4C VE BN TAKVİYELİ ALÜMİNYUM MATRİSLİ KOMPOZİTLERİN BASINÇLI DÖKÜM İLE FABRİKASYONU VE KARAKTERIZASYONU

Alüminyum matrisli kompozitler (AMK) çeşitli seramik takviyelerle birlikte verimli özelliklere sahip malzemelere olan yüksek talepten dolayı belirgin bir şekilde dikkati çekmektedir. Al-B_4C ve Al-B_4C-BN kompozit üretimine yönelik olarak gerçekleştirilen bu çalışmada, farklı hacimsel oranlarda bor karbür (B_4C) ve bor nitrür (BN) seramikleri kullanılmış, elde edilen malzemeler değişik basınçlarda sıkıştırılmıştır. Dövme ve sürekli kalıp döküm işlemlerinin bir bileşimi olan basınçlı döküm, sıvı metalin basınç altında yeniden kullanılabilir kalıba dökülmesi üzerine kurulu bir üretim yöntemidir. Çalışma, iki aşamada gerçekleştirilmiştir. İlk aşamada, çeşitli B_4C içerikleri (% 3, % 5 ve % 10) ve değişik sıkıştırma basınçlarının (0, 75 ve 150 MPa), gerilim dayanımı, sertlik karakteristiği, işlenebilirlik, yoğunluk ve mikroyapı üzerindeki etkileri incelenmiştir. İkinci aşamada, hibrid Al-B_4C-BN AMK örnekleri, sabit sıkıştırma basıncı (75 MPa) altında ve B_4C hacimsel oranında (% 5), üç farklı BN hacimsel oranında (% 3, % 5 ve % 10) üretilmiştir. Toplam 105 numune üretilmiş ve test edilmiştir. Üretim aşamasında karşılaşılan zorluklardan biri, B_4C'ün ve BN parçacıkların alüminyum eriğiyle olan düşük ıslanabilirliğidir. B_4C ilavesinde K_2TiF_6 flaks katkısı kullanılarak ve BN ilavesinde yüksek sıcaklık uygulanarak ıslanılabilirlik sorununun başarılı bir şekilde üstesinden gelinmiştir. Bu araştırmanın temel amacı, öncelikle B_4C parçacık takviyesinin ve sıkıştırma basıncının AMK üzerine etkilerini incelemektir. Çalışmanın ikinci amacı, BN parçacık ilavesinin, B_4C'ün aşındırıcı özelliği nedeniyle düşük işlenebilirliğe sahip olduğu bilinen Al-B_4C AMK'in işlenebilirliğinin üzerindeki etkilerinin araştırılmasıdır. Son olarak, endüstriyel kullanıma yönelik olarak AMK'nin optimum bileşen oranlarının belirlenmesi hedeflenmiştir. Bunların yanı sıra, K_2TiF_6 'ın B_4C partiküllerinin alüminyum eriğiyi ile ıslanabilirliğinin değerlendirilmesi amaçlanmıştır.

TABLE OF CONTENTS

LIST OF FIGURES

LIST OF TABLES

LIST OF SYMBOLS

Al	Aluminium
Al_2Cu	Aluminium Cupper
Al_2O_3	Aluminium Oxide
Al_4C_3	Aluminium Carbide
AlB_2	Aluminium Diboride
AlN	Aluminium Nitride
B	Boron
b	Burger's vector
B_2O_3	Boron Trioxide
B4C	Boron Carbide
Bi	Bismuth
BN	Boron Nitride
Ca	Calcium
CaB_6	Calcium Hexaboride
CaO	Calcium Oxide
Cl	Chlorine
CO_2	Carbon Dioxide
Cr	Chrome
Cu	Cupper
$CuSO_4$	Copper (II) Sulfate
D	Diameter of the ball
d	Particle size
E_C	Young's modulus of the composite material
E_M	Young's modulus of the matrix
E_P	Young's modulus of the particle
Fe	Iron
G	Shear modulus
g	Gram
Ga	Gallium
Gr	Graphite

H_2O	Dihydrogen Monoxide
h-BN	Hexagonal Boron Nitride
HCl	Hydrogen Chloride
K_2TiF_6	Potassium Fluorotitanate
Mg	Magnesium
Mg_2Si	Magnesium Silicide
MgO	Magnesium Oxide
Mn	Manganese
Na	Sodium
Na_3AlF_6	Sodium Hexafluoroaluminate
NH_3	Ammonia
Ni	Nickel
P	Force
Pb	Lead
S	Geometry factor
Sc	Scandium
Si	Silicon
Si_3N_4	Silicon Nitride
SiC	Silicon Carbide
SiO_2	Silicon Dioxide
Sn	Tin
SO_4	Sulfate
T_d	Temperature of the die
Ti	Titanium
TiB_2	Titanium Diboride
TiC	Titanium Carbide
T_m	Melting temperature
T_f	Equilibrium freezing temperature
V	Vanadium
V_f	Specific volume of the liquid
V_s	Specific volume of the solid
W_a	Adhesion work

w-BN	Wurtzite Boron Nitride
Zn	Zinc
Zr	Zirconium
ZrO_2	Zirconium Dioxide
ΔC	Difference in thermal expansion coefficient between matrix and particle
ΔH_f	Latent heat of fusion
$\Delta R_{p,C}$	Increase in tensile strength of aluminium materials by particle addition
ΔT	Freezing range
$\Delta\sigma_{\alpha}$	Influence of induced dislocations
$\Delta\sigma_{KF}$	Strain hardening contribution
$\Delta\sigma_{KG}$	Yield dtrength contribution from changes in grain size
$\Delta\sigma_{SKG}$	Yield strength contribution due to changes in subgrain Size
γ_{LV}	Liquid-vapor interface energy
γ_{SL}	Solid-liquid interface energy
γ_{SV}	Solid-vapor interface energy
θ	Angle between the liquid drop and the solid phase
ρ	Dislocation density
$\sigma_{interface}$	Interface strength
$\sigma_{p,f}$	Particle strength
φ_P	Volume content of particles

LIST OF ACRONYMS/ABBREVIATIONS

AHC	Aluminium Hybrid Composite
AMC	Aluminium Matrix Composite
CBN	Cubic Boron Nitride
CMC	Ceramic Matrix Composite
DAS	Dendrite Arm Spacing
EDAX	Energy-dispersive X-ray Spectroscopy
FEGV	Fan Exit Guide Vane
MMC	Metal Matrix Composite
MMNC	Metal Matrix Nano Composites
MSLAB	Materials Science and Manufacturing Laboratory of Boğaziçi University
PAMC	Particulate Aluminium Matrix Composite
PCD	Poly Crystalline Diamond
PM	Powder Metallurgy
PMC	Polymer Matrix Composite
SEM	Scanning Electron Microscope
UTS	Ultimate Tensile Strength
YS	Yield Strength

1. INTRODUCTION

Composites are composed of at least two phases of matrix and reinforcement and they have compound properties of both phases which typically cannot be found in each phase solely. Among matrix and reinforcement combinations, aluminium alloys are the most favorite matrices due to their low density, high strength, high toughness, corrosion resistance and good machinability. In the case of reinforcement materials boron carbide is ceramic material which has superior hardness, high elastic modulus, high thermal stability, excellent chemical inertness, very good corrosion resistance, high impact strength, exceptional corrosion resistance and similar physical, mechanical and chemical outstanding properties. Also as another potential reinforcement material hexagonal boron nitride (generally called “white graphite”) can be used, because it is a lubricious material with the same anisotropic layered hexagonal structure as carbon graphite. The difference is that that BN is a very good electrical insulator. It offers very high thermal conductivity and good thermal shock resistance. BN is stable in inert and reducing atmospheres up to 2000 °C, and in oxidizing atmospheres to 850 °C. Key properties of h-BN can be listed as: high thermal conductivity, low thermal expansion, good thermal shock resistance, high electrical resistance, low dielectric constant, microwave transparency, non-toxic, easily machined (non-abrasive and lubricious), chemically inert and not wet by most molten metals in natural situation.

Squeeze casting which is combination of die forging and permanent die casting, is a manufacturing method in which molten metal solidifies under pressure in a reusable die. Apart from the fact that squeeze casting is a unique method in manufacturing metal matrix composites, it is a method which can finalize a metal matrix composite production done with other manufacturing routes. Since squeeze casting is normally applied on light metals, it is a favorite technology for researchers who use it in order to eliminate porosities and improve the mechanical and microstructural properties of aluminium matrix composites [1].

2. LITERATURE REVIEW

2.1. METAL MATRIX COMPOSITES

In the world of materials and within three groups of metallic materials, ceramic materials and non-metallic materials, there is a large space filled with materials which are composition of these three main groups. These distinct materials are being called composites, because they are composed of at least two phases of matrix and reinforcement and they have compound properties of both phases which typically cannot be found in each phase solely. Generally the dominant material is called matrix and the material to be added is called reinforcement. The reason why industries have emerging demand for composites is that monopolized properties of each metallic (crystalline, conductive, ductile and chemically unstable), non-metallic (amorphous, poor conductive, ductile in high temperature and chemically stable) and ceramic (crystalline or amorphous, poor conductive, non-ductile and chemically stable) materials cannot meet all the requirements of the industry and sometimes there is a need for versatile properties [1].

Based on matrix and reinforcement, composites can be classified into three main groups [2]:

a) Metal Matrix Composites (MMC's): Having a metal as the matrix and fibers, whiskers or particulates as the reinforcement, metal matrix composites are mostly used in aerospace and automotive industries.

b) Ceramic Matrix Composites (CMC's): Having a ceramic as the matrix and ceramic fibers, ceramic whiskers and ceramic particulates as the reinforcement, ceramic matrix composites are mostly used in very high temperature environments such as jet engines. As typical reinforcements in CMC's, carbon, silicon carbide, titanium diboride, silicon nitride and alumina can be named [3].

c) Polymer Matrix Composites (PMC's): These materials are also defined as FRP's which stands for Fiber Reinforced Plastics. The matrix in these

materials are polymeric resins which are typically polyester, vinyl and epoxy and the reinforcements are variety of fibers but mainly fiberglass [2, 4].

Among three types of composite materials, MMC's have attracted attention in many industries for decades. For almost all scientists the word metal matrix composites is often equal to the term light metal matrix composites. Since these light weight metals are reinforced with materials having properties different than their embedded matrix, the resulting composites come first for application in areas which weigh reduction has high priority. The pre-defined aim is to improve the properties of main material. The development purposes for light metal composite materials are:

- Increasing the yield strength and tensile strength while keeping the ductility and toughness,
- Increasing the creep resistance at higher temperatures
- Increasing the fatigue strength, especially at higher temperatures,
- Upgrading the thermal shock resistance,
- Improving the corrosion resistance,
- Increasing the Young's modulus,
- Reducing the thermal elongation

Briefly, the aim by creating metal matrix composite is to expand the application area and substitution of typical materials and optimizing the properties.

There are several ways to classify MMC's but among them the classification based on type of reinforced material is popular. In this approach, MMC's are categorized to Particulate Composite Materials, Continuous Fiber Composite Materials and Short Fiber Composite Materials (Figure 2.1) [1].

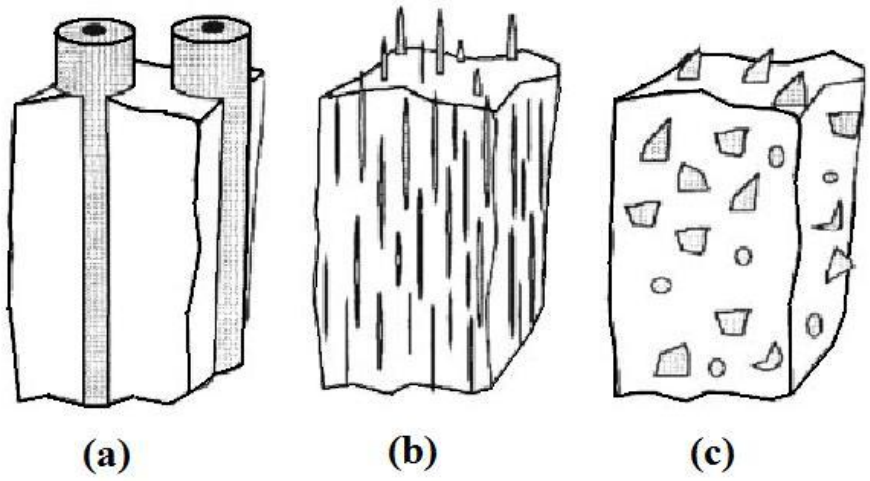

Figure 2.1. Schematic Presentation of three shapes of metal matrix composite materials: a) Continuous Fiber Metal Matrix Composites, b) Short Fiber Metal Matrix Composites and c) Particulate Metal Matrix Composites [1].

2.1.1. Aluminium Matrix Composites

By beginning of 1980s, researchers and industries focused on developing aluminium, magnesium, iron and copper matrix composites for automotive, aerospace, heat treatment and tribology fields and by late 1980s MMC's has been applied in aerospace and automotive industries practically. Among matrix and reinforcement combination, aluminium alloys are the most favorite matrices due to their low density, high strength, high toughness, corrosion resistance and good machinability. Therefore uses of AMC materials are emerging endlessly, especially in the fields of automotive and aerospace. Aluminium composite materials with aluminium matrix, are being used in various parts e.g. pistons, cylinders, engine blocks, brakes etc, in automotive industry. Besides aluminium based composites reinforced with micro/nano Al_2O_3, B_4C, SiC, TiB_2, ZrO_2, graphite and SiO_2 particles, changes the micro-structural features that result in superior mechanical and physical properties suitable for automotive and aerospace applications [5, 6].

2.1.2. Matrix Materials

Aluminium, magnesium, copper, titanium and their alloys are practically used as matrix in MMCs. Aluminium is the most plentiful metal in the earth crust and the third most plentiful element after Oxygen and Silicon. 8 % weight of earth is made of aluminium. Titanium alloys are expensive light materials with acceptable corrosion and oxidation resistance, has applications in aerospace industry and specifically in the parts which need to remain strong in high temperatures. In aforementioned matrix candidates Magnesium has got the lowest density which is 1.7 g/cm^3. Copper is another suitable matrix material due to its good thermal and electrical conductivity and decent machinability and formability. Among materials applied as matrix in MMCs, aluminium is the most used metal because in addition to its unique mechanical advantages it is; light weight, highly corrosion resistant, unscented and impermeable and completely recyclable, excellent heat and electricity conductor and decent ductile material. Based on European Aluminium Association, aluminium consumption in the year 2013 reached 50.2 million tones worldwide which more than 15 % was produced from recycled materials by refineries [5, 7].

Aluminium alloys may be separated into two groups: heat treatable and non-heat treatable alloys. The strength of non-heat-treatable aluminium alloys is originally comes from alloying the aluminium with other elements. These alloys consist of the pure aluminium alloys (1xxx series), manganese alloys (3xxx series), silicon alloys (4xxx series) and magnesium alloys (5xxx series). An additional growth in strength of these alloys is got via cold working or strain hardening. Cold working or strain hardening is finalized by rolling, drawing through dies, stretching or similar processes where area reduction is gained. Regulating the amount of total reduction in area of the material controls its final properties. Heat-treatable aluminium alloys are the ones which their initial strength obtained from adding alloying elements to pure aluminium, similar to non-heat-treatable aluminium alloys. These elements include copper (2xxx series), magnesium and silicon, which can be found in forms of magnesium silicide (6xxx series), and zinc (7xxx series) [8, 9]. Table 2.1 resembles mechanical properties of some aluminium alloys which normally are used as matrix in the composites.

Table 2.1. Typical mechanical properties of some aluminium alloys

Material	0.2 % Proof Stress (MPa)	Tensile Strength (MPa)	Elongation (%)	Reference
LM24	110	200	2	[10]
LM25	240	310	3	[10]
HGZL-01	380	320	8	[11]
LM5		230	10	[12]
LM18		150	6	[12]
Pure Aluminium	35	90	35	[13]
A390	297	351	0.8	[14]
A5083	115	260	22	[15]
A2014	410	480	13	[15]
A2024	450	480	6	[15]
A7075	430	500	13	[15]
A201	345	415	5	[15]
A213	185	220	0.5	[15]
A355	235	280	1	[15]
A356	265	310	1	[15]
A357	248	313	7	[10]
A360	365	310	1	[15]
A6061	276	310	12	[10]
A7010	495	568	15	[10]

2.1.3. Reinforcement Materials

In order to choose the best reinforcement material for the metal matrix composites, conditions such as compatibility with matrix material, easy supplying, tensile strength, density, melting temperature, shape and size, chemical composition and crystal structure should be considered and evaluated. Among all types of reinforcement materials, ceramics are good candidates due to their suitable rigidity, hardness, strength and density. SiC [14], B_4C, graphite [16], Al_2O_3 [17], MgO [18], Si_3N_4 [19], TiB_2 [20], TiC [21], BN [22] and

similar oxide, carbide, nitride and boride materials in forms of particles, whiskers and fibers are normally used as reinforcement materials in MMCs and AMCs. Regarding improvement in mechanical properties, continuous fibers are the most suggested reinforcement applicants but they are expensive. The other choice is whiskers and short fibers which are less expensive but gives out less improvement in mechanical properties too. Among these, particulates owing to their relatively low prices and isotropic properties are optimum in the fields that a share of responsibility to increase the mechanical properties is on the shoulder of matrix material. Typical properties of some reinforcement materials have been shown in the Table 2.2

Table 2.2. Typical properties of some reinforcement materials [23-25]

Material	**Form**	**Elastic Modulus (GPa)**	**Density (g/cm^3)**	**Thermal Conductivity (W/mK)**	**Coefficient of Thermal Expansion ($\times 10^{-6}/K$)**
B_4C	Particulate	450	2.52	29	5-6
SiC	Particulate	448	3.21	120	3.4
BN	Particulate	90	2.1	25	3.8
Al_2O_3	Particulate	300	3.6	0.3-0.9	10.3
TiC	Particulate	320	4.93	29	7.4
TiB_2	Particulate	370	4.5	27	7.4

2.1.4. Mechanical Properties of AMCs

The main advantages of AMCs compared to unreinforced materials are as follows:

- Higher strength
- Better stiffness
- Reduced density (weight)
- Enhanced high temperature properties
- Thermal/heat management
- Improved and custom-made electrical performance
- Developed abrasion and wear resistance

- Enhanced damping capabilities.

For instance, elastic modulus of pure aluminium can be enhanced from 70 GPa to 240 GPa by reinforcing with 60 vol. % continuous aluminium fiber. On the other hand combination of 60 vol. % alumina fiber in pure aluminium results in decreasing the coefficient of expansion from 24 ppm/◦C to 7 ppm/◦C. Also composition of Al-9% Si-20 vol. % SiCp can give rise to wear resistance of grey cast iron. So it can be found out that it is possible to change several technological properties of aluminium/aluminium alloy by including suitable reinforcement in adequate fraction. AMC material systems offer superior combination of properties (profile of properties) in such a way that today no existing monolithic material can compete. Over the years, AMCs have been applied in several structural, non-structural and functional applications in diverse engineering segments. The first intentions for the utilization of AMCs in these sectors include but is not limited to performance, economic and environmental benefits. As instance the key benefits of AMCs in transportation sector are vehicles with lower fuel consumption, less noise and lower air pollution [26].

To achieve a required mechanical property in AMCs, the first needed condition is the interface of matrix and reinforcement to be firmly bonded. Moreover with homogenous distribution of reinforcement and processes like precipitation hardening can give out a material with up to 60 % better tensile strength comparing to the matrix [27]. Typical mechanical properties of AMCs are going to be detailed below.

2.1.4.1. Yield and Tensile Strength. One of the most important features of engineering materials is yield strength. In engineering applications, in order to guarantee the sound running of the parts, high yield strength of the material is required. In addition, if a part is going to be utilized in high temperature, the needed property would be high yield strength in high temperature. In aluminium metal matrix composites the basic reason of increase in yield strength comparing to the matrix material is higher elastic modulus of reinforcement material. Similarly tensile strength obeys same rules. The comparison of yield and tensile strength with different reinforcement materials has been tabulated in Table 2.3.

Table 2.3. Tensile properties of AMCs with different matrices and reinforcements [28]

Material	Yield Strength (MPa)	Tensile Strength (MPa)	Elastic Modulus (GPa)	Elongation (%)
A356	200	255	75.2	4
A356-10 % SiC	262	276	77.2	0.7
A356-15 % SiC	296	303	92.4	0.4
A356-20 % SiC	296	317	95.8	0.5
Al-Si-Mg-10 % SiC	359	372	87.6	0.3
Al-Si-Mg-10 % SiC	101	372	101	0.1
Al-Si-Cu-Mg-Fe- 10 % SiC	221	310	91	0.9
Al-Si-Cu-Mg-Fe-Ni- 10 % SiC	248	303	108.2	0.5
Al-Cu	345	434	70	12
Al-Cu-20 % TiC	358	400	96	1.2

Strength improvement in AMCs can be explained in two approaches. When a force is applied on the AMC, the stress transfers from matrix to reinforcement which means from less strength materials to higher strength material. This is called direct strength improvement. The other approach is indirect strength improvement in which the increase in strength happens in the matrix, but in the microstructure and properties of the material. Due to the thermal expansion coefficient mismatch and decrease in temperature from manufacturing temperature to environment temperature and also the temperature changes in the time of application, dislocation density raises in the regions close to matrix and reinforcement interface which causes plastic deformation. This high density of dislocations in the interface acts as a barrier to any other dislocation movement which is the necessity for plastic deformation. So there are two ways for the material; to either accept elastic deformation or standstill to high tensile strength values and at the end break plastically as a brittle material. This is why strength of composites normally increases with increase in the volume fraction of reinforcement. Besides it is seen that decrease in the grain size of reinforcement results in improvement of AMC materials [5, 29, 30].

2.1.4.2. Ductility. In AMC materials, when the volume fraction rate of reinforcement materials increases, which causes an increase in yield and tensile strength, normally a decrease in elongation percentage is seen. An instance of such situation is demonstrated in Figure 2.2 in which, increase in % content of reinforcement material which increases the strength, results in decreasing strain.

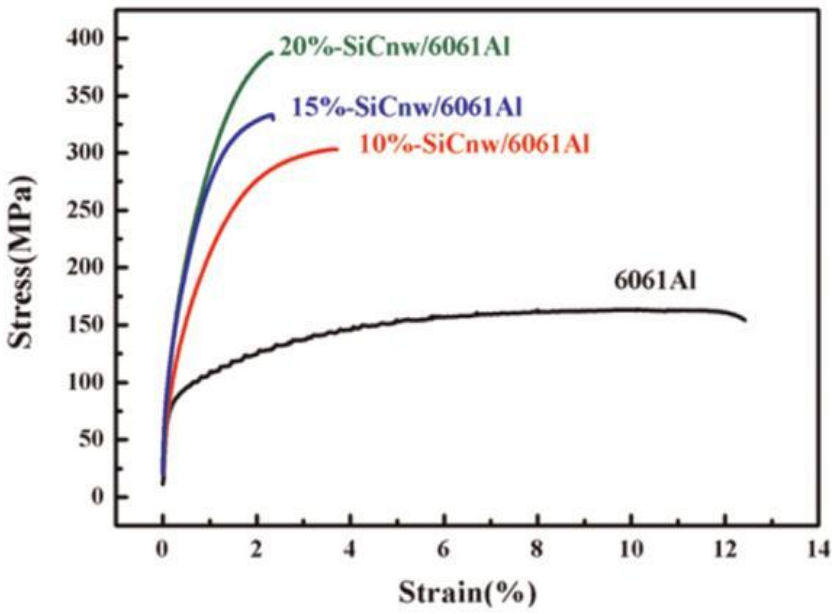

Figure 2.2. Tensile behavior of AMC with different contents of reinforcement [31].

Similarly it can be said that if reinforcing a matrix material causes decrease in the strength of material, elongation should be logically increased. Such condition is reported by Emamy *et al*. (Figure 2.3) [32].

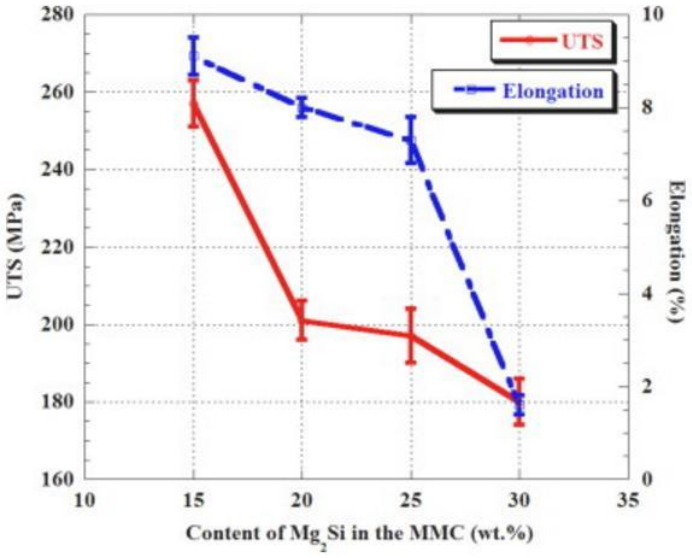

Figure 2.3. Tensile behavior of AMC with different contents of Mg_2Si [32].

Generally the fracture in the composite materials might take place in the reinforcement material, matrix/reinforcement interface or in macro-porosities created due to the particulate agglomeration. Considering these facts, coarse particulates have more tendency to be subjected to failures than fine particulates [33]. Harichandran *et al.* examined different particle size of B_4C reinforcement in pure aluminium and found out that with reduction in particulate sizes from micro to nano-size, up to 5 % of improvement in elongation percentage is possible. Also in such situation, up to 18 % increase in strength values is possible [34].

Beside the volume fraction of particles, and their sizes, distribution in a metal matrix composite plays an important role in controlling the material's mechanical properties. In other words, in order to achieve the optimum properties of the AMC, the distribution of the reinforcement material in the matrix alloy must be uniform. With all this in AMCs manufacturing in liquid phase, it is a real challenge to settle the reinforcement particles during melting or casting. This happens as a result of density differences between the reinforcement particles and the matrix alloy melt. The reinforcement distribution is influenced during several phases including (a) distribution in the liquid as a result of mixing, (b) distribution in the liquid after mixing and before solidification, and (c) redistribution as a consequence of solidification. Appropriate dispersion of the particles in a matrix is also depends on pouring rate, pouring temperature and gating systems [33]. It is

reported that for the spherical particles, failure starts in porous regions close to the interface ($\sigma_{interface}<\sigma_{p,f}$) and for the needle shape reinforcements it occurs by failure in the reinforcement itself ($\sigma_{interface}>\sigma_{p,f}$). So it is suggested in the literature to employ spherical reinforcement materials and avoid the ones with sharp edges (Figure 2.4) [5, 35].

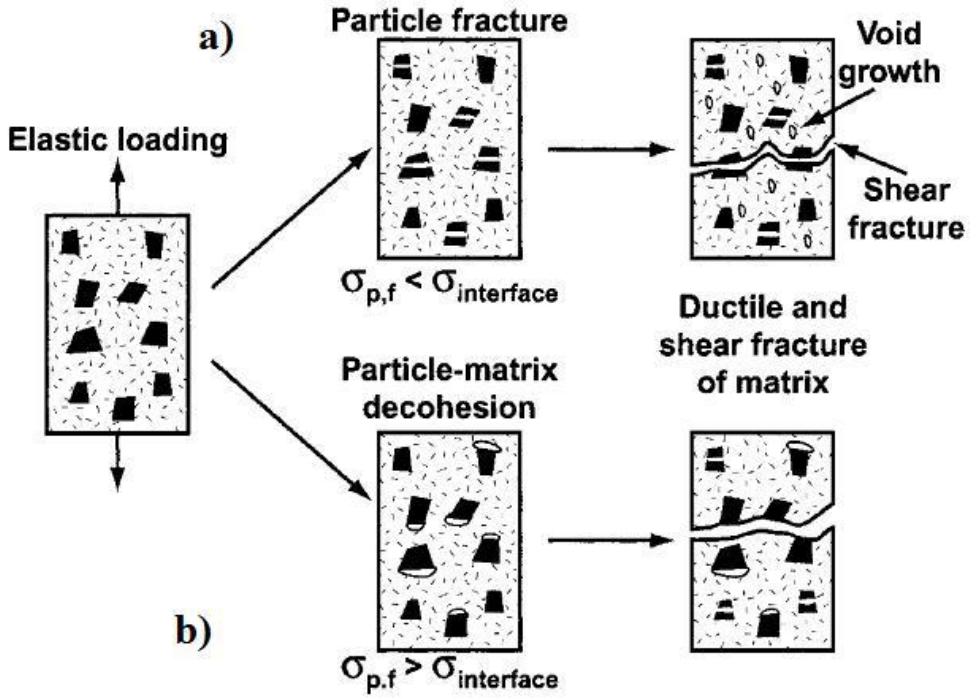

Figure 2.4. Schematic of the two possible types of tensile damage evolution in particle reinforced MMCs: (a) interface strength greater than particle strength and (b) interface strength less than particle strength [5].

2.1.4.3. Elastic Modulus. An objective in the development of aluminium matrix composite materials is to increase the modulus of elasticity (Young's modulus) which is the main reason for the modification in the tensile stress and strain values (Table 2.3). It is reported that although in case of continuous reinforcements, the elastic modulus achieved from experiments are close to the values gained from classic mixing formulations, in case of non-continuous reinforcements like particles, it is far below the classic theories. This is why for the particulate reinforced metal matrix composites another formulations are applied.

The universally used models are the following linear and inverse mixture rules which are:

- Linear mixture rule or Voigt-model (ROM) which can be shown as

$$E_C = \phi_P E_P + (1 - \phi_P) E_M \quad (2.1)$$

- and Inverse mixture rule or Reuss-model (IMR)

$$E_C = \left(\frac{\varphi_P}{E_M} + \frac{1 - \varphi_P}{E_M}\right)^{-1} \quad (2.2)$$

where φ_P is the volume content of particles or fibers, E_C the Young's modulus of the composite material, E_P the Young's modulus of the particle or fiber and E_M the Young's modulus of the matrix. The Voigt model is just valid for long-fiber reinforced composites, though the Reuss model is suitable for layer composite materials. By applying an active geometry factor, which can be found out analyzing the structure of the composite materials as a function of the load direction, the geometry and the orientation of the reinforcement can be re-written as follows:

$$E_C = \frac{E_M(1 + 2S_q\varphi_P)}{1 - q\varphi_P} \quad (2.3)$$

In which q can be shown as:

$$q = \frac{\left(\frac{E_P}{E_M}\right) - 1}{\left(\frac{E_P}{E_M}\right) + 2s} \quad (2.4)$$

where S is the geometry factor of the fiber or particle (1/d) [1].

2.1.4.4. Strengthening Mechanisms in Particulate Reinforced Metal Matrix Composites.

Two tactics are known to explain mechanical properties of AMCs which are the continuum approach and micro mechanistic approach. Continuum approach assumes that the properties can be described by global parameters. Micro mechanistic approach uses models

found out from deformation science in atomic level. In this part, various strengthening mechanisms that are derived for particulate reinforced metal matrix composites using micro mechanistic approach will be discussed. In fact, most of these mechanisms are first derived for conventional particle containing alloys but in some extent they can be applied to particulate reinforced metals. The first mechanism is quench strengthening. As discussed before, the large difference in thermal expansion or CTE between the matrix metal and the particulate results in the generation of dislocations on quenching from the recrystallization or solution treatment temperature. The dislocation density generated on quenching is a function of reinforcement size, reinforcement volume fraction and the product of the thermal mismatch and the temperature change. The influence of ceramic particles on the strength properties of particle reinforced light metals can be described by using the following micromechanical model:

$$\Delta R_{p,C} = \Delta\sigma_{\alpha} + \Delta\sigma_{KG} + \Delta\sigma_{SKG} + \Delta\sigma_{KF} \tag{2.5}$$

In the equation above, $\Delta R_{p,C}$ is the increase in tensile strength of aluminium materials by particle addition, $\Delta\sigma_{\alpha}$ is the influence of induced dislocations, $\Delta\sigma_{KG}$ is the yield strength contribution from changes in grain size (for example recrystallization during thermo-mechanical treatment of composite materials, analogue Hall-Petch), $\Delta\sigma_{SKG}$ is the yield strength contribution due to changes in sub-grain size (e.g., in a relaxation process during thermomechanical treatment of composite materials) and $\Delta\sigma_{KF}$ is the strain hardening contribution.

The influence of yield strength contribution due to geometrical necessary dislocations and inner tension (induced dislocations) $\Delta\sigma_{\alpha}$ can be shown as:

$$\Delta\sigma_{\alpha} = \alpha . G . b . \rho^{1/2} \tag{2.6}$$

In which the dislocation density ρ can be found from:

$$\rho = 12\Delta T \frac{\Delta C \varphi_P}{bd} \tag{2.7}$$

where α is a constant between 0.5 and 1, G is the shear modulus, b is the Burger's vector, ΔT the temperature difference, ΔC the difference in thermal expansion coefficient between matrix and particle, φ_P the particle volume content and d the particle size.

This analysis assumes that the dislocations are distributed uniformly and all dislocations generated contribute to strength. It is also indicated that this may not be true for a solution hardened matrix.

The second mechanism related also to the present work as well as quench strengthening is grain strengthening. In the presence of grain refiners, particles may act as nucleation sites for grains and grain sizes considerably finer than the grain size of unreinforced alloys might occur. This might contribute to the strength of the material formulated by the Hall-Petch equation given below:

$$\Delta\sigma_{KG} = K_{Y1} D^{-1/2} \tag{2.8}$$

with

$$D = d\left(\frac{1-\varphi_P}{\varphi_P}\right)^{1/3} \tag{2.9}$$

where K_{Y1} is a constant and D is the resulting grain size.

As discussed above, there are other mechanisms which are effective in occasions such as sub structure strengthening and work hardening (strain hardening) but in many cases they cannot be applied linearly, because the various mechanisms will interact with each other. For instance $\Delta\sigma_{KG}$ occurs during secondary processing routes such as heat treatment or work hardening [1, 36, 37].

2.1.5. Machinability

Forming and shaping the AMCs has become a matter of importance due the emerging request for these materials in the industry. After casting which is the most common route of manufacturing, machining is the next favorite choice of industry. The

processing parameters affecting machinability of a material are the values of cutting speed according to selected set of material properties of work piece and machining parameters.

Studies about machinability of B_4C and BN reinforced AMCs are very limited. Ozben *et al.* [38] stated that machinability of MMC is very different from traditional materials since it normally contains abrasive reinforcement element. This is because the abrasive elements induce more wear on cutting tools. Flank wear of cutting tool are also increased with increase in reinforcement ratio. It is also found out that by decreasing the cutting speed, the surface quality can be improved and increase in the particle ratio effects roughness, negatively. Prabagaran *et al.* [39] studied machinability of AA6061 aluminium matrix composites reinforced with 10 % B_4C and 3 % graphite particles. They have tried different cutting conditions using carbide, CBN (Cubic Boron Nitride) and PCD (Poly Crystalline Diamond) tools. It was shown that surface roughness is more for carbide tools in comparison with PCD tools which are minimum. PCD tools perform better than CBN and carbide tools. This is found to be due to the daubing effect and dismissal of softer and amorphous graphite particles on the surface of the composite specimen, which produces pits on the machined and hence reduces the surface finish level. Also it was observed that by increase in the boron carbide ratio, surface roughness was improved. This is completely in disagreement with the report by Pandi *et al.* [40] that the addition of graphite content to aluminium composites improves the tensile strength, elastic modulus and machinability due to the solid lubricating property of the graphite particles. In this work, it is mentioned that machinability can be improved by increasing graphite amount up to 7% and tool life up to 130%. In another work by Najem [41] it is said that addition of B_4C as reinforcement to the master alloy produces higher tool wear, surface roughness and minimizes the cutting forces.

2.1.6. Applications of Aluminium Matrix Composites

The applications of aluminium matrix composite materials are rising endlessly, especially in the fields of automotive and aerospace due to their high physical, mechanical and tribological properties comparing to base alloys.

In aerospace field, a study by Song. W. Q. *et al.* [42] showed that AMCs can be used as airframes and engines. Also large conventional titanium engine parts have been produced by the casting, rapid solidification and mechanical alloying such as number of aerospace components, i.e. landing gear wheel, cast engine parts, engine compressors, etc. Particle reinforced aluminium metal matrix composites are employed as fan exit guide vane (FEGV) in the gas turbine engines. PAMCs are likewise applied as rotating blade sleeves in helicopters. Moreover flight control hydraulic manifolds made of 40 vol. % SiCp reinforced aluminium composites have been effectively benefited. Besides carbon fiber (continuous) reinforced AMCs have been used as antenna wave guides for the Hubble Space Telescope. Furthermore 6061 Al-boron fiber (continuous) composites have been used as struts in main cargo bay of space shuttle.

In Automotive industry, Froes F.H. [43] presented that lightweight materials can make a considerable contribution to enhanced fuel consumption, since a 10 % reduction in vehicle weight translates to a 5.5 % enhancement in fuel economy. Anthony Macke *et al.* [44] reported that usage of AMCs as aluminium engine block, suspension components, body panels and frame members are very common. Aluminium-graphite pistons and liners were tested in gas and diesel engines in addition to racing cars, resulting in reduced friction coefficients and wear rates. Aluminium matrix nano Al_2O_3 composites are used for connecting rods, A/C pump brackets, timing belt/chain conveyors, alternator housing, transmission housing, valve covers and intake manifolds. SiC reinforced aluminium brake rotors are incorporated in vehicles such as Lotus Elise, Chrysler Prowler, General Motors EVI, Volkswagen Lupo 3L, and Toyota RAVA-EV.

AMC's are being employed in other fields as well. For Instance in electric and electronic industry they can be utilized as packaging for electronic parts and electric transport lines. In nuclear plants, Al-B_4C composite materials are used as neutron absorber in nuclear shields. Similarly SiC whisker-reinforced aluminium matrix composites have been produced and used as track shoes in advanced military tanks. Use of whisker-reinforced AMCs as track shoes help in reducing the weight of the tank. Also short fiber-reinforced AMCs are being used in piston and cylinder liner applications. Another modification of AMCs known as hybrid AMCs have been developed and are utilized to some extents. Hybrid AMCs fundamentally contain more than one type of reinforcement.

For example, mixture of particle and whisker, or mixture of fiber and particle or mixture of hard and soft reinforcements. Aluminium matrix composite containing mixture of carbon fiber and alumina particles used in cylindrical liner applications is an example of hybrid composite [6, 26].

2.1.7. Aluminium Matrix Hybrid Composites

Aluminium hybrid composites (AHCs) are a new generation of MMCs that takes attention these days for application in advanced mechanical application. This attention is taken due to improved mechanical properties, accountability to conventional processing technique and decrease in production cost of AHCs. The accountability of these materials is typically dependent on choosing the right combination of reinforcing materials since most of the improvements in mechanical properties are linked with the reinforcing particulates. Not many groupings of reinforcing particulates have been studied in the design of AHCs [29].

Based on a work by Devaraju *et al.* [45], SiC + Al_2O_3 composites compared to SiC + Gr composites have higher hardness values due to higher hardness of Al_2O_3 to that of Gr but inferior wear resistance because of better solid lubricating effect of Gr to that of Al_2O_3. Ramnath *et al.* [27], reported that hybrid composites containing mica and SiC have higher hardness, tensile strength and wear resistance than the single reinforced silicon carbide aluminium composites. Ravindran *et al.* [46] investigated microstructure and mechanical properties of 5 % SiC reinforced aluminium composites with the additions of 5 % and 10 % of solid lubricant which was graphite. Results showed that the hardness and wear resistance of the AHC were increased significantly by increasing the graphite content.

Hybrid MMCs of Al/SiC/Gr and Al/Si10Mg/Fly ash/Gr can easily be machined by EDM and a good surface quality can be obtained by controlling the machining parameters. In Al/Gr/SiC hybrid composites, graphite acts as a solid lubricating agent and lowers the friction coefficient. However, it reduces the mechanical properties of the composite. The presence of hard SiC particles in these hybrid composites increases the hardness and strength and compensates for the weakening effects of graphite. These materials are developed for bushes, bearings and cylinder liners in cast aluminium engine blocks. It is

also reported that boron nitride which like graphite is an effective solid lubricant, improved the machinability of aluminium matrix composite in presence of SiC as initial reinforcement material [47]. It can be concluded that the combining reinforcing materials has significant effect on the improvement of the tensile strength, hardness machinability and tribological properties of the composites. This was ascribed to the load bearing capacities and pinning effect of the hard ceramic particulates and the solid lubricating effect possess by selected reinforcement such as graphite, alumina and boron nitride. From the literature it is clear that addition of a reinforcement material like B_4C with unique specifications, improves some of mechanical properties of composite material but at the same time decreases the machinability of it. Therefore another reinforcing material is required which has lubricating features in order to betterment of the machinability too [40, 48].

2.2. MANUFACTURING METHODS OF PARTICULATED METAL MATRIX COMPOSITES

Number of manufacturing methods have presented in the literature in order to optimize the microstructures and mechanical properties of PAMCs. These methods can be categorized based on the temperature of the aluminium matrix during processing. Accordingly, the processes can be classified into two groups of solid phase and liquid state manufacturing [49].

2.2.1. Liquid state manufacturing routs

In liquid-phase methods, the ceramic particulates are mixed into the molten aluminium matrix benefiting mixing and in the end casting of the final composite mixture into the ultimate part. The procedure starts with a careful selection of the reinforcement considering the matrix alloy. Most of the ceramic materials are not properly wetted by the molten aluminium. Thus, appropriately introduction and mixing ceramic particulate sometimes requires addition of wetting agents to the melt or coating the ceramic particulates before mixing [49]. Usually there are three liquid state fabrication methods or casting ways, which are practical today. Squeeze casting, Stir casting (Figure 2.5) and liquid metal infiltration, which squeeze casting will be discussed later on.

2.2.1.1. Stir Casting. In this method, the ceramic particles are incorporated into a molten matrix using various techniques, followed by mixing or pressing, and casting the subsequent AMC. In this process, a durable bond between the matrix and reinforcement is reached by working in high temperatures, and frequently, alloying aluminium with a material which has good interaction with the reinforcement material can lead in creating a new phase which can improve the wettability. There are number of ways in stir casting methods, like vortex method which is totally in liquid state or compocasting which is in partially solid state. In the vortex method, the reinforcement is mixed during a vortex created in the liquid metal by stirring. Reinforcement is efficiently distributed throughout the melt, and the product composites may be cast. While in the compocasting, or rheocasting techniques, the melt is vigorously stirred till the temperature comes below the

liquidus.

Stir casting is the most preferred liquid phase method for manufacturing MMCs, due to its low expenses. In order to get the best result in this process, it is needed that wettability and homogenous distribution of particles can be achieved. Besides, porosity, agglomeration, oxidation and interface reaction should be controlled as well.

In case of vortex method, one main challenge other than wettability can be high porosity in the resulting composite. When the vortex encounters, proses are created normally and with adding more volume fraction of particles the value of porosity will increase. It is reported that if the process is not properly controlled the rate of porosity can reach to 30 % or more. In order to prevent such situations, it is needed to control the atmosphere by applying inert gas, control the surface of the melt or applying squeeze casting so that the created porosities can be removed at the end of process.

Stir casting is the most preferred liquid phase method for manufacturing MMCs, due to its low expenses. With mechanical mixing it is possible to have a mixture of up to 20 % reinforcement particles into metal melt but it is very important to optimize the factors such as: particle size, particle surface erea, distance between particles and metal matrix alloying system. Depending on these parameters, more than a specific volume fraction of particles will be rejected by the aluminium melt [1, 50, 51].

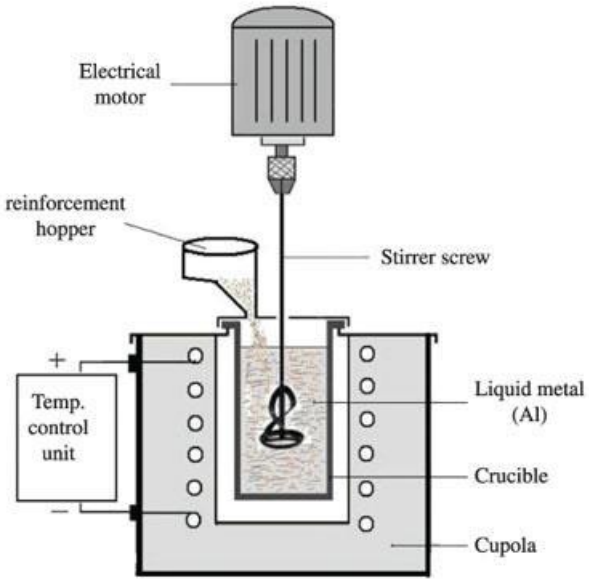

Figure 2.5. Schematic of stir casting method [52].

2.2.1.2. Infiltration Method. In this method, aluminium alloy is introduced into a porous ceramic pre-form benefiting an inert gas or a mechanical part like pressurizing device. Viscosity of aluminium melt matrix in the time of filling the ceramic preform is a matter of importance due to the effect of friction on the required pressure. Wetting of the ceramic by the liquid aluminium is dependent to alloy composition, features of ceramic preform, surface treatment of ceramic, surface geometry, interfacial reactions, adjacent atmosphere, time and temperature [49].

2.2.2. Solid state manufacturing routes

Manufacturing of AMCs in solid phase has advantages such as much homogenous distribution of reinforcement materials, less porosities and no segregation which are not completely controllable in liquid state processes. This is mostly due to the reduction of most of the non-required interface reactions [53].

2.2.2.1 Powder metallurgy. It is reported that PM is the most suggested method for manufacturing discontinuous reinforcement metal matrix composites. This method has advantages such as: less unrequired interface reactions due to low temperature process and manufacturing of AMCs with whisker and particulate reinforcements are easier but it is relatively expensive, needs high level of cleanliness and it has limitations of final parts [53]. The process starts with blending elemental or alloy metal powders and additives (lubricants and blinders), then follows with die compacting and sintering.

2.2.2.2 Diffusion bonding. This is another method in solid state manufacturing of MMCs. Diffusion bonding is an advanced material process for joining metallic or non-metallic materials. This bonding technique is based on the atomic diffusion of elements at the joining interface. In other words it is the transport of mass in form of atom movement or diffusion through the lattice of a crystalline solid. Diffusion of atoms proceeds by many mechanisms, such as exchange of places between adjacent atoms, motion of interstitial atoms or motion of vacancies in a crystalline lattice structure. The latest is the preferable mechanism due to low activation energy required for atom movement. Advantages of this method are the possibility of using several matrix materials and opportunity of controlling

fiber direction and volume content rate. However this method is counted as an expensive one which had restrictions in dimensions of final product, requires long process periods and has necessity of high process temperature and high pressure [54].

2.3. SQUEEZE CASTING

Squeeze casting which is categorized to direct and indirect squeeze casting (Figure 2.6. Schematic diagram to show two forms of the direct squeeze casting process) is a die casting method based on slower, continuous die filling and high metal pressures in a reusable steel die. It is, in other words, combination of permanent die casting and die forging. Some of the weaknesses of most of advanced casting methods, like high pressure die-casting are the formation of defects such as porosity, segregation defects of hot tears, A and V segregates and banding. Actually the key differences between squeeze casting and high-pressure die casting are in the gate design, injection velocities and intensification pressures. Squeeze casting uses wider gates and the metal enters in a laminar or plug flow regime. This reduces the entrainment of air into the molten metal, thus minimizing porosity and resulting high density which is a goal in squeeze casting [55-57].

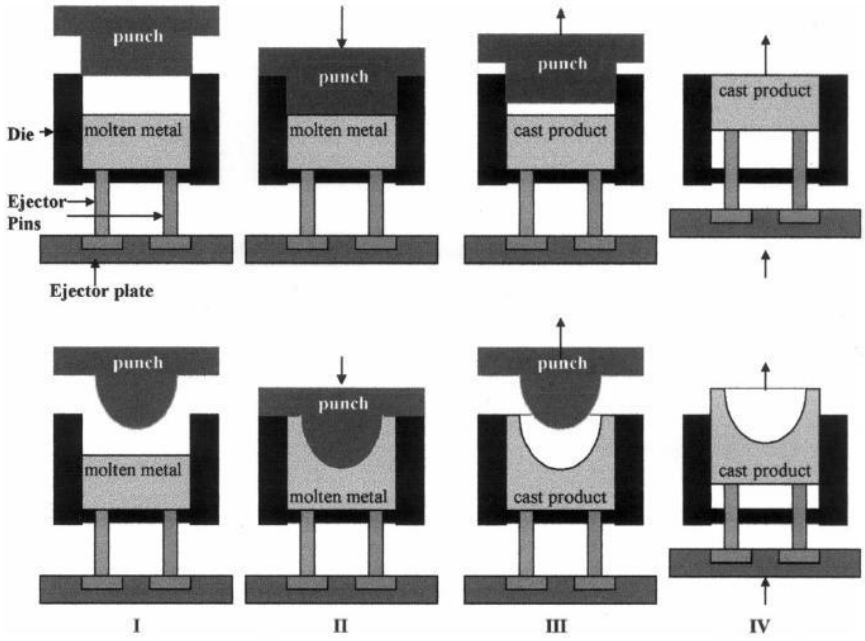

Figure 2.6. Schematic diagram to show two forms of the direct squeeze casting process [58].

There are numerous studies which used reinforcements like WO_3, $Al_3Zr + Al_2O_3$, ZrO_2, Ca, SiC, Fe and B_4C reported that regardless of effect of alloying and reinforcement addition, the squeeze cast parts have superior mechanical properties compared to the gravity die cast alloys [59-65].

2.3.1. Squeeze Casting of Aluminium Matrix Composites

Apart from the fact that squeeze casting is a unique method in manufacturing metal matrix composites, it is a method which can finalize a metal matrix composite production. Since squeeze casting is normally applied on light metals, it is most likely that researchers use it in order to eliminate porosities and improve the mechanical and microstructural properties of aluminium matrix composites. There are number of studies in which the effect of squeeze pressure has been evaluated in manufacturing aluminium matrix composites. In a study by Chen *et al.* [66], it is shown that reinforcing aluminium matrix composite with SiC particles and making it hybrid by addition of titanium particles can reserve ductility while increasing the strength of material in presence of squeeze casting. R. B. Bhagat [67] found out that squeeze casting is a very promising fabrication method for stainless steel fiber reinforced AMCs. In their research pouring temperature of 850°C, die preheating temperature of 550°C, and a squeeze pressure of 110 MPa resulted in high quality composites having a wide range of fiber volume fraction. Referring to a work by Dhanashekar *et al.* [68] who reviewed papers in which squeeze casting has been employed in manufacturing or post processing of aluminium matrix composites, it can be concluded that:

- Pressure as the main process parameter in squeeze casting should be optimized in order to get the best results.
- The selection of the reinforcement particle size affects the strength of the material in the squeeze casting process. The smaller the grain size, the superior the improvement in the properties.
- The suggested melt and die temperature during the squeeze casting of Aluminium alloys and composites are 600°C to 700°C and around 250°C respectively.
- Normally a refinement in the microstructure is expected in the process with the combined effect of undercooling and a higher cooling rate, due to the high pressure level in the squeeze casting.
- The mechanical properties are expected to be improved for the composites when fabricated through the squeeze casting technique, under controlled process parameters.

2.3.2. Advantages and Disadvantages of Squeeze Casting

The major advantages of Squeeze Casting are elimination of porosity and shrinkage, 100% casting yield, ability to manufacture parts with more details, acceptable surface finish, good dimensional accuracy, resistance to high temperature, high strength to weight ratio, better corrosion resistance, improved wear resistance, superior hardness, improved fatigue and better creep strength. The components manufactured by this casting method requires less or no post machining processes and they have improved mechanical properties like higher strength and ductility [69]. Squeeze casting also provides a fine-grained equiaxed structure with small dendrite arm spacing and small constituent particles. Also it is counted as the most popular fabrication route for MMC products [70, 71]. Based on literature, advantages of squeeze casting can be categorized as below which is also illustrated and compared to other casting techniques in Figure 2.7 :

(i) Manufactured part are without gas porosity and shrinkage porosity;

(ii) Feeders or risers are not required and therefore no metal wastage occurs;

(iii) Alloy fluidity (cast-ability) is not a challenge in squeeze casting, due to the fact that both cast alloys and wrought alloys can be manufactured by squeeze casting to finished shape with the aid of pressure;

(iv) Squeeze castings can have mechanical properties as good as wrought products of the same composition;

(v) Minimum material and energy utilization are used for process;

(vi) The cast structure exhibits more isotropic and improved mechanical properties.

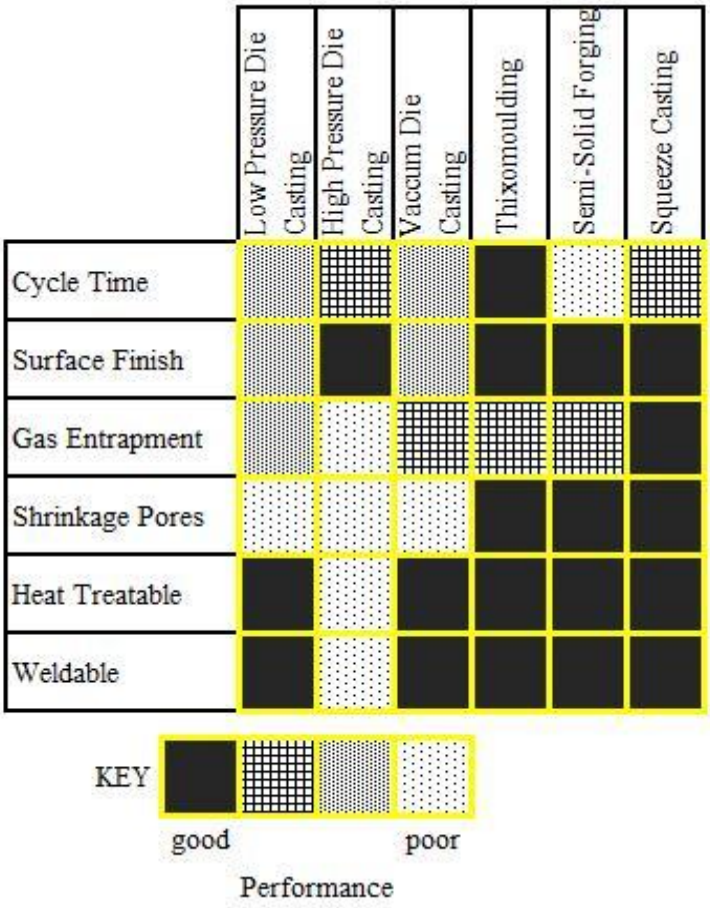

Figure 2.7. A graphical representation of casting quality with respect to the casting technique [72].

Regarding disadvantages of squeeze casting it can be briefed that, unlike the gated systems, oxidation of melt is a challenge in squeeze casting. Also the process requires a careful control of die, punch and melt temperatures and a good timing for pressure application because these parameters affect the quality of the casting vastly. Moreover it is difficult to apply squeeze casting on alloys with narrow freezing ranges, because there would be need for high overheating temperatures which cause leakage of molten metal through tooling interfaces and shrinkage porosity in thick sections. Likewise lubrication and preheating of die is very important because high pressure might cause a weld between die and the melt and also to provide good surface finish and to increase die life which is another challenge in squeeze casting. Besides all aforementioned drawbacks one critical disadvantage of squeeze casting is high capital cost and limitations in as cast parts size and weight [58].

2.3.3. Variables in Squeeze Casting

Alike all casting processes, there are number of variables which should be controlled during squeeze casting which can be different for different AMCs and as cast part geometry.

i. *Melt Volume:* It is important to precisely control the volume of melt to be poured into die cavity. This is both for dimensional control of final product and also to be sure about the sound application of pressure on the melt.

ii. *Pouring Temperature:* Casting temperature mainly depends on the material and its alloying system used as the matrix in metal matrix composites. Too low casting temperature causes insufficient fluidity in the melt and results in incomplete die fill as well as cold laps on the casting surfaces. On the other hand too high casting temperature can cause extrusion of liquid metal through the tooling interfaces and can also result in shrinkage porosity in thick sections of the casting. Also the die life is unfavorably affected by high pouring temperatures. 6 to 55 °C above the liquidus temperature has been reported as the pouring temperature. Effect of pouring temperature in aluminium matrix composites will be discussed vastly in explaining effect of pressure on microstructure of AMCs.

iii. *Die and punch Temperature:* In the case of die, normally temperature of 190 to 315 °C is used while the temperature of punch is mostly chosen 15 to 30 °C less than die temperature. This is because if the punch temperature is close to that of die, the melt can be extruded between them and results in an eroded surface.

iv. *Pressure:* Applied pressure for metal matrix composites with aluminium and magnesium alloys generally varies between 50 and 150 MPa. Depending on the geometry of the part to be cast and the material and also the required level of mechanical properties, this value can be adjusted but it should be concerned that after a specific pressure value which is called optimum pressure no added advantages in mechanical properties will be obtained.

v. *Time Delay before Pressure Application:* In order to avoid shrinkage cavities, the melt is needed to be decreased to below the liquidus temperature and for this a time delay is needed before pressure application. With aluminium alloys, it is

frequently necessary to provide a time delay of 10 to 20 seconds before die closure and pressure application.

vi. *Pressure Duration:* Again this parameter is directly dependent on the part geometry but it normally takes 30 to 120 s for a 9 kg part. Applied pressure after composite solidification and temperature equalization will not contribute any property enhancements and will only increase the cycle times.

vii. *Lubrication:* In case of aluminium, magnesium and copper alloys as the matrix material, a spraying a lubricant like graphite on the die will be promising [55, 58, 73].

2.3.4. Effect of Pressure on Micro/Macrostructure and Mechanical Properties

Pressure is the main process parameter in squeeze casting which causes almost all the improvements in mechanical properties and microstructure of materials.

There are usually two theories to explain the grain refinement mechanism under applied pressure: One theory considers the improvement of heat transfer during squeeze casting process. In most conventional casting processes, an air gap is formed immediately after pouring, between the mold and the solidified shell of the component. Then the heat transfer mechanism changes dramatically due to the existence of the air gap and results in a significant decrease of the cooling rate. The other theory considers the change of phase diagram under applied pressure. Consider the Clausius–Clapeyron equation:

$$\frac{\Delta T_f}{\Delta P} = \frac{T_f(V_f - V_s)}{\Delta H_f} \tag{2.10}$$

where T_f is the equilibrium freezing temperature, V_f and V_s are the specific volumes of the liquid and solid respectively, and ΔH_f is the latent heat of fusion. The effect of pressure on the freezing point may be roughly estimated as follows:

$$P = P_0 \exp\left(\frac{-\Delta H_f}{RT_f}\right) \tag{2.11}$$

where P_0, ΔH_f and R are constants. According to Equation 2.11, T_f should increase with increasing pressure. Increase of T_f can induce a higher undercooling compared to conventional castings. According to the calculation result reported by Han *et al.* [74], the undercooling in squeeze casting is less than 15 K and the nucleation rate increases evidently with increasing undercooling in this undercooling range. Squeeze casting also leads to the morphology modification of second phases. Pressurized solidification and high cooling rate promote the nucleation of second phases and correspondingly restrict their growth. Consequently, the plate-like second phases grow much thinner when solidified under high pressure. Generally, it can be said that the improvement of mechanical properties in squeeze casting is attributed to the reduction of shrinkage and gas porosities and the refinement in the microstructure. According to Hall-Petch relation, yield strength of a given alloy is proportional to $d^{-1/2}$, where d is the average grain size and YS would increase when d decreases. Moreover, it might be the result of a higher dislocation density in the samples prepared by the squeeze casting [75]. The increase in the amount of dislocations increases the lattice strains that interact with active dislocations, impeding their motion and causing an increase in YS [76]. Al in all, the effect of pressure on a molten metal during solidification can be categorized as:

i. *Change in the melting point*. As discussed above, melting point (liquidus temperature) of most metals and alloys increases under pressure and the increase satisfies Clausius–Clapeyron equation. This characteristic can be utilized to create sudden large undercooling in the melt upon application of pressure if the melt temperature and timing of pressure application are accurately controlled.

ii. *Change of solidification rate.* In most casting processes an air gap is formed shortly after pouring between the die and the solidified outer shell of the casting [6]. This is due to simultaneous contraction of the shell and expansion of the die. Air gap formation changes heat transfer mechanism from conduction to convection and radiation and causes a significant decrease in heat transfer rate and consequently decreases the cooling rate. In squeeze casting, air gap formation is eliminated as a result of the applied pressure on the casting and therefore heat transfer and cooling rate increases considerably. Higher cooling rate, especially if coupled with a prompt large undercooling as mentioned above, can causes significant improvements in the structure and mechanical properties of the castings.

iii. *Structural changes.* Applied pressure causes structural changes through affecting cooling rate of the melt and its undercooling. These structural changes include decrease in dendrite arm spacing (DAS), more homogeneous distribution of structural features and refinement and modification of intermetallic phases. These factors cause improvement in the mechanical properties of squeeze cast components.

iv. *Reduction of gas and shrinkage porosities.* It has been shown that gas solubility in the melt increases under an applied pressure. This makes gas bubble nucleation more difficult. It is also well established that application of an external pressure during solidification of a casting activates the different feeding mechanisms and hinders the shrinkage porosity formation. Consequently, if a high enough pressure is used, formation of both gas and shrinkage porosities may be completely eliminated [77].

For squeeze casting minimum pressure level of 70 to 105 MPa is necessary in order not to face shrinkage and gas porosity. However, the geometry of casting dictates the use of higher pressure for controlling porosity formation and die filling. There is a critical pressure for each composition at which density nearly reaches saturation. The saturation values are almost equal to the ideal (theoretical) density of alloy of that composition. This pressure level is also called as 'the critical pressure for density'. There is also critical pressure above which no defects (porosity, shrinkage etc.) are detected (by dye penetrant checking) and this pressure is called 'the critical pressure for defects'. Usually the critical pressure for defects is higher than the critical pressure for density and it dictates 'the minimum pressure level' for a sound casting. In general, a pressure of 105 MPa was necessary to eliminate porosity in alloys with a narrow freezing range ($\Delta T \approx 10°C$), whereas 70 MPa was adequate for alloys with extended freezing range ($\Delta T \approx 100°C$). Extended freezing range alloys were found to require less applied pressure because of shorter feed length between the semi-liquid pool and solidifying metal than for narrow freezing range alloys. The pressure level in squeeze casting is usually in the range of 70-105 MPa for simple shapes and rises to 140-210 MPa for thin sections and complex shapes. The shapes and the section thickness of the casting govern the duration of pressure necessary to ensure complete solidification under pressure.

As discussed before, the timing of pressure application is critical, since if it is applied at a temperature of $T > T_m+\Delta T$, ΔT being the expected increase in Tm due to pressure, the effect of undercooling is negligible and thus increase in the heat transfer coefficient is the dominant mechanism. If however, the pressure is applied at a temperature $T_m \leq T \leq T_m+\Delta T$, then under cooling would be the dominant mechanism [58, 77]. Figures below show effect of pressure on different properties of squeeze cast materials.

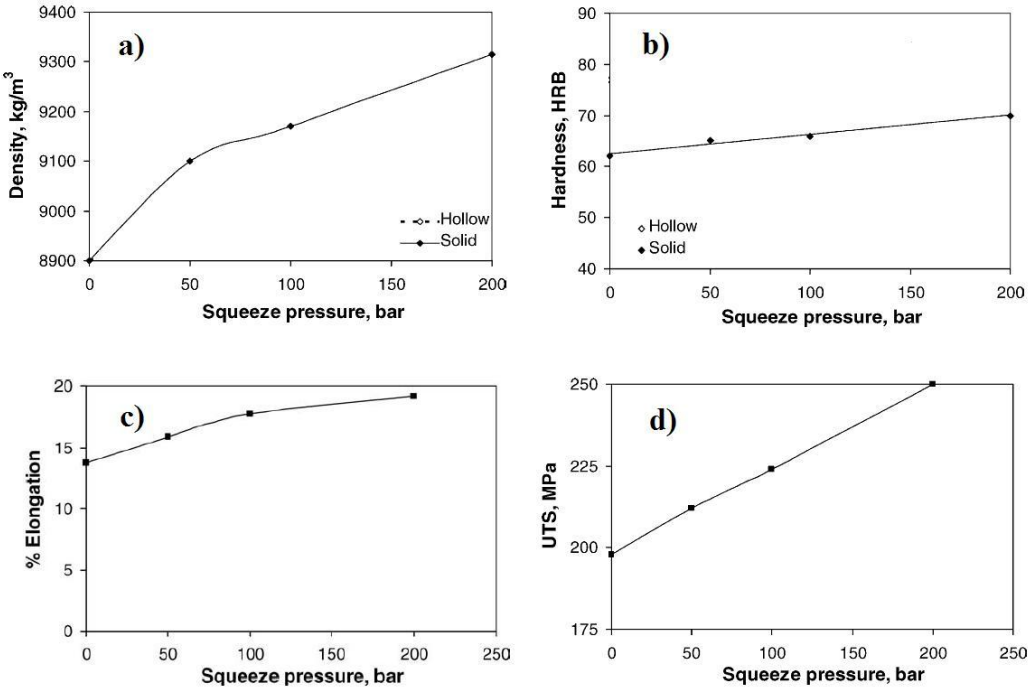

Figure 2.8. Effect of pressure on a) density, b) hardness, c) elongation and d) UTS of squeeze cast pure gunmetal (Cu 85 % , Zn 5 % , Sn 5 % , Pb 5 %) [78].

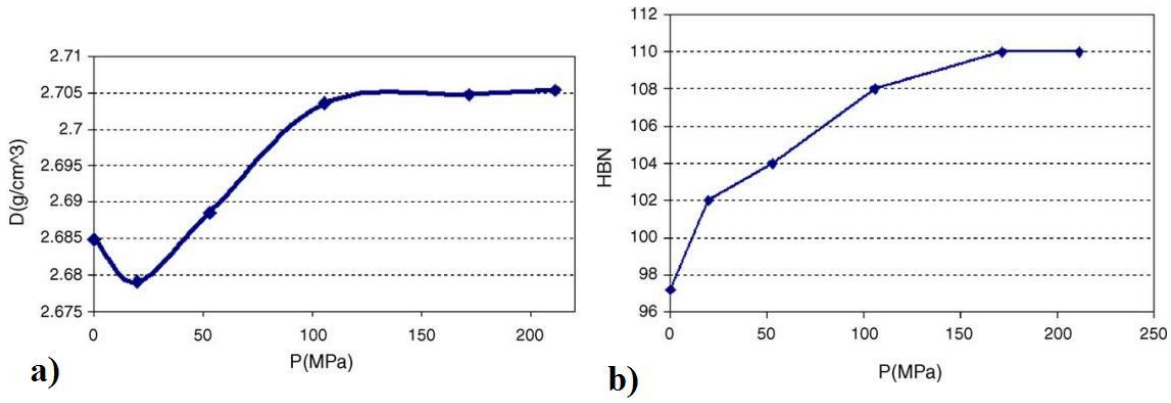

Figure 2.9. Effect of external pressure on a) density and b) hardness of squeeze cast LM13 alloy (T_m = 730 °C and T_d = 200 °C) [77].

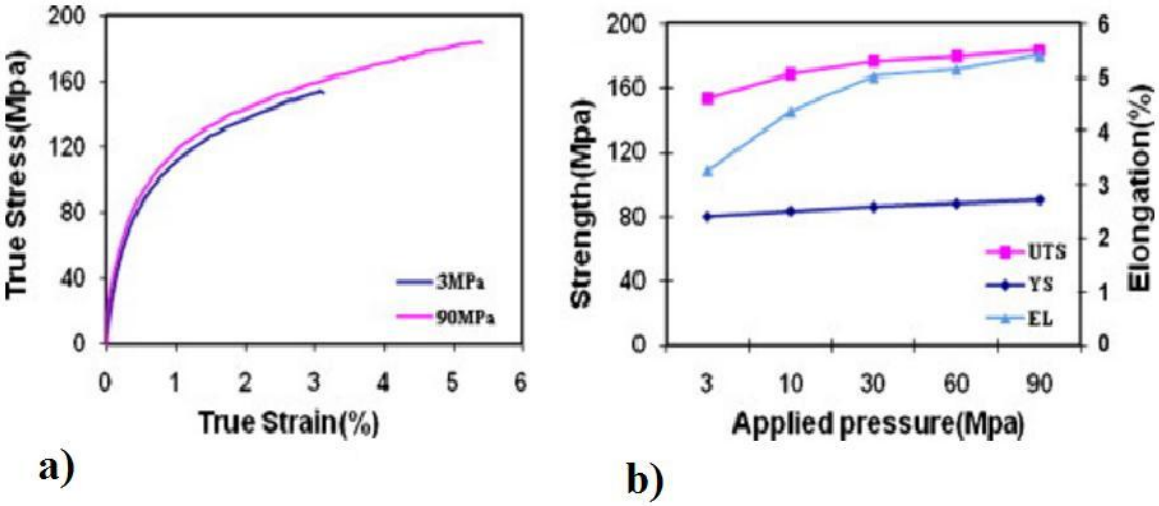

Figure 2.10. (a) Typical true stress vs. strain curves of AX51 alloys squeeze cast under 3 and 90 MPa and (b) effect of pressure levels on UTS, YS and elongation of AX51 alloy [75].

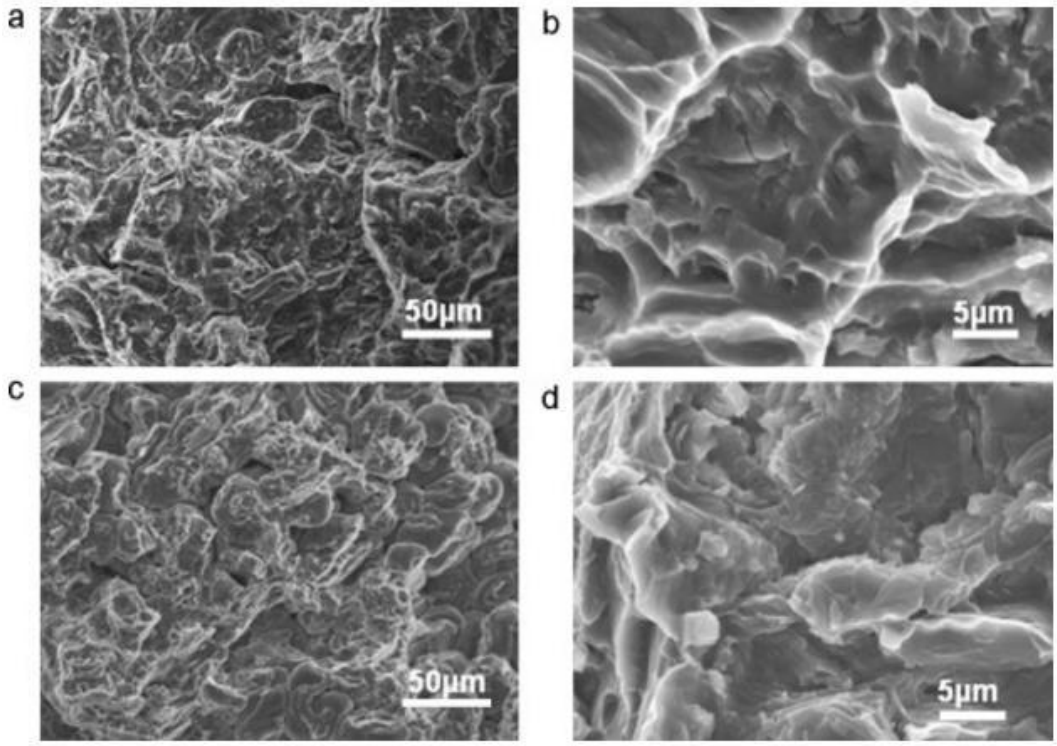

Figure 2.11. SEM fractographs of squeeze cast AX51 under (a and b) 90 MPa (c and d) 3 MPa ((a and c) low magnification and (b and d) high magnification) [75].

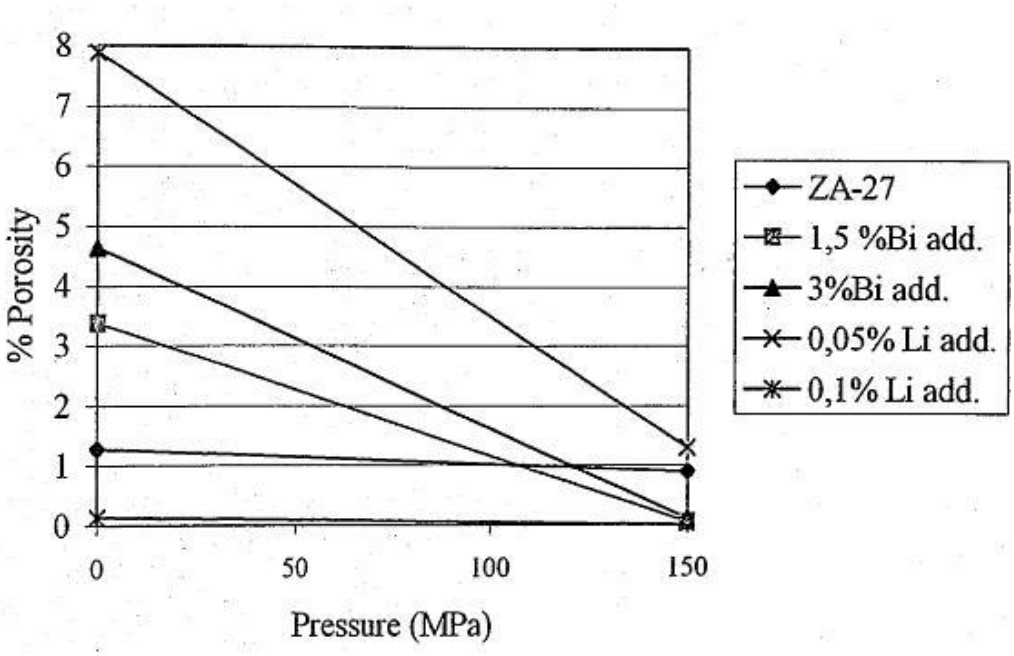

Figure 2.12. % porosity in casting vs. squeeze casting [73].

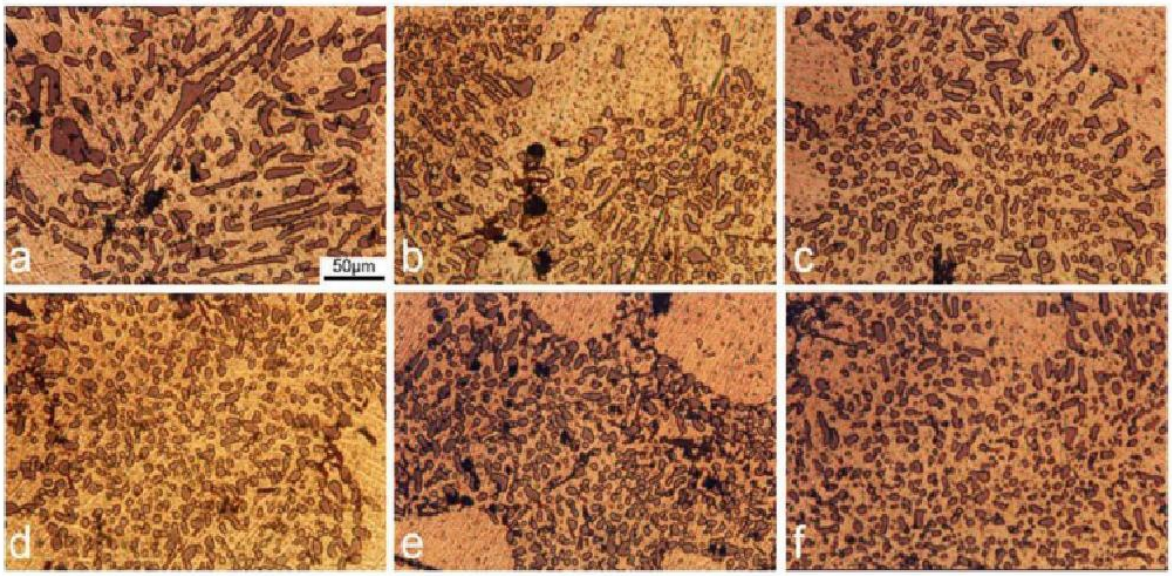

Figure 2.13. Effect of external pressure on the morphology of eutectic silicon particles of squeeze cast LM13 alloy: (a) 0 (Atmospheric Pressure), (b) 20 MPa, (c) 53 MPa, (d) 106 MPa, (e) 171 MPa (f) 211 MPa (T_m = 730 °C and T_d = 200 °C) [79].

2.4. COMPOSITES WITH B_4C AND BN AS REINFORCEMENT MATERIALS

Boron (B) is the group III-A element in the periodic table, occurs in borates and borosilicates in the earth crust which was discovered in 1808 by French chemist Gay Lussac and English chemist Humphrey Davey. Boron containing minerals (borates) have been used by human in 300 years B.C. in Chinese ceramics. On the basic of equivalent B_2O_3 content, boron reserves are known as 1.176 billion tons. 72.2 % of the reserves of 851 million tons are known to exist in Turkey but the figures are 35 % in the production and trade. Two main ceramic materials to be produced from boron are boron nitride and boron carbide which have vast applications in the industry [80].

Country Name	Region and type	Total Ore	Contained B_2O_3	B_2O_3 Reserve	B_2O_3 Reserve Base	B_2O_3 Total Reserve
Turkey	Bigadic-Balikesir					
	(Ca-NaCa types)	935	330	(1030-360)		
	Emet-Kütahya (Ca-type)*	545	200	(890-310)		
	Kestelek (Ca-type)	7	3	(8-3)		
	Kırka (Na-type)	520	140	(519-130)		
	Subtotal	2007	673	227	624	851
USA	Boron-(Na-type)	113	26			
	(Ca-type)	198	20			
	Subtotal	311	46			
	Searles Lake, Death Valley, Hector, Owens Lake, Salton Sea, Four Corners, Muddy Mountains, etc.	255	77			
	Subtotal	566	123	40	40	80
Russia	Dalnegorsk, etc.	700	64	40	60	100
China	Liaoning, etc.	480	65	27	9	36
Mexico	Mesa del Amo, Vitro, Tubutama, etc.	140	13.5			
Argentina	Loma Blanca, Sijes, Tincalayu, Salars, etc.	100	20.5	2	7	9

Figure 2.14. World boron reserves high ranked 6 countries in million metric tons [80].

2.4.1. Boron Carbide (B_4C) Reinforcement

Boron carbide is a ceramic material which has superior hardness, high elastic modulus, high thermal stability, excellent chemical inertness, very good corrosion resistance, high impact strength, exceptional corrosion resistance and similar physical, mechanical and chemical outstanding properties. These properties make boron carbide a

material of choice for a wide range of engineering applications. Boron carbide is used in refractory applications due to its high melting point and thermal stability; it is used as abrasive powders and coatings due to its extreme abrasion resistance; it excels in ballistic performance due to its high hardness and low density; and it is commonly used in nuclear applications as neutron radiation absorbent. In addition, boron carbide is a high temperature semiconductor that can potentially be used for novel electronic applications. This ceramic has rhombohedral lattice system and is covalently bonded [81, 82].

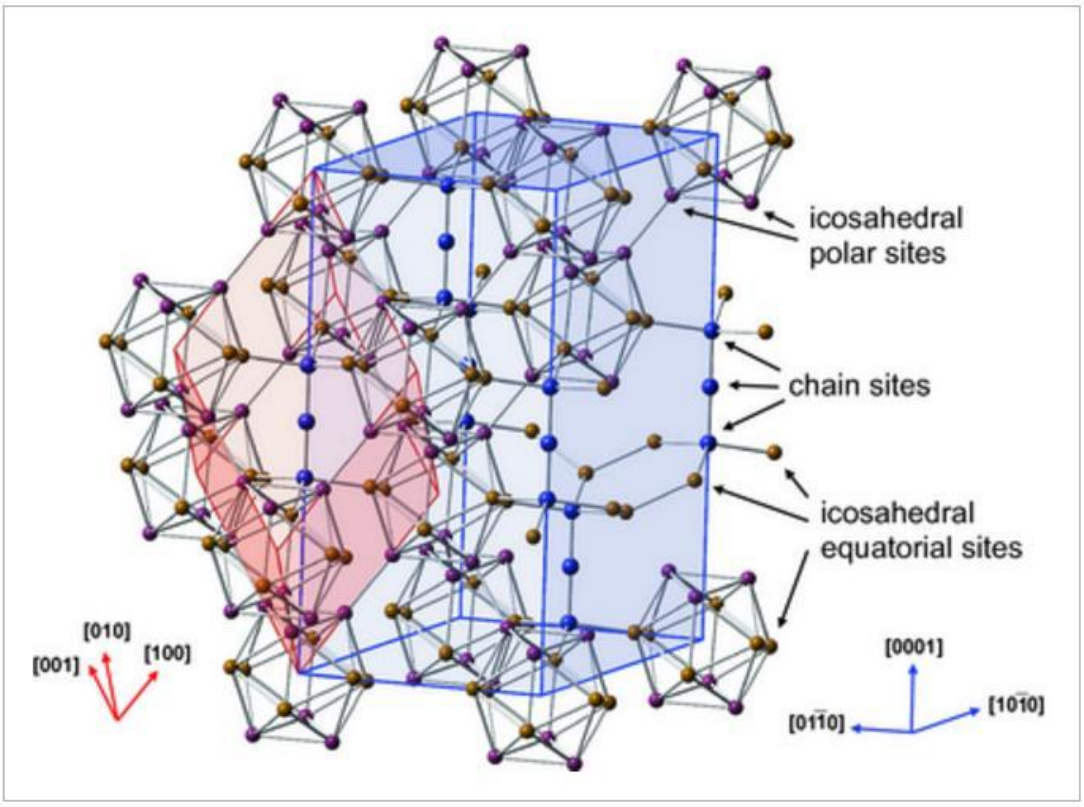

Figure 2.15. Boron carbide lattice showing correlation between the rhombohedral (red) and the hexagonal (blue) unit cells. Inequivalent lattice sites are marked by arrows [82].

Industrial preparation of boron carbide is done either by reduction of boron anhydride (or acid) with carbon ($2\ B_2O_3 + 7\ C \rightarrow B_4C + 6CO$), or by reduction of boron anhydride with magnesium in the presence of carbon black ($2\ B_2O_3 + 6\ Mg + C \rightarrow B_4C + 6\ MgO$) in an electric arc furnace, which are normally expensive processes making boron carbide, an expensive ceramic [82]. Currently, boron carbide is produced in the form of large ingots, produced by mixing petroleum coke with boron oxide at temperatures of up to 2000 °C. These ingots then have to be ground into fine grains before being fabricated into

the required shape. This method uses a lot of energy and time, making boron carbide products up to 10 times more expensive than other, less hard wearing ceramic materials which currently dominate the market. A team led by Isaac Chang has devised a method which substitutes a carbohydrate-based compound for the petroleum coke. The boron oxide and carbohydrate are mixed in water to form a solution which mixes the carbon and boron sources at a molecular level. The solution is then atomized into fine droplets which convert into a powder on cooling. When this powder is heated at a temperature below 1500 °C fine boron carbide particles are produced, ready for processing. The raw materials used in this method are very cheap and also highly active, which means much lower temperatures are required to make the chemical reaction which means less energy is needed. Also, since the end product of this process is a powder, rather than an ingot, there is no need for grinding, which removes a costly and inefficient step from the process [83-86]. In Figure 2.16 some of current applications of boron carbide ceramics have been shows as: a) superior abrasives for polishing and cutting, b) bulletproof armor materials used for bulletproof armor material, such as bulletproof vests bulletproof plates, military aircraft cockpit bulletproof ceramic tiles and modern armored personnel carriers and tanks, ceramic bulletproof plate, c) advanced refractory like antioxidant additives for carbon brick, d) nuclear material control and making nuclear reactor control rods and closed columns, making for radiation protection of boron carbide tile, sheet or neutron absorber (B10 with a high content of powders), or mixed with cement for the production of nuclear reactor shield, e) sand blasting nozzle cutting machine, sealing rings and ceramic mold and f) alloy powder coating for electrodes, in order to enhance abrasion resistance weld surface.

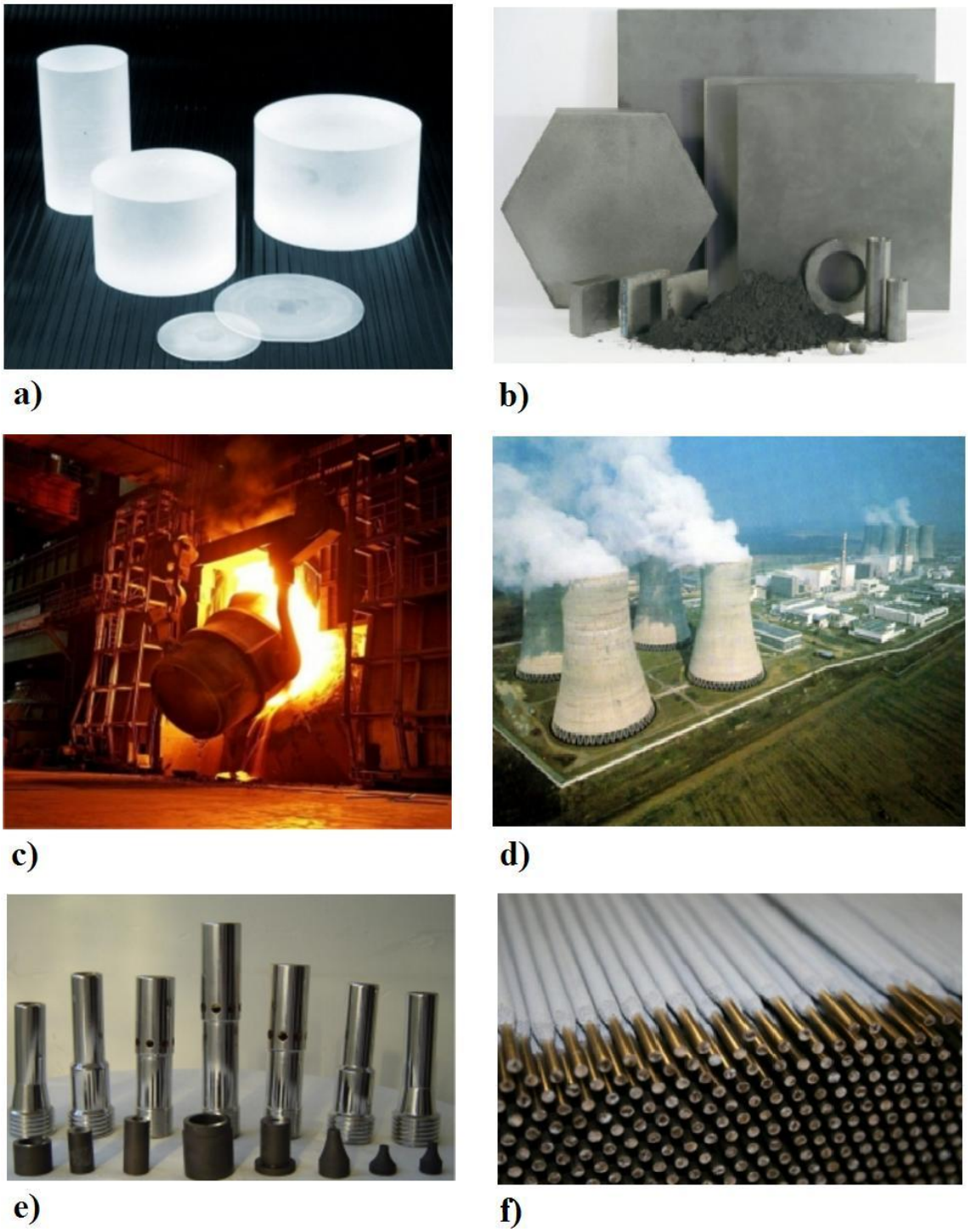

Figure 2.16. Example applications of B_4C in the industry a) superior abrasives, b) bulletproof material, c) advanced Refractory, d) nuclear Material Control, e) sand blasting and f) alloy powder [87].

Although B_4C has superior properties compared to alumina and silicon carbide, Al_2O_3 and SiC are the most used reinforcement materials in aluminium matrix composites.

The reason relies on the higher expenses of manufacturing Al-B_4C composites due to higher prices of boron carbide particles, which is going to be solved as discussed in upper lines. However, comparing to Al-Al_2O_3 and Al-SiC, less density, higher elastic modulus and higher specific rigidity are reachable with reinforcing aluminium with B_4C. This makes Al-B_4C a good choice in applications in which wear resistance and lighter composite is required. Some properties of B_4C have been shown in the Table 2.4.

Table 2.4. Properties of boron carbide

Property	**Value**	**Reference**
Density	2.52 g/cm^3	[82]
Hardness	3900 HV_{980N} / 2800 Knoop 100g (kg.mm^{-1})/ 29.1 GPa	[82,83]
Melting Temperature	2445 °C	[82]
Elastic Modulus	460 GPa	[82]
Coefficient of Thermal Expansion	5.73 ppm/°C	[82]
Fracture Toughness	3.6 ± 0.3 MPam$^{1/2}$	[82]
Poisson Ratio	0.17	[82]
Electrical Conductivity	~10^3 1/ohm cm	[82]
Thermal Conductivity	0,35 – 0,16 (25–800°C) W/cm K	[83]

Based on a study by Ravi *et al.* [88], A6061-B_4C has been fabricated by stir casting. In this study an increase in the volume fraction of boron carbide particles increases the hardness (about 6 %), ultimate tensile strength (about 14 %) and decreases the grain size in the composite (Figure 2.17).

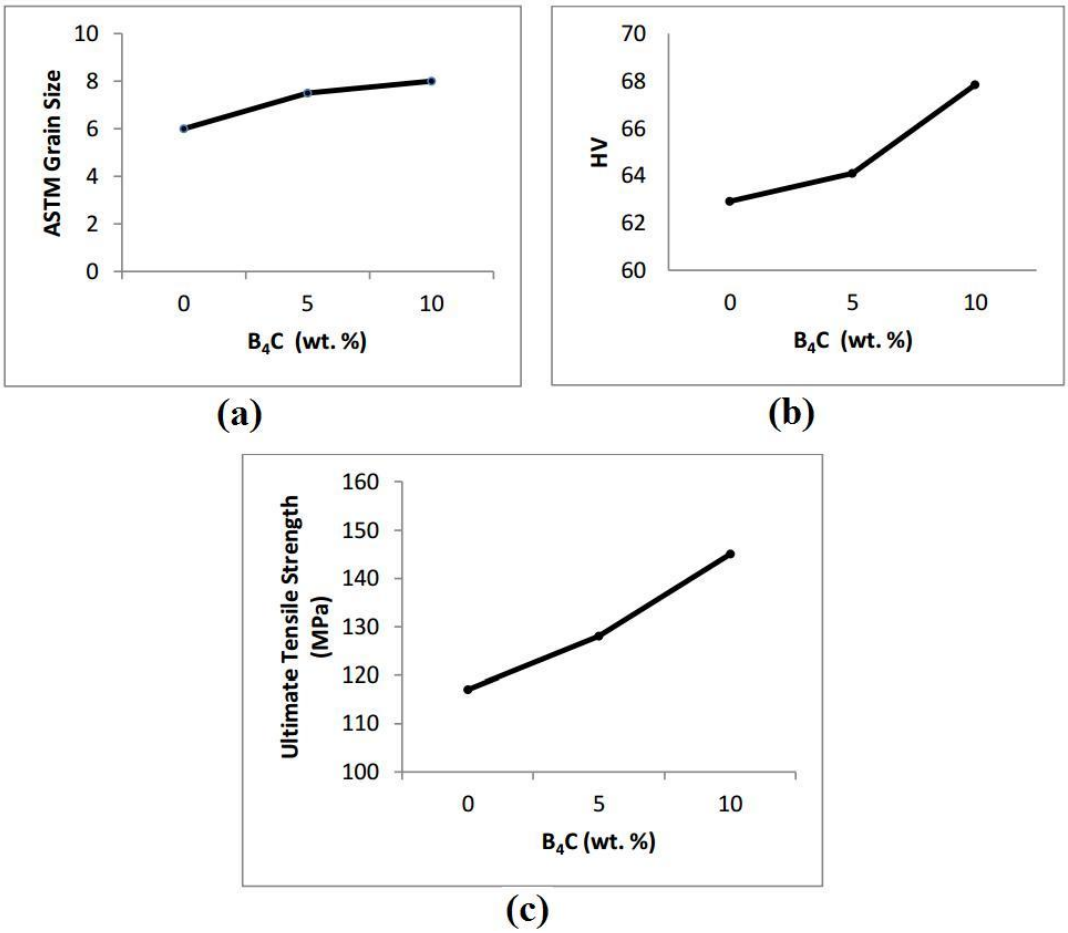

Figure 2.17. The effects of percentage of B_4C particulates on the a) grain size b) hardness and c) ultimate tensile strength of stir casted AMCs [88].

In another work, Ibrahim *et al.* [89] studied impact toughness of Al-15 vol. % B_4C metal matrix composites and the results exhibited that; introduction of Ti improved the particle wettability with no microporosity. However, Ti may react with B_4C particles leading to the formation of Al-Ti-B compound. The combined addition of Ti with Zr and/or Sc reduced this reaction. Also it was seen that cracks were always initiated at the particle/matrix interfaces and propagate either through the B_4C or along the protecting layer or both, depending upon the particle/matrix adhesion.

Furthermore Lashgari *et al.* [90] assessed the effect of strontium on the microstructure, porosity and tensile properties of A356–10 % B_4C cast composite and found that adding strontium (0.05 % and 0.2 %) has a negligible effect on UTS and YS, but considerably improves the elongation values of Al–B_4C composite. In another work,

Harichandran *et al.* [34] evaluated effect of nano/micro B_4C particles on the mechanical properties of pure aluminium matrix composite. They found out that the nanocomposites were stronger and more ductile than the aluminium composites reinforced with micro-sized B_4C particles. The stress and strain curve shows that increasing the amount of B_4C particles increased the ultimate tensile strength and decreased the ductility. The nanocomposite is more ductile than the micro B_4C-reinforced composite but increasing the wt. % of B_4C nanoparticles beyond 6 %, leads to the decrease of the strength and ductility of the MMNCs due to the particle agglomeration and porosity (Figure 2.18 and Figure 2.19). Besides, The hardness of composites is positively correlated with the weight % of micro- and nano-boron carbide particles up to 8 wt. % of B_4C.

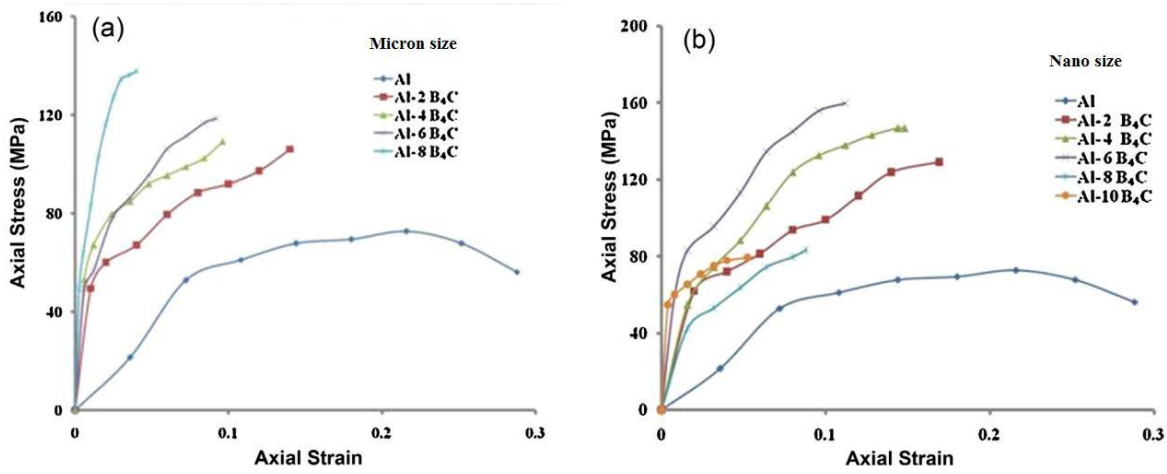

Figure 2.18. (a) The tensile stress–strain curves of the Al-B_4C (μm) composites. (b) The tensile stress–strain curves of the Al-B_4C (nm) composites [34].

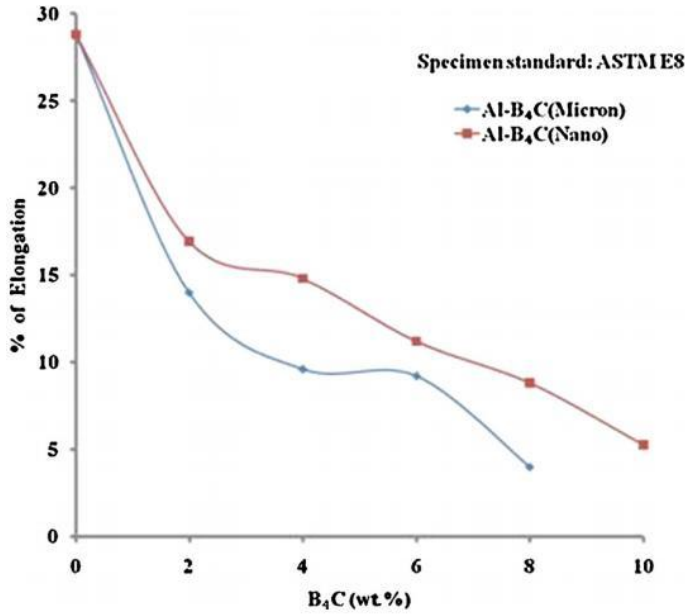

Figure 2.19. Variation of elongation of the Al–B_4C (μm) and Al–B_4C (nm) composites [34].

Furthermore influence of B_4C on the tribological and mechanical properties of Al 7075–B4C composites has been studied by Baradeswaran *et al.* [91]. In this work, an increase in B_4C particulates volume fraction from 0 to 20 % resulted in an increase in hardness from 114 BHN to 210 BHN and improvement in ultimate tensile strength values from 220 MPa to 301 MPa.

An important factor in an experimental work of manufacturing Al-B4C composites, is interface between matrix and the reinforcement material. Two critical cases in this issue are low wettability of B_4C by aluminium melt and the fact that the system is highly reactive. Specifically the phases created in temperatures above 900 °C are more complicated ones. In Al-B_4C system and in the temperatures between 600-700 °C, AlB_2 is expected. In 700-900 °C, AlB_2 and Al_4BC are potential phases and in 900-980 °C Al_4BC is reported. Also reports showed presence of $AlB_{24}C_4$ and Al_4C_3 phases in 1000-1050 °C. Among these phases, Al_4C_3 is a detrimental phase which has been reported also in 985-1370 °C and 1200-1400 °C temperatures. [92, 93].

2.4.2. Boron Nitride (BN) Reinforcement

The elements boron and nitrogen are both neighbors to carbon in the periodic table, mutually form 1:1 compounds which are isostructural to the polymorphs of carbon:

i. α-BN (h-BN): Is a hexagonal modification with a layered structure like graphite, which is called "white graphite" and its theoretical density is equal to 2.27 g/cm3 (Figure 2.20-a);
ii. β-BN (c-BN): Is a high pressure modification with cubic zinc blend structure very similar to diamond and its theoretical density is equal to 3.48 g/cm^3 (Figure 2.20-b);
iii. γ-BN (w-BN): Is a dense hexagonal modification with wurtzite structure and its theoretical density is equal to 3.48 g/cm3 (Figure 2.20-c) [94].

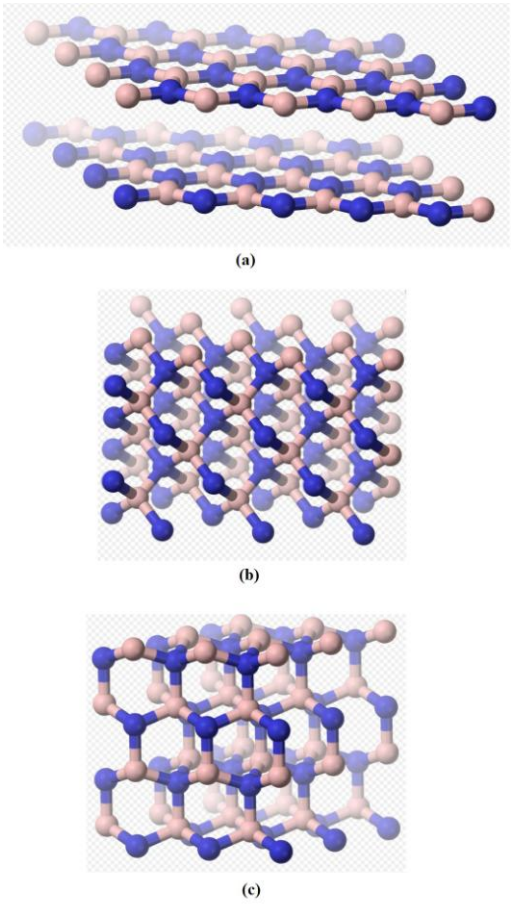

Figure 2.20. Crystal structures of a) h-BN, b) c-BN and c) w-BN [95].

As mentioned previously, hexagonal boron nitride is generally called “white graphite” because it is a lubricious material with the same anisotropic layered hexagonal structure as carbon graphite with this difference that BN is a very good electrical insulator. It offers very high thermal conductivity and good thermal shock resistance. BN is stable in inert and reducing atmospheres up to 2000 °C, and in oxidizing atmospheres to 850 °C. Key properties of h-BN can be listed as: high thermal conductivity, low thermal expansion, good thermal shock resistance, high electrical resistance, low dielectric constant, microwave transparency, non-toxic, easily machined (non-abrasive and lubricious), chemically inert and not wet by most molten metals in natural situation (Table 2.5) [96].

For the first time hexagonal BN was manufactured by Balmain in the mid-19th century. It remained a laboratory interest until the mid-20th century, when hot-pressed α-BN products were made for the first time. There are lots of general methods for the preparation of h-BN powders but three main reactions have become practical in the industry:

i. Reaction of boric oxide with ammonia in the presence of a filler material (i.e. tricalcium orthophosphate) in 900 °C:

$$B_2O_3 + 2NH_3 \rightarrow 2BN + 3H_2O \qquad (2.12)$$

and a second heat treatment for purification and crystallization is performed at temperatures higher than 1500 °C under N_2.

ii. Reaction of boric oxide (or borax) with organic nitrogen compounds (i.e. urea, melamine) at temperatures higher than 1000 °C:

$$B_2O_3 + CO(NH_2)_2 \rightarrow 2BN + CO_2 + 2H_2O \qquad (2.13)$$

iii. Nitridation of calcium hexaboride in the presence of boric oxide at the temperatures higher than 1500 °C:

$$3CaB_6 + B_2O_3 + 10N_2 \rightarrow 20BN + 3CaO \qquad (2.14)$$

Table 2.5. Properties of hexagonal boron nitride

Property	Value	Reference
Density	2.1 g/cm^3	[94]
Hardness	15-285 HV / 400 Knoop 100g (kg.mm^{-1})/ 0.15-0.24 GPa	[97]
Melting Temperature	2600 °C	[94]
Elastic Modulus	19.5-102 GPa / 32 GPa	[94, 98]
Fracture Toughness	2.6 MPam$^{1/2}$	[98]
Poisson Ratio	0.225	[98]
Thermal expansion coef.	1-2 ppm/°C	[99]
Thermal Conductivity	30 (@RT) W/m K	[99]

Applications of boron nitride can be categorized into two groups based on nature of raw material used:

a. *h-BN powder:* As solid lubricant for high-temperature bearings, active filler for rubber, resin and plastic, mold release for die casting, additive to oils and high-temperature grease, as parting agent for deposited metal films, ultrahigh-pressure transmitting agent, coatings for evaporation plants, coating for graphite hot-pressing molds, embedding medium for heating wires and boron feed for preparation of other boron mixtures.

b. *h-BN hot pressed shapes*: Crucibles for melting glass and metals, break rings for horizontal continuous castings, components for high-temperature electric furnaces, structural parts for magnetic hydrodynamic devices, dielectric for radar antennas and windows, insulators for low and high frequency equipment, insulators for plasma-jet furnaces, arc pulse generators and ion engines, holders, mounting plates, substrates and heat sinks in valve and transistor circuits, pump components, pipes and nozzles for handling liquid metals, protective tubes and insulating sleeves for thermocouple, protective sleeves for electrodes in automatic welding, wafers for boron-doping of semiconductors, molds for hot-pressing of ceramics like B60 and finally neutron absorbers and shields for nuclear reactors. It should be noticed that the increasing application of h-BN hot-pressed shapes is due to the unique

combination of the properties such as: high temperature refractoriness, chemical inertness and non-wetting property, high thermal conductivity, excellent thermal shock resistance, insulator of electricity and ease of machining [94].

As mentioned there are very suitable applications for pure hexagonal boron nitride and boron nitride composites in high temperature situations. For instance in an experiment Eichler *et al.* [100] found out that MYCROSINT® SO which is a commercial BN/m-ZrO2-composite is a very suitable material to be used as a side dam for thin-strip casting (Figure 2.21).

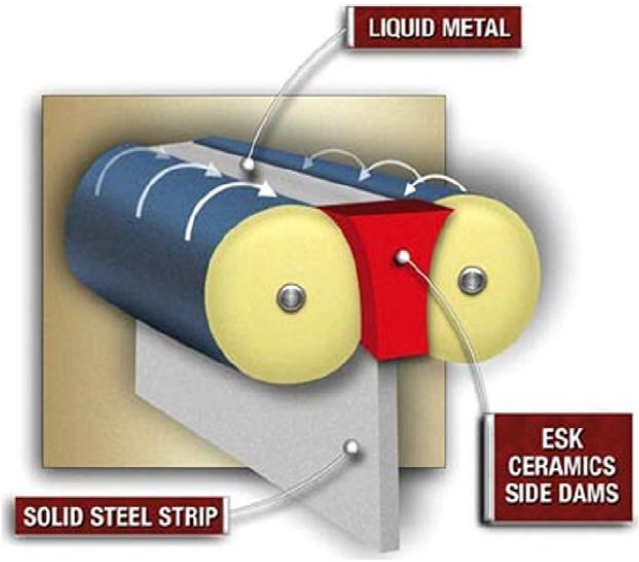

Figure 2.21. Schematic of thin-strip caster with BN/m-ZrO_2 side dam [100].

Zhang *et al.* [101] conducted a paper in which they showed that the phase transformation of c-BN to hexagonal boron nitride depends on the second phases, sintering aids and sintering parameters. In another work by Jin *et al.* [102], researchers found out that the SiC/h-BN nano-composites have the characters of not only lower hardness and good machinability, but also higher bending strength and fracture toughness (693.4 MPa and 6.23 MPa $m^{1/2}$). Li *et al.*, studied mechanical properties of machinable Al_2O_3/BN composite ceramics. They concluded that there was no significant decrease in the fracture strength of Al_2O_3/BN nano-composite ceramics, including the nano-sized BN up to 30 vol.

% ceramics with the increase of h-BN content. Moreover presence of the h-BN contents positively affected the machinability of the composite material and it could be said that improvement in machinability is equal to decrease in the hardness of the material. Also there are some research on improving the mechanical properties and machinability of Si_3N_4, ZrO, Al_2O_3, AlN, etc. with nano-sized h-BN phase [103].

2.4.3. Wettability of B_4C and BN by Aluminium Melt

The wettability is the ability of a liquid to spread over a solid surface. In liquid phase fabrication of MMCs, the contact between the reinforcement and the matrix should be done properly and this needs good wettability between them. The rate of wettability depends on numerous factors such as processing temperature and time, Stoichiometry, concentration of valance electron in ceramic, reactions in the interface, atmosphere, porosities and crystallography of ceramic material. As it is seen in Figure 2.22 the role of contact angle between melt droplet and the ceramic is explained. Wettability is measured by the angle between the solid phase and the liquid drop and it can be calculated by Young's equation:

$$\gamma_{SV} = \gamma_{SL} + \gamma_{LV}\,\mathrm{Cos}\theta \qquad (2.15)$$

in which γ_{SV} is Solid-vapor interface energy, γ_{SL} is solid-liquid interface energy, γ_{LV} is liquid-vapor interface energy and θ is the angle between the liquid drop and the solid phase. When a drop of liquid places on a solid face, part of solid-vapor interface exchanges with solid-liquid and liquid-vapor interfaces. The liquid only spreads on the solid surface when a reduction happens in the total free energy of the system.

Bond strength between liquid and solid (adhesion work) or W_a can be defined as below:

$$W_a = \gamma_{LV} + \gamma_{SV} - \gamma_{SL} \qquad (2.16)$$

Combination of two equations yields:

$$W_a = \gamma_{LV}(1 + \cos\theta) \quad (2.17)$$

θ can be determined by experimental methods like sessile drop from which the behavior of melt and ceramic can be predicted in terms of wettability:

i. θ =0° which means complete wetting will happen
ii. θ =180° which means no wetting will happen
iii. 0° < θ <180° which mean partial wetting will happen between reinforcement and matrix materials [104, 105].

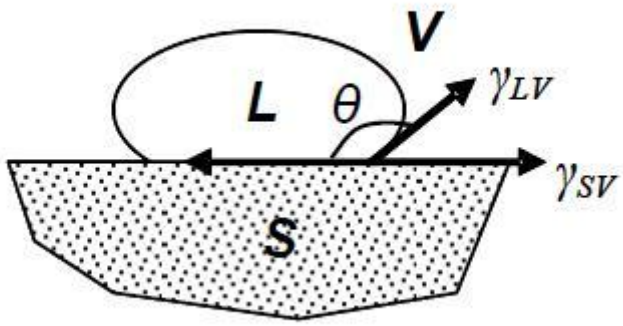

Figure 2.22. Surface energy balance for a liquid droplet on its solid [106].

There are three main methods which can improve the wettability of ceramic by molten metal which can be listed as:

I. *Addition of alloying elements:* For example, the addition of magnesium, calcium, titanium, silicon, nickel or zirconium to the melt may improve wetting by creating new carbide and boride phases and reducing the surface tension of the melt, decreasing the solid–liquid interfacial energy of the melt or aiding wettability by chemical reaction. For a given liquid metal, transition metal carbides, borides and nitrides are better wetted than covalently and ionically bonded ceramics and the tendency for a ceramic to wet decreases as its heat of formation becomes more negative. Titanium is one of the reactive metals used in Al-B_4C systems in order to increase the

wettability.

Probable reactions in aluminium-titanium-boron carbide systems which are all thermodynamically possible ($\Delta G<0$) and exothermic ($\Delta H<0$) are as follows:

$$\frac{10}{13}Al + \frac{3}{13}B_4C \rightarrow \frac{6}{13}AlB_2 + \frac{1}{13}Al_4C_3 \quad (2.18)$$

$$\frac{3}{4}Al + \frac{1}{4}Ti \rightarrow \frac{1}{4}TiAl_3 \quad (2.19)$$

$$\frac{10}{13}Al + \frac{3}{13}B_4C \rightarrow \frac{6}{13}AlB_2 + \frac{1}{13}Al_4C_3 \quad (2.20)$$

$$\frac{3}{4}Ti + \frac{1}{4}B_4C \rightarrow \frac{1}{2}TiB_2 + \frac{1}{4}TiC \quad (2.21)$$

$$\frac{1}{4}Al_4C_3 + \frac{3}{4}Ti \rightarrow \frac{3}{4}TiC + Al \quad (2.22)$$

In some studies, researchers have used K_2TiF_6 flux in order to put titanium into system and received good results in terms of wettability. [16, 93, 107]. If other metals are added for reaction, fluxes like Na_3AlF_6 can be used [108].

II. *Treatment of the ceramic particles:* Heat treatment of particulates prior to dispersion in the melt helps their transmission by removing adsorbed gases from the particle surface.

III. *Coating of the ceramic particles:* Wetting could be promoted by coating the particles with a wettable metal. This is because the liquid metals almost always wet solid metals, and wettability is highest in the case of mutual solubility or formation of inter-metallic compounds [93, 109, 110].

Based on the literature, normally the volume fraction of used boron carbide particles hardly exceed 15 %, but in some works 20 % of boron carbide reinforcement have been used too. The main reason is wettability of boron carbide particles by aluminium melt is very low especially in temperatures below 1100 °C. Other challenges could be

homogenous distribution of particles and preventing porosities. In liquid phase manufacturing of particulate reinforced AMCs and specifically in stir casting, the most successful method is creating vortex in the time of mixing but this can lead to large amount of porosities if it is done in absence of inert gas. It is reported that with increase in the amount of particles and decrease in their sizes, the amount of porosity is increased. [65]

In the case of boron nitride wettability, very limited works have been done in the literature but the clear thing is wettability of BN by molten aluminium is still very challenging. Based on the literature potential reaction in solid/liquid phase of boron nitride ceramics and aluminium molten metal is initially:

$$BN_{(S)} + Al_{(L)} \rightarrow AlN_{(S)} + B_{(in\ Al)} \quad (2.23)$$

Then reactions follow by:

$$BN_{(S)} + Al_{(L)} \rightarrow AlN_{(S)} + B_{(in\ Al)} + \alpha AlB_{12\ (S)} (> 1258K) \quad (2.24)$$

$$BN_{(S)} + Al_{(L)} \rightarrow AlN_{(S)} + B_{(in\ Al)} + AlB_{2\ (S)} (< 1258K) \quad (2.25)$$

Two kinds of boron compounds were detected in the aluminium of a 1373 K drop cycle as, a rectangular shaped compound and a round-shaped compound. $\alpha AlB_{12\ (S)}$ must have been produced at 1373 K during the experiments. Also, $AlB_{2\ (S)}$ can be produced in the sample during cooling after the experiments. It is considered that the round shape, which has a stronger peak of boron, is $\alpha AlB_{12\ (S)}$ and the rectangular one, which has a weaker peak of boron, is $AlB_{2\ (S)}$. The original contact angle between the boron nitride and the aluminium (phase II) is about 132 ° and it is known that B, $\alpha AlB_{12\ (S)}$ and $AlB_{2\ (S)}$ do not affect the wetting very much. Therefore, it is considered that the production of A1N at the interface causes the contact angle to decrease to 0 °. In order to measure the change in the contact angle between hexagonal boron nitride (h-BN) and aluminium over time, an improved sessile drop technique was devised in the literature, to prevent the oxidation of aluminium. Finally it was confirmed that above a certain temperature the contact angle of A1 on BN also progresses through the following four phases, on a logarithmic time scale:

i. Original wetting phase: in 0-5 seconds of process and contact angle of 180 °.
ii. Quasi-equilibrium phase: The original contact angle (the contact angle between non-reacted BN and aluminium) is about 143°, 135° and 132° at 1173, 1273 and 1373 K respectively.
iii. Interfacial-reaction-wetting phase: It was observed at and above 1173 K, while phase IV was observed at and above 1273 K.
iv. Equilibrium phase: The equilibrium contact angle is 0°. This value is much lower than those of typical ceramics. This value means that BN is an optimum material for use as an aluminium matrix composite material from the standpoint of wetting.

In a comprehensive study named "Interfacial reaction wetting in the boron nitride/molten aluminium system", Fuji *et al.* studied wettability of BN in aluminium melt. The degree of decrease in the contact angle depends on the initial quantity of oxide film on the aluminium. Thermodynamics considerations have indicated that the conditions for the reduction are easily achieved when the initial oxide film on aluminium surface is partially removed. When the oxidation of the aluminium is prevented, the contact angle becomes 0° [111]. In another study by Chen *et al.* [112], they stated that due to the high relative density, significant grain refinement and the presence of reasonably distributed hard particulates (nano-Al_2O_3) and intermetallic phases (Al_2Cu) in the matrix, the h-BN/Al–Cu composite with the 2μm Al powder by the semi-solid powder forging showed the best mechanical performance, including the Brinell hardness, compressive strength and fracture strain. Also they have found out that the hardness of the composite was increased by 17 %, 12.6 % and 14.3 % with d=35, 12 and 2μm Al powder, respectively, due to the addition of the h-BN powder particles.

3. MATERIALS AND METHODS

3.1. Materials Applied in the Experiment

As the matrix material, commercial pure aluminium has been used, which was provided by Şahinler Metal Co.. Chemical analysis of the matrix material is shown in the Table 3.1 and initial shape of it can be seen in Figure 3.1. Reinforcement materials used in the AMC are B_4C particles (black color) with size of 65 μm and BN particles (white color) with size of 5 μm. Also in order to increase the wettability of the reinforcement material with the molten aluminium, flux of potassium fluorotitanate (K_2TiF_6) has been applied with size of 75 μm (Table 3.2). Reinforcement materials and the flux material are shown in Figure 3.2 registered by an optical microscope with different magnifications. Also in order to ball mill the particulates with the flux, distilled water has been employed.

Table 3.1. Chemical analysis of matrix material (commercial pure aluminium)

Commercial Name	**Si**	**Fe**	**Mn**	**Mg**	**Cu**	**Ti**	**Zn**	**Cr**
A7EC INGOTS	0.1	0.176	0.002	0.001	0.00043	0.001	0.004	0.0005
	Sn	**Na**	**V**	**B**	**Ga**	**Ni**	**Bi**	**Al**
	0.0005	0.00039	0.003	0.004	0.01	0.001	0.0005	99.7

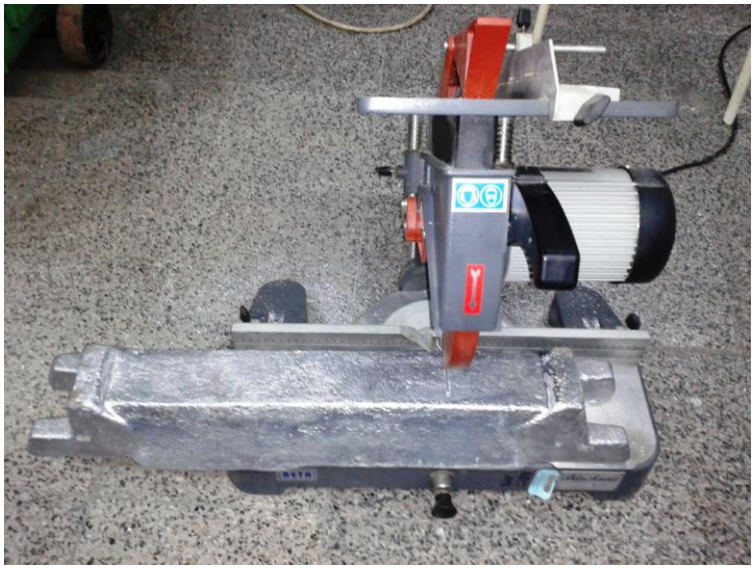

Figure 3.1. Pure aluminium ingot as the matrix material.

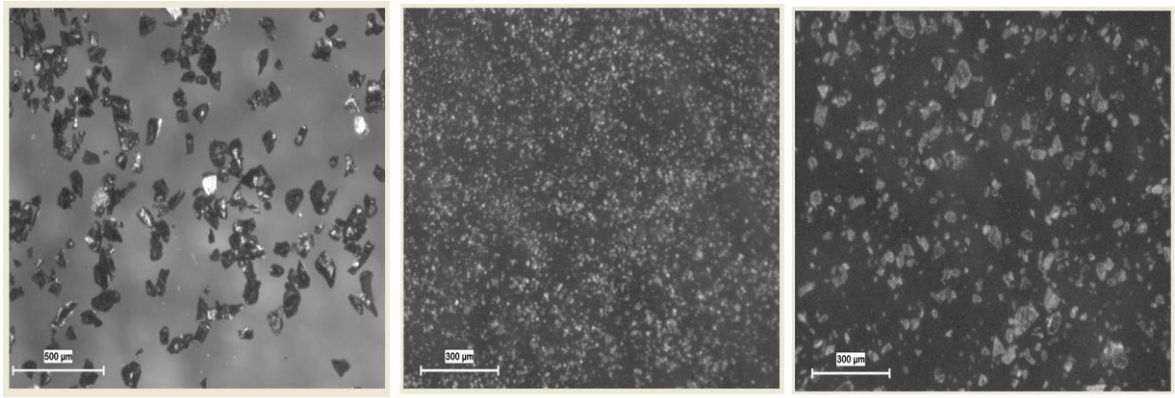

Figure 3.2. Boron carbide particles (a), boron nitride particles (b) and potassium fluorotitanate used in this work.

Table 3.2. Chemical analysis and density value of the flux

Material Name	**Cl**	**SO_4**	**H_2O**	**Mg**	**Pb**	**SiO_2**	**Fe**	**Ca**	**K2TiF6**	**Density (g/cm^3)**
Potassium fluorotitanate	0.05	0.01	0.05	0.001	0.01	0.2	0.02	0.01	=>98	3.01

3.2. Flowchart of Experiments

The experimental study has been done in two phases (each in "a" and "b" sections) which are summarized in and the phases of the experiment are illustrated in the flowcharts in Figure 3.3 and Figure 3.4. As it is concluded in Table 3.3, firstly pure aluminium is cast into squeeze cast die and pressurized under 0 (gravity), 75 and 150 MPa in which 7 samples are produced related to each value of squeezing pressure (total of 21 samples). Then Al-B_4C composites with 3 different volume fractions of boron carbide particles reinforcement (3 %, 5 % and 10 %) have been fabricated and again squeezed under 0, 75 and 150 MPa pressure to give out another total number of 63 samples. At the end, hybrid aluminium matrix composites of Al-B_4C-BN have been manufactured with constant volume fraction of B_4C (5 %) and three different volume fractions of BN (3 %, 5 % and 10 %) and went under one single pressure value of 75 MPa, to give out 21 samples.

As it is obvious in Figure 3.3 and Figure 3.4, in the first phase the aim was manufacturing Al-B_4C composites, pressurizing the products and evaluating the as cast specimens. Firstly in the phase 1-a, pre-process has been done on the particulate reinforcement materials, where B_4C particles were mixed with K_2TiF_6 and ball milled in presence of distilled water. This will aid to create the reaction phases of TiC and TiB_2 which greatly improve the wettability during AMC manufacturing. Then the reinforcement is added to the molten aluminium in the oven called "AMC oven" and stirred. The product of phase 1-a was an ingot called "master ingot 10 % B_4C-Al". In the phase 1-b, required amount of master ingot 10 % B_4C-Al is taken based on percentages indicated in Table 3.3. This amount of AMC is then added to needed amount of pure aluminium in the oven called "squeeze cast oven". Then the molten AMC is stirred manually and pressurized into the die. At the end evaluation of mechanical and physical properties of the as cast material is done.

In the second phase the aim was firstly manufacturing Al-BN composites, add it to Al-B_4C composites to make hybrid Al-B_4C-BN composites, pressurizing the product and evaluation. Firstly in the phase 2a, the BN reinforcement was added to the molten aluminium in the oven called "AMC oven" and stirred at high temperature. The product of phase 2a were ingots called "master ingot 10 % BN-Al". In the phase 2b, required amount

of master ingot 10 % B_4C-Al and master ingot 10 % BN-Al is taken based on the amounts indicated in Table 3.3. These amounts of AMCs are then added to the required amount of pure aluminium in squeeze cast oven. Then the molten AMC is stirred manually and pressurized in the die. At the end again the evaluation of mechanical and physical properties of the as cast material is done.

Table 3.3. Summarized phases of manufacturing Al-B_4C composites, Al-B_4C-BN hybrid composites and then squeeze casting and implemented tests.

Composition	Pressure (Mpa)	No of Samples	Tests on Samples
Al (control)	0	7	5 Samples for evaluating machinability and examining strength"
	75	7	
	150	7	
Al-3 % B_4C	0	7	
	75	7	
	150	7	
Al-5 % B_4C	0	7	2 Samples for studying microstructure and hardness"
	75	7	
	150	7	
Al-5 % B_4C	0	7	
	75	7	
	150	7	
Al- 5 % B_4C- 3 % BN	75	7	7 Samples to examine density change
Al- 5 % B_4C- 5 % BN	75	7	
Al- 5 % B_4C- 10 % BN	75	7	

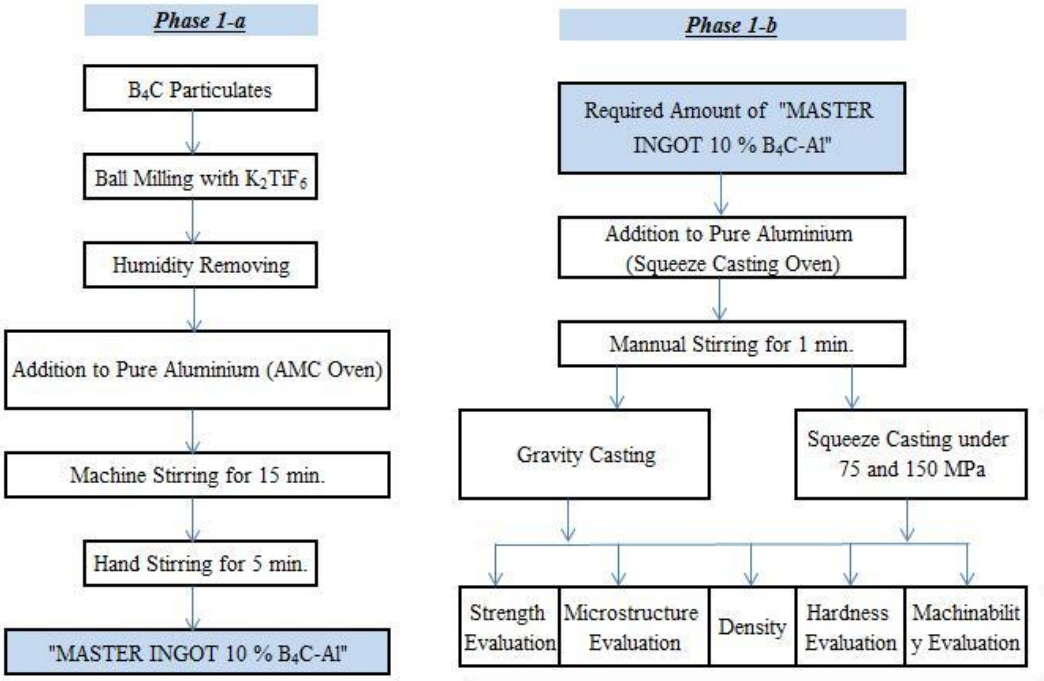

Figure 3.3. Flowchart of phase 1a and b.

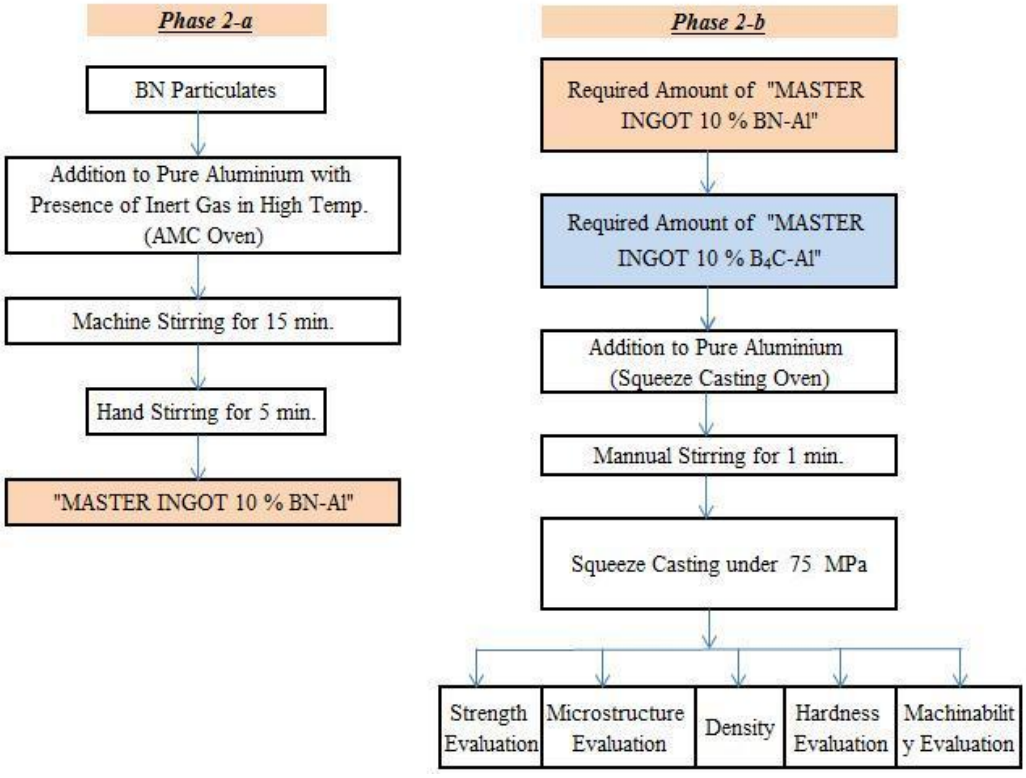

Figure 3.4. Flowchart of phase 2a and b.

3.3. Materials Preparation

3.3.1. Aluminium Preparation

In this step, aluminium ingot is cut into small pieces with different weighs so that the exact required amount aluminium can be taken where needed in the process . Then the aluminium pieces are weighed on the digital scale and put into separate plastic bags to be used later on.

3.3.2. Mixing Reinforcement Particulates with the Flux

In some future stages of the process there would be a need for boron carbide particles enriched and mixed with K_2TiF_6 flux in order to improve the wettability. With the intention of homogenous mixture of the flux and the reinforcement, these two powders were weighed on a digital scale and mixed in equal volume fractions with distilled water and then ball milled for 7 hours using 10 mm alumina balls in a ball milling machine with speed of 85 rpm. Resulting wet powders were put into an oven with the temperature of 110 °C for 2 hours in order to dry them. It was observed that after complete drying of the powders, some parts stacked to each other and formed clod shaped bulks. These parts have been removed and carefully grinded in the manual ceramic mortar to have the bulks in powder form. Also it was observed that in some sections grey mass stuck to the glass plates containing powders. It is likely that there is some free potassium in the K_2TiF_6 flux and since the melting temperature of potassium is around 63 °C, it has been melted and stuck to the glass plate walls.

3.3.3. Melt Stirring Set-up Preparation

Since casting is a process of high temperature, some safety measures should be taken into account such as using safety casting gloves and clothes, wearing masks and also careful and ordered implementation of works so that every single risk can be predicted.

A casting setup used in order to manufacture the master ingots which is called AMC setup. The AMC oven and the whole related setup have been demonstrated in Figure 3.5.

In this figure as it is seen, a vertical induction oven and a stirring machine have been used. The process has been done in presence of inert gas and vacuum pump to prevent oxidation as much as possible, although the effectiveness was not perfect.

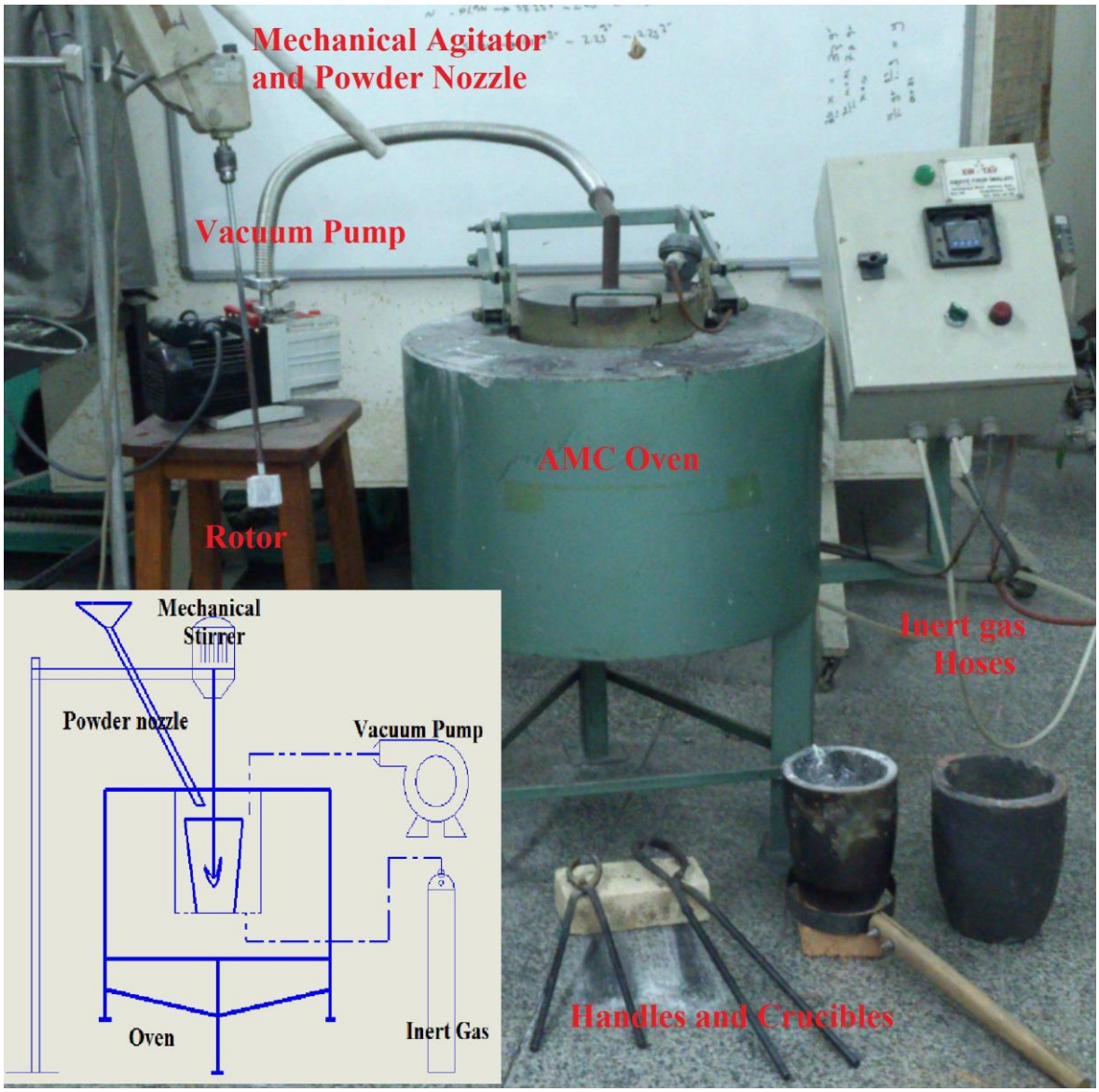

Figure 3.5. Master ingot preparation setup called "AMC set up" in this work.

3.3.4. Experimental Methods of Manufacturing Metal Matrix Composites

Based on Table 3.3 initially the amount of material used in the phase 1-a should be calculated. For this reason the volume and weight of final samples which will be manufactured after squeeze casting should be known. From Figure 3.10 and considering the volume of die cavity (~16265 mm^3), the prepared melt for each sample of squeeze

casting can be calculated as 45 gr (in case of pure aluminium). Considering Table 3.4, required amount of pure aluminium and related boron carbide particles ball milled with potassium fluorotitanate (K_2TiF_6) were weighed on a 600 gr x 0.01 gr digital scale. In order to stand on the safe side, 40% more of each material was applied. The aluminium is melted in the crucible in the AMC oven. When the temperature reached to 850 °C, the flux-enriched-reinforcement material was added manually in a constant rate, as much as possible. At the same time mechanical stirrer is turned on with 250 rpm rotation speed. A stainless steel shaft has been used armed with a graphite rotor manufactured in the MSLAB (Materials Science and Manufacturing Laboratory of Boğaziçi University). Different sizes and mixing angles of graphite rotors have been tried in order to choose the most effective one. It should be considered that all the devices in contact with the melt should be preheated prior to the process. In this stage, rotors, ladles and skimmers are coated with graphite and preheated up to 280 °C in order to prevent shocks in the melt. This should be mentioned that unlike the vortex method in which a vortex is needed to improve the mixing, in this process due to the weak vacuum and isolation situation, a vortex will result in a fully oxidized molten metal. Therefore the method in this work is mixing the metal under the oxide layer without breaking it. The particles are vigorously agitated mechanically for 15 min. to activate the interfaces between the melt and particles, and hence to form a uniform mixed slurry.

After mechanical stirring, it is expected that the melt temperature is decreased about 90 °C. So the oxide layer is removed and again the temperature is increased to mixing temperature. At that point a manual stirring is done for 5 min. prior to casting. Manual stirring is done in the motions which brings up the particles close to the surface and left them and again repeat the flow. This mixing should be vigorous enough to make effective movement under the melt but not so vigorous to break the oxide layer.

At the end, the slurry matrix composite is cast into rectangular and cylindrical graphite dies to produce the master ingot 10 % B_4C-Al. It is valuable to say that initial intention in this work was to manufacture aluminium matrix composites with higher volume fraction of B_4C contents but as the manufacturing started it was observed that reinforcing with more than 10 % B_4C with present facilities are not practically feasible. It was experienced that in the attempts for more than 10 % of boron carbide, fraction of

powders are rejected by the melt due to the low wettability and also high viscosity caused the casting process problematic.

The same method was used in manufacturing master ingot 10 % BN-Al with some variations. The temperature applied in this process was 950 °C which is chosen information given in the literature stating that the temperature can affect the wettability. But the main challenge was due the variation between density of BN powders and aluminium melt, appropriate dispersion of the particles in the matrix was difficult, so in some cases more time to stirring has been assigned.

Table 3.4. Mass fraction values calculation based on volume fraction of compositions.

Sample Code on Plastic Bags	Samples by Volume Fraction in Compositions	**Pressures (Mpa)**	**Volume per sample (mm3)**	**AL Mass per sample (gr)**	**B_4C Mass per sample (gr)**	**BN Mass per sample (gr)**	**K_2TiF_6 Mass per sample (gr)**
Al0	Al (Control)	0	16265	44	0.00	0.00	0.00
Al75		75	16265	44	0.00	0.00	0.00
Al150		150	16265	44	0.00	0.00	0.00
01-000	Al-3 % B_4C	0	16265	43	1.23	0.00	1.48
01-075		75	16265	43	1.23	0.00	1.48
01-150		150	16265	43	1.23	0.00	1.48
02-000	Al-5 % B_4C	0	16265	42	2.05	0.00	2.47
02-075		75	16265	42	2.05	0.00	2.47
02-150		150	16265	42	2.05	0.00	2.47
03-000	Al-10 % B_4C	0	16265	40	4.10	0.00	4.93
03-075		75	16265	40	4.10	0.00	4.93
03-150		150	16265	40	4.10	0.00	4.93
01-01-075	Al-5% B_4C-3% BN	75	16265	40	2.05	1.02	2.47
02-01-075	Al-5%B_4C-5% BN	75	16265	40	2.05	1.71	2.47
03-01-075	Al-5% B_4C-10% BN	75	16265	37	2.05	3.42	2.47
			Total:	621	197.97	43.04	238.36

Figure 3.6. Different rotors used in the stirring processes.

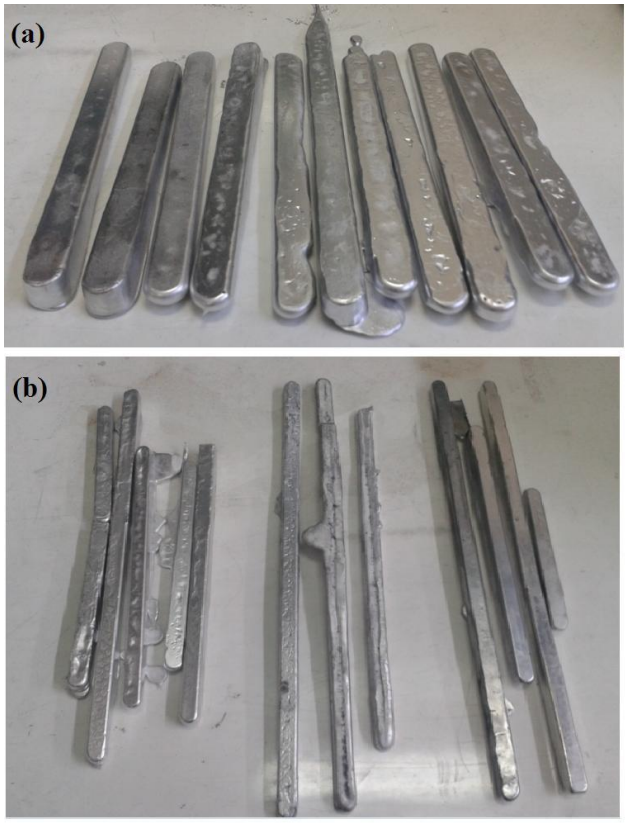

Figure 3.7. Samples of (a) Master ingot 10 % BN-Al (b) master ingot 10 % B_4C-Al.

3.3.5. Squeeze Casting Set up Preparation

Referring to Figure 3.3 and Figure 3.4, in the phase 1b and phase 2b, squeeze casting has been applied to the aluminium matrix composites and final samples were manufactured. In this section the melting and stirring was done in an induction oven with maximum temperature of 1200 °C which was very promising for specially hybrid AMCs containing boron nitride. In order to pressurize the cast composites a squeeze pump has been used. The hydraulic system's equipment are a hydraulic tank, a cylinder, pump motor, manual control lever, pressure regulator and indicator. Squeezing machine is produced by MAG San. ve Tic. A.Ş. (Turkey) and available in MSLAB of Boğaziçi University. The type of hydraulic cylinder is KHS-Ø100×200. The diameter and stroke of cylinder are 100 mm and 200 mm, respectively.

Figure 3.8. Squeeze casting machine.

Regarding squeeze casting machine some issues should be taken into account in order to have a safe and appropriate work:

i. Before operating the pump, all hose connections must be tightened with the proper tools.
ii. No poorly-balanced or off-center loads should be applied on the cylinder. The load can tip and cause personal injury. (This happened once and broke the die)
iii. Pump must be plugged into corresponding voltage power source. It was seen that when the ovens are working, voltage changes can damage the pump motor. Also it should be noted that the rotation direction of electromotor is chosen properly otherwise the pump won't push the oil.
iv. For adjusting the pressure regulating valve: The locknut on the pressure regulating valve should be loosen and with an allen wrench, the bolt can be adjusted counterclockwise a few turns. This will decrease the setting to a lower than desired pressure.
v. The oil level in the reservoir should be checked periodically.
vi. It is also very important not to stand in the same direction with die's bolts and nuts, because it was experienced that when the die was broke, nuts and bolts were shoot like bullets.

Two dies used in this study were; first one was a die used previously in a thesis in MSLAB [73] and the second one manufactured in exact sizes and specifications similar to the first one using DIN1040 steel. The images and technical drawings of the manufactured die and punch are provided in Figure 3.9, Figure 3.10 and Figure 3.11.

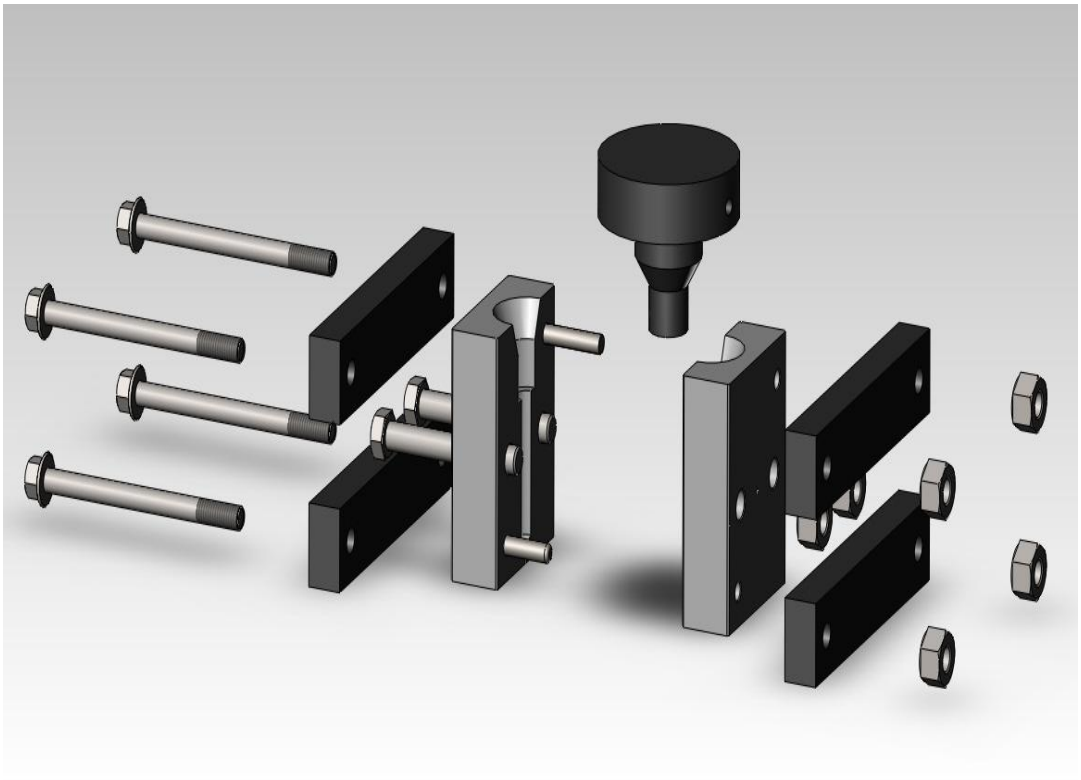

Figure 3.9. Exploded view of die and punch.

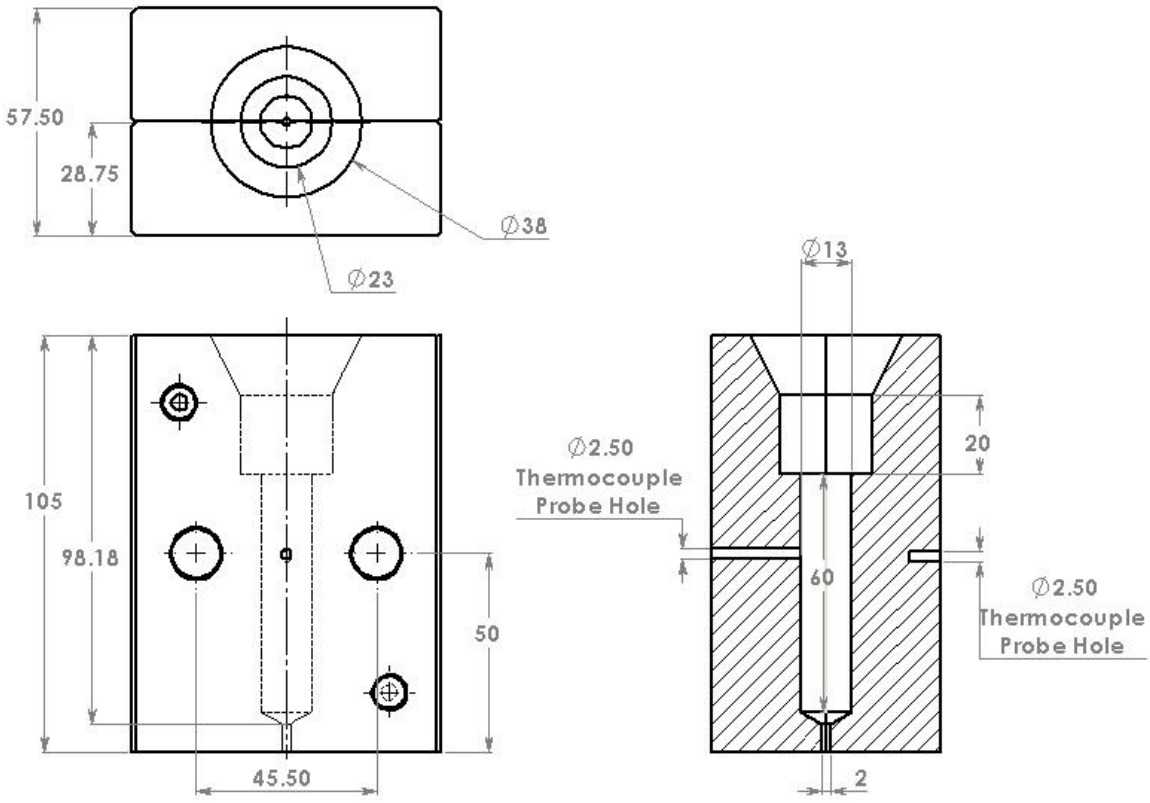

Figure 3.10. Drawing details of the die (units are mm).

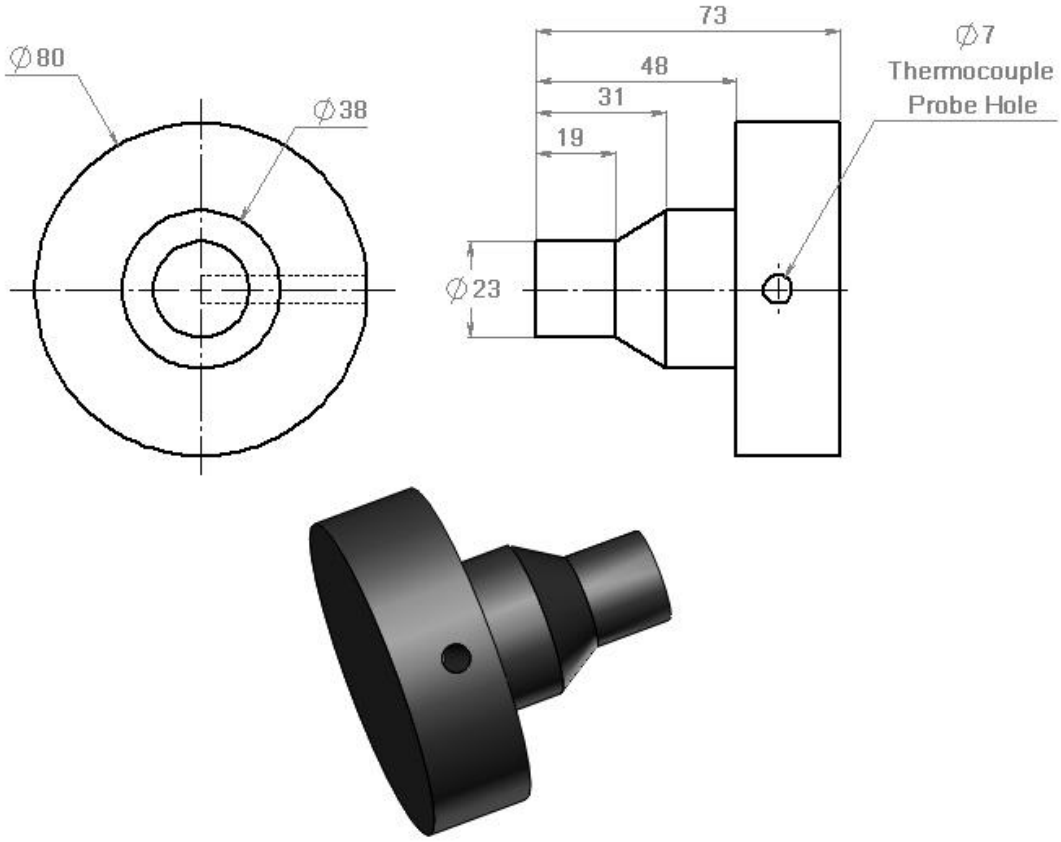

Figure 3.11. Drawing details of the punch (units are mm).

Figure 3.12. Manufactured die and punch.

The squeeze casting setup for pre-heating the tools and temperature controlling is shown in Figure 3.13. In addition to the K-type thermocouples in this figure which controls the temperature of die and punch for preheating and also in the time of molten metal pouring, another thermocouple (Lutron TM-906A) has been used in order to assess the temperature of melt in different steps of process. This dual portable thermometer is capable

of sensing from -50 °C to 1230 °C and an appropriate instrument to read the temperature of molten composite or tools.

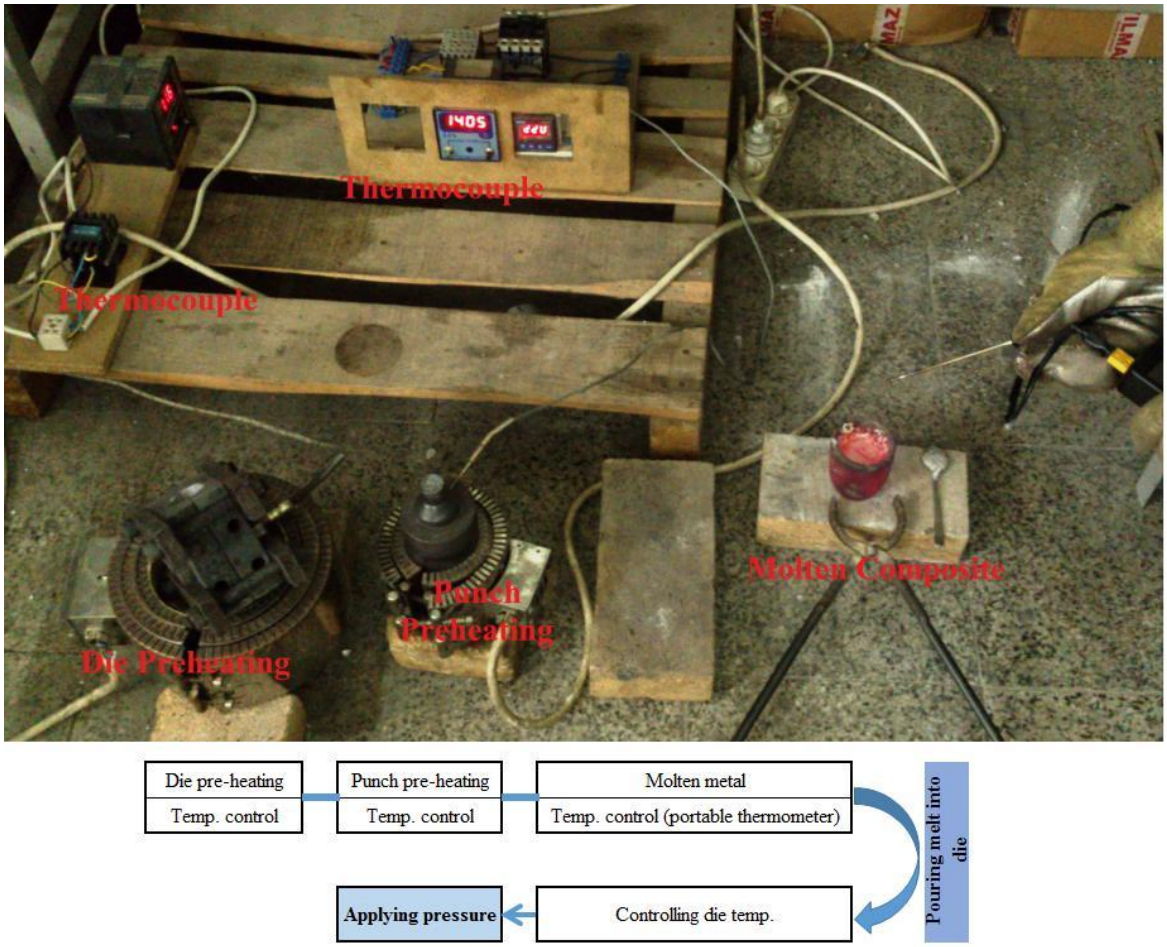

Figure 3.13. Setup for pre-heating the die and punch along with the temperature control in squeeze casting process.

3.3.6. Experimental Method of Squeeze Casting

In this section, firstly samples of pure aluminium for control has been manufactured with three different pressures. Then AMCs reinforced with boron carbide produced and finally hybrid aluminium matrix composites containing boron nitride and boron carbide have been manufactured.

For manufacturing aluminium control samples, required amount of aluminium pieces (45 gr for each sample) were taken and melted in the squeeze casting oven up to 850 °C. At the same time the die and the punch were preheated up to 350 °C simultaneously.

Then the die was put on the casting brick and when its temperature decreased to 300 °C, aluminium melt was taken out of furnace, the slag was removed and the molten metal was poured into the die (Figure 3.14). In case of gravity casting the die was remained in this situation until complete solidification. However in case of 75 and 150 MPa squeezed samples, the melt is poured into the die and waited and once the temperature decreased to 730 °C the pressure was applied (Figure 3.15). Duration of pressure holding was 60 seconds, due to the fact that in all of the test samples, complete solidification took place in a temperature below 50 seconds and therefore more time could not cause any further improvement. After pouring the molten aluminium into the die cavity the punch was put and fixed on it when its temperature was 280 °C. If the temperature of the punch was selected equal to that of die, it could cause extrusion of liquid metal through the tooling interface between die and punch and could also result in shrinkage porosity on top of samples.

It is good to mention that in order to calculate the number to be seen on the hydraulic indicator below equations was used considering that $D_{Cylinder}$ was equal to 100 mm, D_{Sample} was equal to 13 mm and aimed pressures were 75 and 150 MPa.

$$F_{Cylinder} = F_{Sample} \tag{3.1}$$

$$P_{Cylinder} \times A_{Cylinder} = P_{Sample} \times A_{Sample} \tag{3.2}$$

$$P_{Cylinder} \times \frac{\pi . D_{Cylinder}^2}{4} = P_{Sample} \times \frac{\pi . D_{Sample}^2}{4} \tag{3.3}$$

$$P_{Cylinder} = P_{Sample} \times (\frac{D_{Sample}}{D_{Cylinder}})^2 \tag{3.4}$$

Considering the above information, $P_{Cylinder}$ was calculated as 12.9 kg/cm^3 and 25.8 kg/cm^3 , convertible to sample pressures of 75 and 150 MPa, respectively.

Figure 3.14. Pouring melt into die.

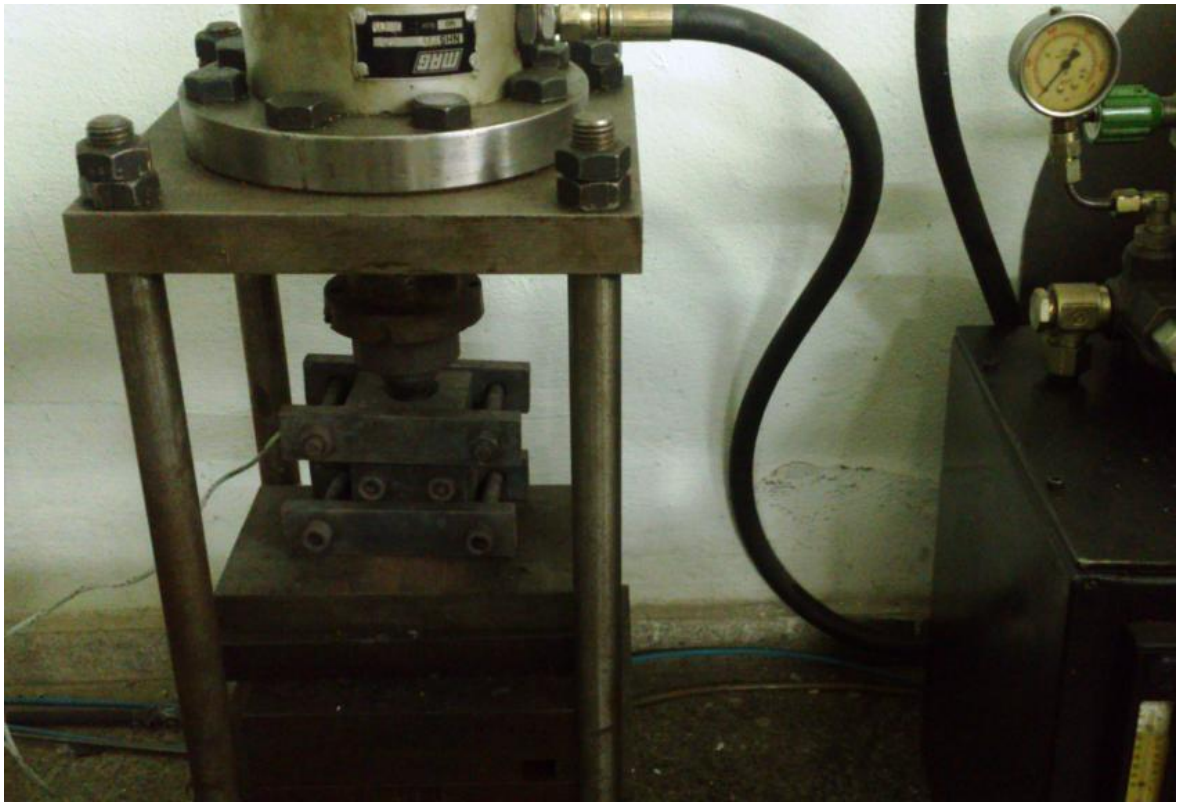

Figure 3.15. Pressure application under squeeze casting machine.

In the second step and for manufacturing Al-B_4C composites, required amount of master ingot 10 % B_4C-Al which was previously cut into pieces was taken and melted with

required amount of matrix material in order to give out the aimed volume fraction. In the production of 3 % B_4C-Al, 5 % B_4C-Al and 10 % B_4C-Al same procedure as control samples were implemented with some modifications. In this process, when the oven reached to a temperature of 850 °C, a manual stirring and mixing was done for 1 min. considering that the oxide layer of the melt should not be broken. It was seen that in 3 % B_4C-Al and 5 % B_4C-Al negligible sedimentation of ceramic reinforcements happens. Sedimentation for the 10 % B_4C-Al was more noticeable, but manual stirring was promising to overcome it. This improved wettability of boron carbide particles by the molten metal relied on the interface reactions which was created in the time of master ingot production as described in the literature review. After pouring the molten composite into the die cavity the punch was put and fixed on it when its temperature was 280 °C. After putting the die and punch under hydraulic press, and right after the molten metal's temperature decreased to defined value, again the lever is activated to pressurize the punch and consequently the molten composite.

It is valuable to mention that cutting master ingot 10 % B_4C-Al was not convenient with regular cutting tools and saws because of high hardness and abrasiveness of boron carbide particles in the composite. Therefore after breaking a number of tools and saws, a cutting machine with diamond cutting tool was applied which is demonstrated in Figure 3.17.

Figure 3.16. Master ingots cut into pieces to be used later in the phase 1-b and phase 2-b.

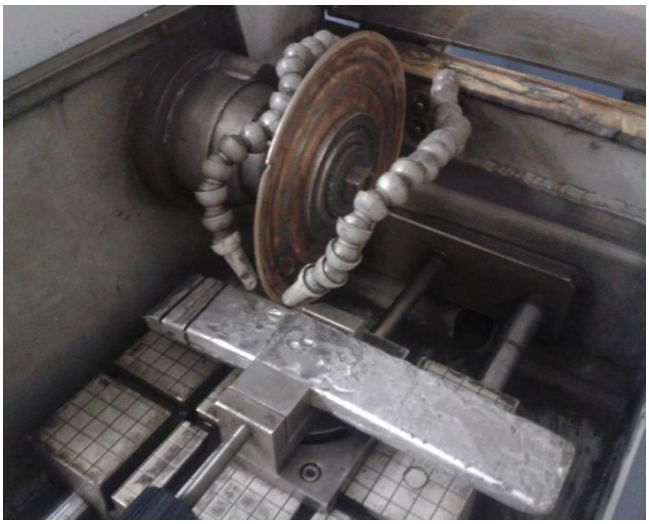

Figure 3.17. Cutting master ingot 10 % B_4C-Al with diamond cutting tool.

In the third step same process was utilized for manufacturing hybrid B_4C-BN-Al composites. In this process again required amounts of master ingot 10 % BN-Al and master ingot 10 % B_4C-Al were selected and melted. At the first place, the same temperature of 850 °C was chosen but it was seen that BN particles were either depositing or coming above the oxide layer. So a higher temperature of 1200 °C was tried and as it was promised in the literature, this higher temperature helped for better wettability. The crucible was taken out of oven at 1200 °C and the content was mixed until the temperature

decreased to 850 °C and then the casting was implemented with constant pressure of 75 MPa.

At the end of squeeze casting processes every sample were taken out by loosening the bolts, though with proper lubrication of die prior to casting it was possible for non-pressurized samples to be taken out without opening the die. One important issue in this process was the amount of molten composite poured into the die cavity and the method of pouring. Samples in which the molten metal in the die cavity was less than 1/3 or more than 2/3 of the runner's depth, were rejected. Also in the time of pouring, it was very important to hold a constant rate of feeding and not pour directly into the sample cavity which was a cause for macro cavities in some samples. Another case to be taken into account was in the time of applying pressure where it was safer to firstly apply a small amount of pressure (close to zero) in order to make the punch's position perpendicular to the surface and prevent any damage to the die.

The result of this section was 105 pieces of samples one of which is shown in Figure 3.18. The samples afterwards went under mechanical, physical and microstructure evaluations which will be discussed in future sections.

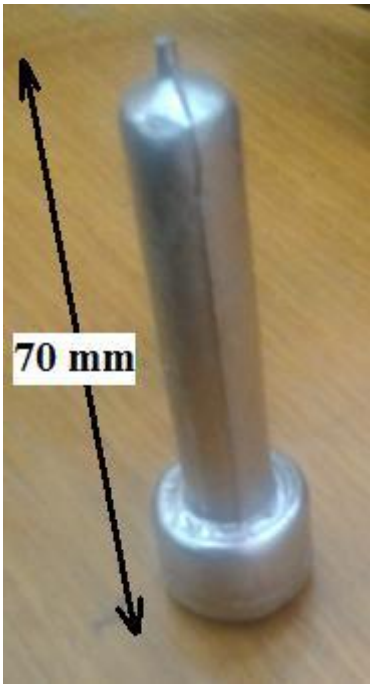

Figure 3.18. Final manufactured sample.

3.3.7. Machinability Testing

Good machinability is one of the factors persuades the industry for using a material. In order to see the effect of different reinforcement materials with different contents and also effect of squeeze casting on the machinability of composite materials a process was designed.

3.3.7.1. Chip length: Chip length is one of the main indicators of the machinability of the material. In this test firstly the headpiece of the samples were cut by normal hacksaw. Then the samples were mounted on a universal lathe machine with two different turning speed and constant axial movement speed.

Machining the samples containing boron carbide particles was very challenging. Firstly different turning and axial speed values were tested in order to find an appropriate range for machining B_4C containing samples. It was seen that low cutting speed rates caused too much of tool wearing (Figure 3.20) so the axial speed value was set on high rate to minimize the tool wear (Table 3.3). Also it was experienced that normal HSS (high speed steel) B DIN 4964 with 65 HRc was not promising for cutting B_4C contained samples and in every cycle (sample length), grinding the tool was needed so DNGA432-Sumitomo ceramic bits was tried. These cutting bits were again damaged after some cycles but they were capable of finalizing the machining process. Spindle turning speed value was chosen constant at 860 rpm while axial speed (feeding speed) was taken to be 0.7 mm/s and 2.68 mm/s.

First, all specimens went under a cleaning pass and then with 1 mm of feeding, the cutting was done in two halves with two different feeding speeds. The resulting samples up to this step are shown in Figure 3.21. For specimens of each category the chips were searched and with eye control, a group of longest chips were collected and among them 4 longest chips were taken and shown in Table 3.5.

3.3.7.2. Roughness Test: Moreover a roughness test was done for further evaluation of machinability of specimens. Since most of the failures start from a defect on the surface of materials, roughness test can be a reliable criterion to evaluate well-functioning of a material. For this test one specimen from each category was selected and went under roughness evaluation in a Dektak XT stylus profilometry machine in Boğaziçi University Kandilli Campus. The aim was to measure Ra value of each specimen which is the most used parameter indicating roughness of a surface. Ra measure gives a good description of height variations on a surface. This machine was armed with a smile size needle shape probe which moved along two specified regions on the samples (each 4 mm) and registered the graph of roughness and roughness parameters. The results of this test are shown in the Table 3.5.

Figure 3.19. Collected chips in the bags.

Figure 3.20. Tool wear (HSS) after one pass on a sample containing 5 % boron carbide.

Figure 3.21. Samples prepared for the density test.

3.3.8. Physical Testing

One of the main factors to be tested in order to evaluate the effect of squeeze casting on reducing porosities of the material is assessing the resulting samples' density. For this purpose, after implementing the machinability evaluation, all the samples brought into size of Ø10 × 60 mm (Figure 3.21). Then they were weighed on a 600 gr × 0.01 gr digital scale. The weight of each specimen were registered (Table 3.7). When all the samples were weighed, they were machined to prepare the samples for the tensile test.

3.3.9. Mechanical Testing

In order to evaluate the mechanical properties of aluminium matrix composites and hybrid AMCs, tensile test and hardness test were implemented on the samples.
For this reason, firstly as the last step of machining, the specimens were machined into shape demonstrated in Figure 3.22 based on ASTM E8 standard [113]. The machining was done by same tools but for shaping the radius section a fillet HSS tool with radius of 6 mm was used (Figure 3.23).

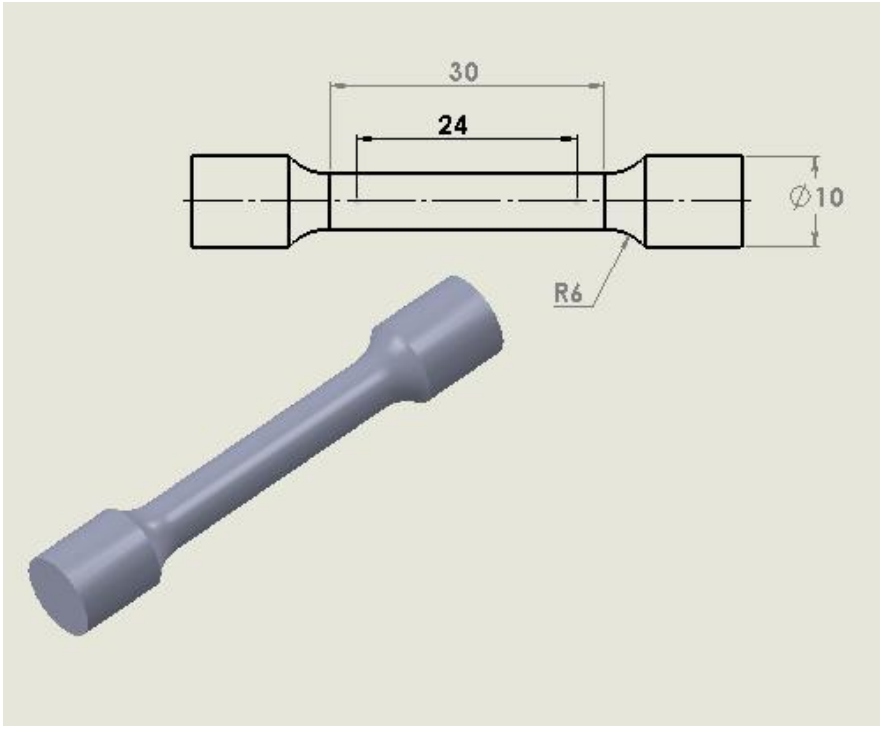

Figure 3.22. Technical drawing of tensile test sample (dimensions are in mm).

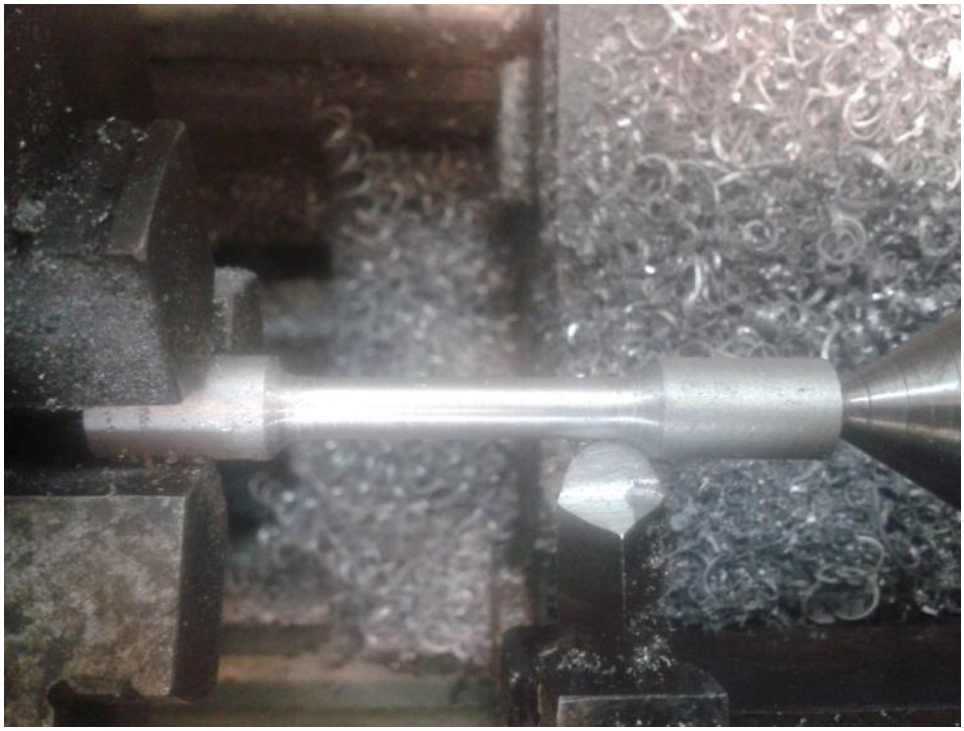

Figure 3.23. Machining of tensile specimen.

Tensile test is the most popular method for determination of the mechanical properties of a material. The process can be simplified as pulling a standard specimen between two jaws in an apparatus until the fracture happens. The result of this process is a stress-strain diagram or its equivalents which can give out values for ultimate tensile strength, yield strength, elongation, reduction of the area and ductility.

The ultimate tensile strength (tensile strength) is the maximum engineering stress level approached in a tension test. Actually the strength of a material is its capacity to endure external forces without fracture. In brittle materials, the UTS will be seen at the end of the linear-elastic section of the stress-strain curve or close to the elastic limit. In ductile materials, the UTS will be far from the elastic section and in the plastic portion of the stress-strain curve. The ductility of a material shows how the material will behave in deformation before fracture. The straight measures of ductility are the engineering strain at fracture (called the elongation) and the reduction of area at fracture. The yield strength (YS) is the stress required to produce a small amount of plastic deformation. The yield strength obtained by an offset method is usually used for engineering purposes because it avoids the practical difficulties of measuring the elastic limit or proportional limit. Also the slope of the line in this region where stress is proportional to strain and is called the

modulus of elasticity or Young's modulus. The modulus of elasticity (E) defines the properties of a material as it experiences stress, deforms, and then returns to its original shape after the stress is removed. It is a quantity of the stiffness of a given material.

In this test 5 pieces of specimen in each category were subjected to the tensile test on a Zwick/Roell Z010 machine with 10 KN load cell (Figure 3.24). The results of this test will be explained in upcoming sections.

Figure 3.24. Tensile testing machine.

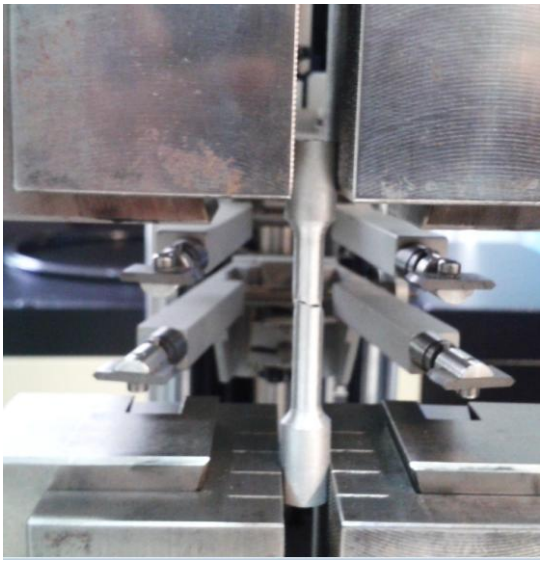

Figure 3.25. The specimen fractured under tensile test.

For the hardness test, pieces from one sample in each category were cut and tested in three different points for each sample. The Brinell hardness test method was used for this section which consists of indenting the test material with a 2.5 mm diameter hardened steel under load of 187.5 Kgf. The full load was applied for 10 seconds. The Brinell hardness number is calculated by dividing the load applied by the surface area of the indentation. Compared to the other hardness test methods, the Brinell ball makes the deepest and widest indentation, so the test averages the hardness over a wider amount of material, which will more accurately account for multiple grain structures and any irregularities in the uniformity of the material.

With hardness test it can be evaluated how the material tolerates the plastic deformation. Generally for hardness test, an indenter is forced into the material's surface which is in shapes of ball, cone or pyramid and its material should be chosen with harder value compared to the material to be tested. Since hardness depends on behavior of material when subjected to plastic deformation, there is a relation between hardness and strength of the material.

In the Brinell hardness test, a ball shape indenter is used with specified diameter of ball and specific force. In case of soft materials the force is reduced to 500 kg in order to prevent large effect of indenter on depth of created hole. In case of hard materials, a ball

with tungsten carbide is used to prevent distortion of the intender. Brinell hardness number (BHN) (kg/mm^2) can be explained with below equation:

$$BHN = \frac{P}{(\pi\frac{D}{2})(D-\sqrt{D^2+d^2})} = \frac{P}{\pi D t} \quad (3.5)$$

In which P (kg) is the force, D (mm) is diameter of ball, d (mm) is the diameter of the hole and t (mm) is the depth of the hole.

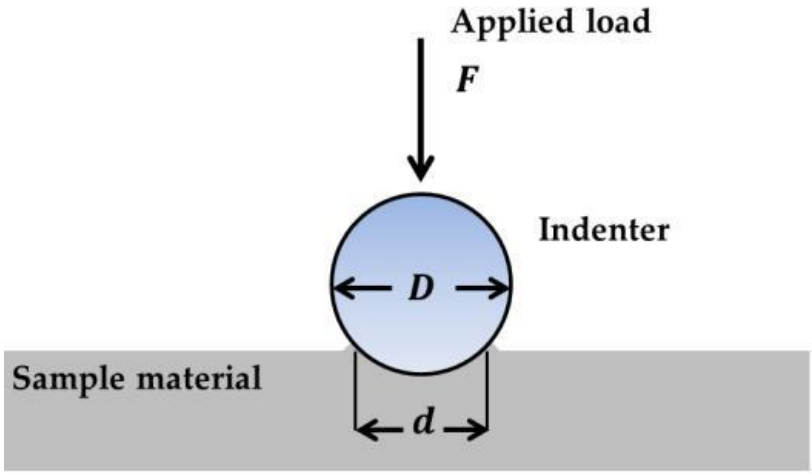

Figure 3.26. Schematic of Brinell testing method.

3.3.10. Microstructural Testing

In the microstructure evaluation the aim is to see if the K_2TiF_6 flux addition was detectable and effective in the structure, to evaluate the effect of pressure and particle addition on the microstructure and also examine if the particle distribution has been done homogenously.

Samples firstly were cut, mounted in bakelite and then polished, observed under an optical microscope (Figure 3.28) with different magnifications (Clemex LV 150) and then examined in Philips XL30 (Figure 3.29) environmental scanning electron microscope (ESEM). Then again samples were etched (Figure 3.27) in Marble's reagent (10 gr $CuSO_4$, 50 ml HCl and 50 ml distilled water) and tested in optical microscope to detect the change in phases and grain sizes.

Figure 3.27. Samples ready for microstructure tests.

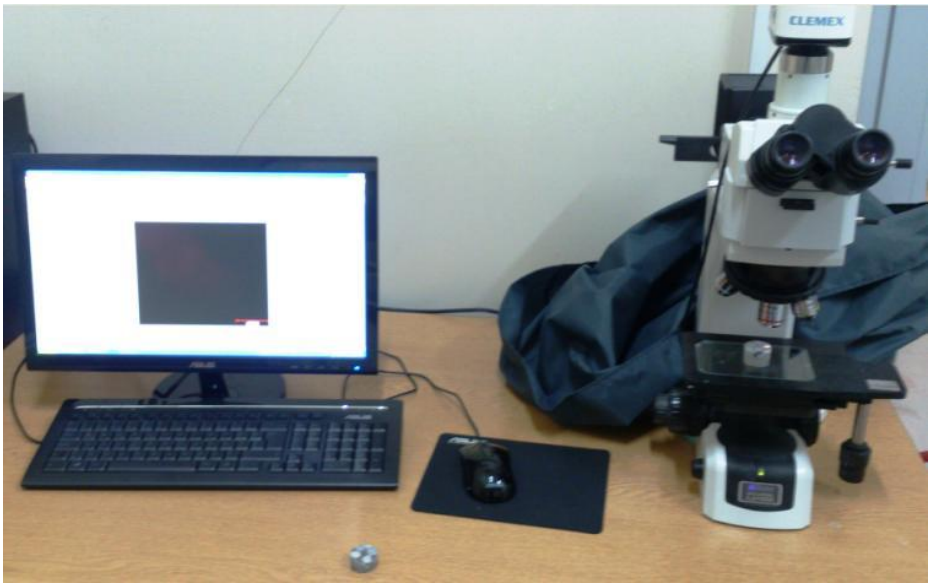

Figure 3.28. Optical microscope with different magnifications.

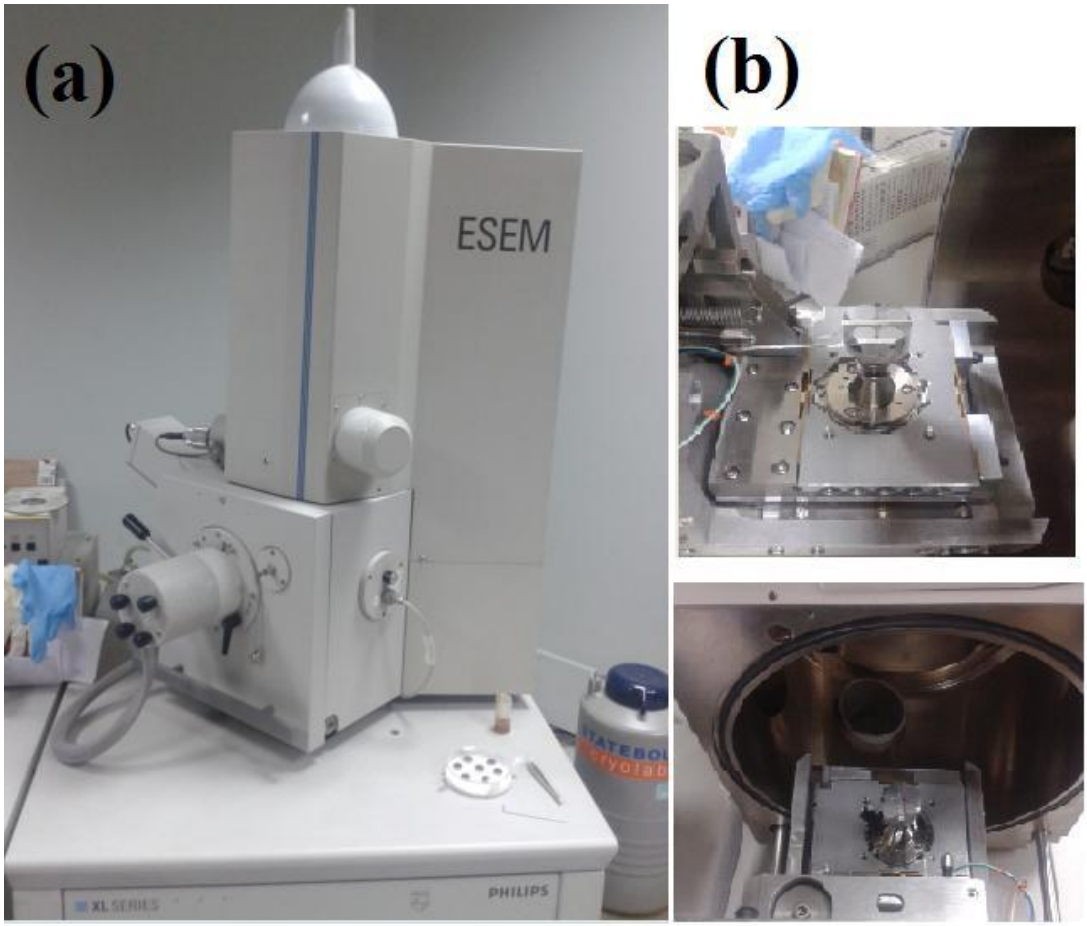

Figure 3.29. (a) Scanning electron microscope and (b) mounting samples in SEM.

3.4. RESULTS AND DISCUSSION

3.4.1. Machinability Evaluation Results

As discussed before the machinability test has been implemented with two indicators.

3.4.1.1. Chip length evaluation results: The length of 4 longest chips of each category can be seen in Table 3.5. The average of each four values is calculated in the table too.

Table 3.5. Chip length values of different sample categories

Specimen Name	Pressure (MPa)	Four Longest Chips (mm)				Average Length (mm)	Standard Deviation
Al Test	0	306	252	195	180	233.25	57.5
Al Test	75	326	284	168	165	235.75	81.7
Al Test	150	281	202	141	127	187.75	70.1
Al-3 % B_4C	0	103	71	52	41	66.75	27.1
Al-3 % B_4C	75	85	72	48	37	60.5	21.9
Al-3 % B_4C	150	89	75	68	32	66	24.2
Al-5 % B_4C	0	61	33	32	28	38.5	15.1
Al-5 % B_4C	75	70	25	20	13	32	25.8
Al-5 % B_4C	150	44	32	27	10	28.25	14.1
Al-10 % B_4C	0	11	8	7	5	7.75	2.5
Al-10 % B_4C	75	10	10	6	6	8	2.3
Al-10 % B_4C	150	6	4	3	3	4	1.4
Al-5 % B_4C-3 % BN	75	83	73	70	39	66.25	18.9
Al-5 % B_4C-5 % BN	75	92	90	81	57	80	16
Al-5 % B_4C-10 % BN	75	164	143	111	95	128.25	31

From Figure 3.30, it is seen that with increasing the amount of boron carbide particles in the aluminium matrix composite, there is an obvious deterioration in the chip

length and consequently the machinability. It is natural due to the presence of abrasive B_4C particles, although some of the literature works reported completely different. At the time of machining it was observed that chips were flowing but once the cutting tool confronted the ceramic particles, the chip was cut and hardly any continuous chip was created. It is also seen that effect of pressure on the chip length in the samples containing reinforcement particulates was negligible but in general with increasing the squeezing pressure, the chip length decreased. This behavior is highlighted in pure aluminium where there is approximately 20 % decrease in the chip length by increasing pressure from gravity to 150 MPa, although there is a slight increase in chip length from zero to 75 MPa of pressure. It can be explained that applied pressure makes the material tougher and this makes the machinability more difficult. For proving this we should control hardness and tensile strength of squeeze cast products in future chapters.

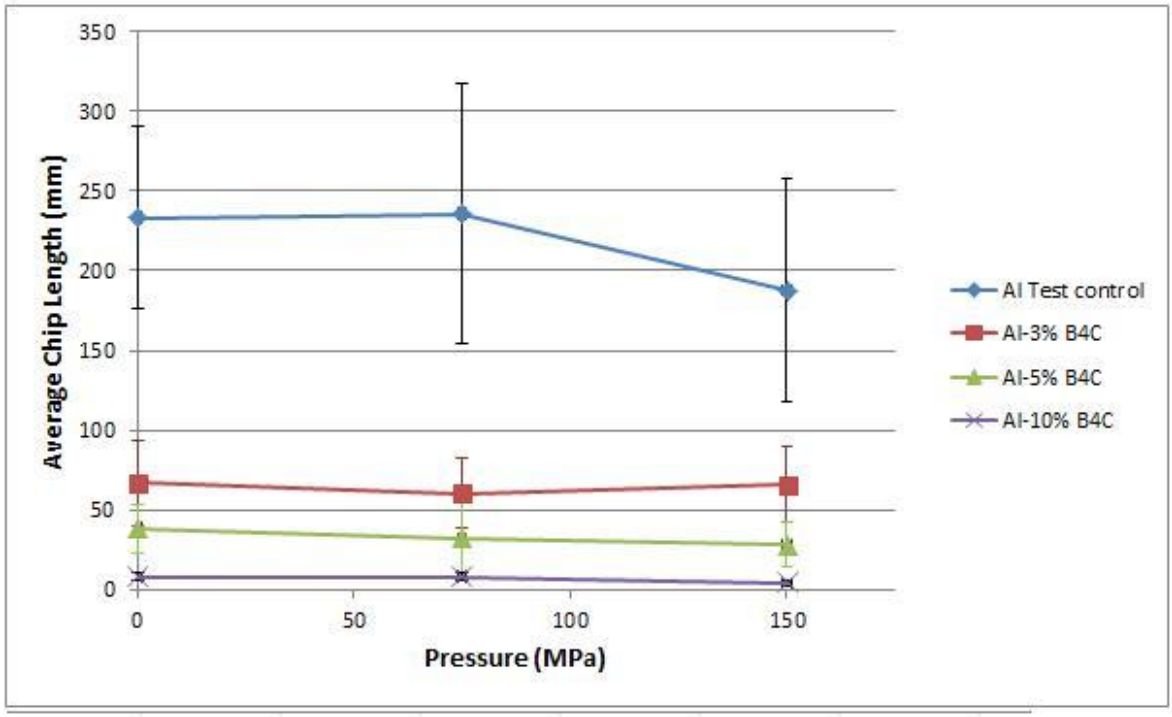

Figure 3.30. Average chip length for different B_4C contents and pressure values.

Regarding addition of BN particles into the AMC and increasing its contents, it can be concluded from Figure 3.31, that there would be a major improvement in machinability by increasing BN particles amount. Boron nitride acts as a solid lubricating agent and lowers the friction coefficient. This is the main reason for improvement of chip length values by adding BN particles in hybrid aluminium matrix of Al-B_4C-BN.

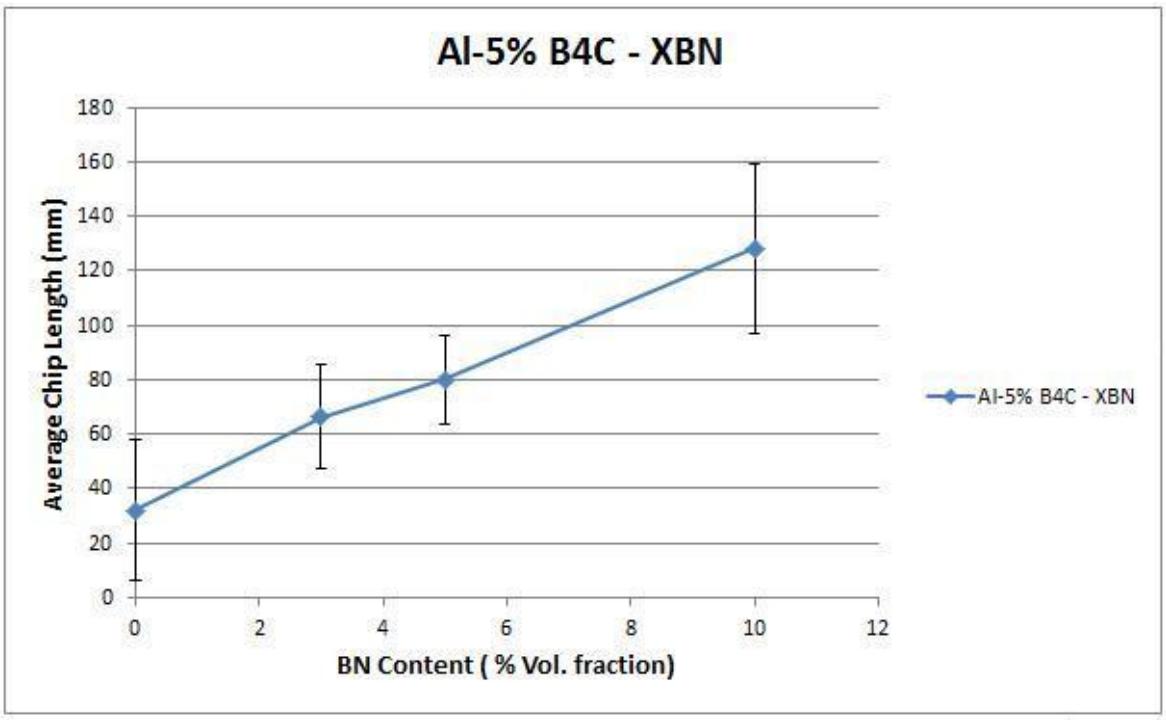

Figure 3.31. Average chip length for different BN contents.

3.4.1.2. Roughness evaluation results. As mentioned before, the roughness of one sample for each category was examined and the results concluded in Table 3.6 for different cutting speeds.

Table 3.6. Roughness (Ra) variations for different materials tested

Specimen Name	**Pressure (MPa)**	**Surface Roughness Values For Different Cutting Speeds (Ra (μ))**	
		0.7 (mm/s)	**2.68 (mm/s)**
Al Test	0	1.8	2.2
Al Test	75	1.6	1.9
Al Test	150	1.5	2.1
Al-3 % B_4C	0	3.8	3.5
Al-3 % B_4C	75	4.1	3.7
Al-3 % B_4C	150	3.9	3.4
Al-5 % B_4C	0	4.6	3.4
Al-5 % B_4C	75	4.2	3.2
Al-5 % B_4C	150	5.1	3.6
Al-10 % B_4C	0	5.6	5.7
Al-10 % B_4C	75	5.9	5.2
Al-10 % B_4C	150	5.4	4.9
Al-5 % B_4C-3 % BN	75	3.2	3.6
Al-5 % B_4C-5 % BN	75	4.6	2.9
Al-5 % B_4C-10 % BN	75	3.5	2.8

As it is demonstrated in Figure 3.32 and Figure 3.33, effect of squeeze pressure and different cutting speed on surface roughness of machined part have been analyzed, respectively. It can be said that this experiment could not draw a pattern for roughness variation by change in the squeeze pressure. However there can be seen a decrease in the surface roughness by increasing pressure in the case of pure aluminium. Also it is concluded that, except for pure aluminium, the increase in the cutting speed has positive effect on the surface roughness. This can be explained in the way that when there are abrasive particles of B_4C in the specimen, higher cutting speed means lower friction of tool on the specimen and consequently less tool wear which decreases the surface roughness.

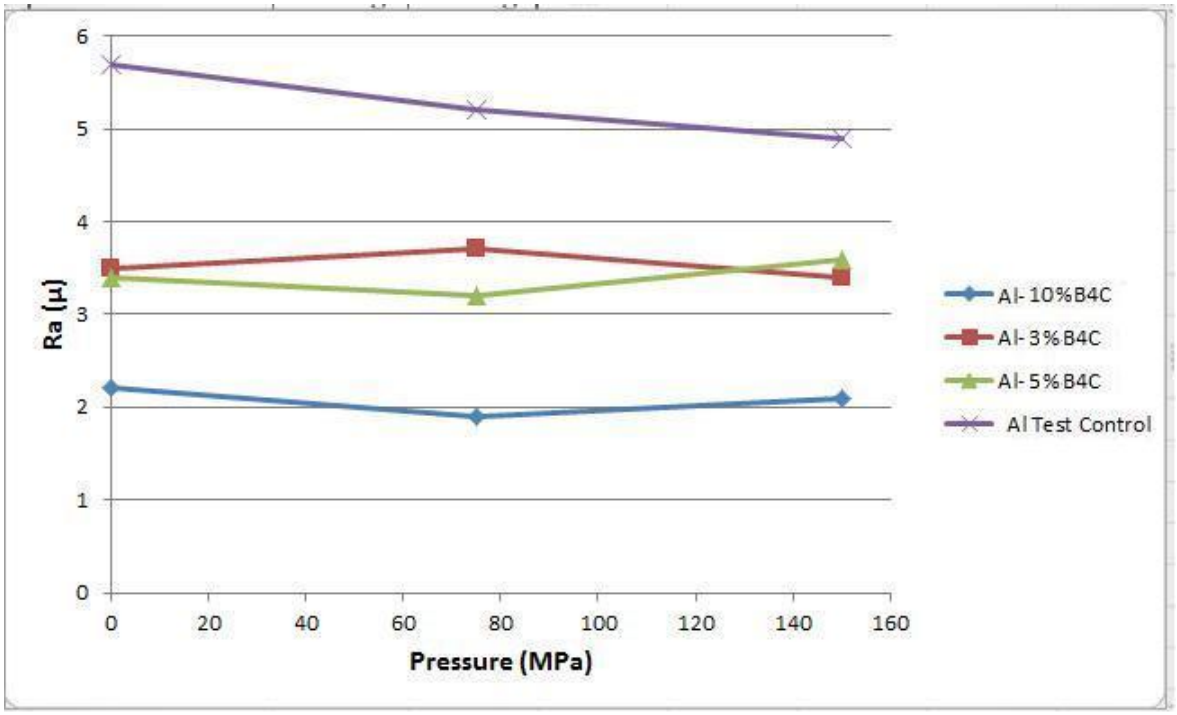

Figure 3.32. Variation in roughness (Ra) for different squeezing pressures.

Regarding effect of boron nitride addition there were versatile behaviors in roughness values, but it might be concluded that, in general, addition of boron nitride is decreasing surface roughness in the samples.

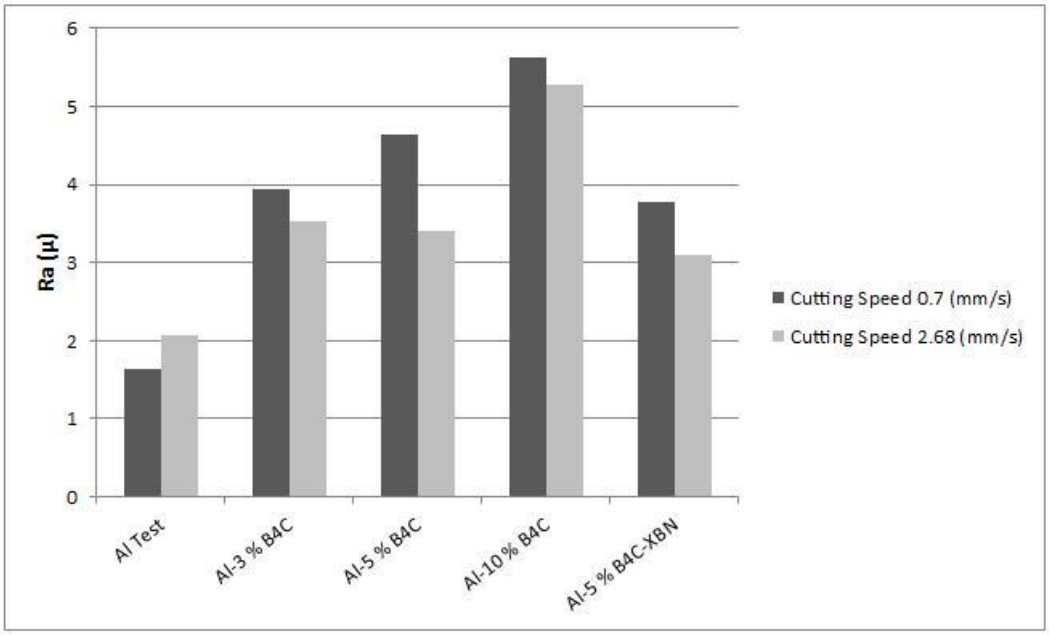

Figure 3.33. Variation in roughness by applying different cutting speeds.

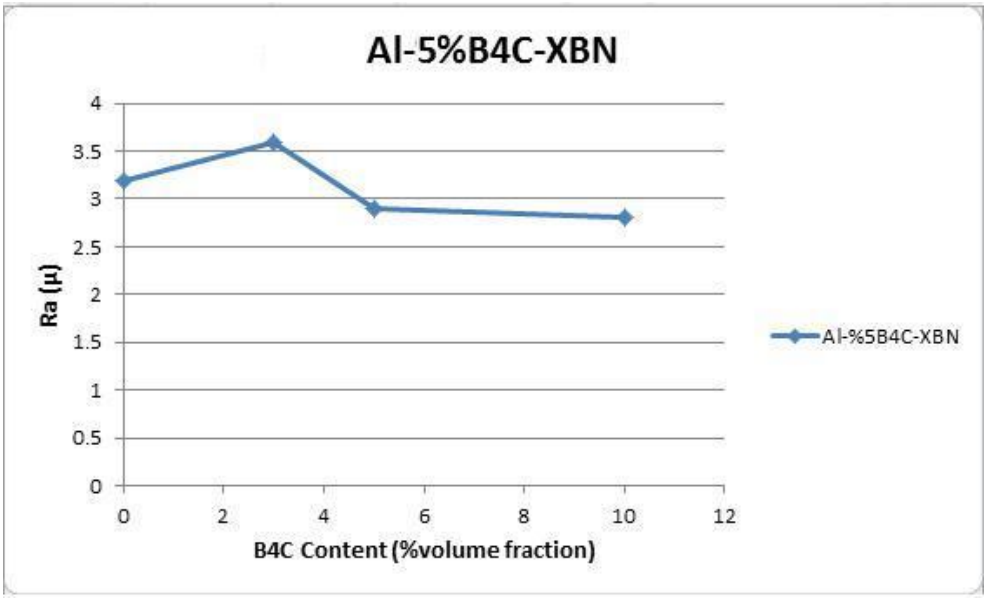

Figure 3.34. Variation in roughness by addition of BN particulates.

3.4.2. Physical Testing Results

The results of density measurements are registered in Table 3.7 and graphically illustrated in Figure 3.35. It can be seen that in all the cases increase in the applied pressure, resulted in higher density values which is equal to lower porosities in the material structure. Since with applying pressure, the gasses are removed from the solidifying molten aluminium, this is logical. This effect can clearly improve the cast quality. The surface quality with less defects and macro-cavities are shown in Figure 3.36.

Table 3.7. Density values for Different Specimens

Specimen Name	Pressure (MPa)	Density Values (g/cm3)							Average Density (g/cm3) ± STD
Al Test	0	2.649	2.647	2.663	2.661	2.648	2.661	2.660	2.656±0.007
Al Test	75	2.667	2.671	2.669	2.673	2.667	2.666	2.666	2.668±0.003
Al Test	150	2.655	2.682	2.674	2.665	2.681	2.695	2.741	2.685±0.028
Al-3 % B_4C	0	2.649	2.643	2.634	2.625	2.650	2.627	2.638	2.638±0.010
Al-3 % B_4C	75	2.665	2.627	2.627	2.640	2.715	2.658	2.635	2.652±0.031
Al-3 % B_4C	150	2.672	2.600	2.686	2.670	2.686	2.682	2.669	2.667±0.030
Al-5 % B_4C	0	2.645	2.626	2.611	2.647	2.641	2.637	2.631	2.634±0.012
Al-5 % B_4C	75	2.641	2.668	2.649	2.660	2.645	2.638	2.662	2.652±0.012
Al-5 % B_4C	150	2.646	2.658	2.662	2.666	2.652	2.669	2.660	2.659±0.008
Al-10 % B_4C	0	2.602	2.580	2.611	2.593	2.589	2.586	2.648	2.601±0.023
Al-10 % B_4C	75	2.638	2.614	2.625	2.639	2.619	2.624	2.601	2.623±0.013
Al-10 % B_4C	150	2.648	2.647	2.660	2.659	2.645	2.639	2.666	2.652±0.010
Al-5 % B_4C-3 % BN	75	2.615	2.621	2.632	2.630	2.624	2.639	2.643	2.629±0.010
Al-5 % B_4C-5 % BN	75	2.618	2.622	2.617	2.604	2.639	2.644	2.600	2.621±0.016
Al-5 % B_4C-10 % BN	75	2.578	2.562	2.583	2.591	2.572	2.588	2.584	2.579±0.010

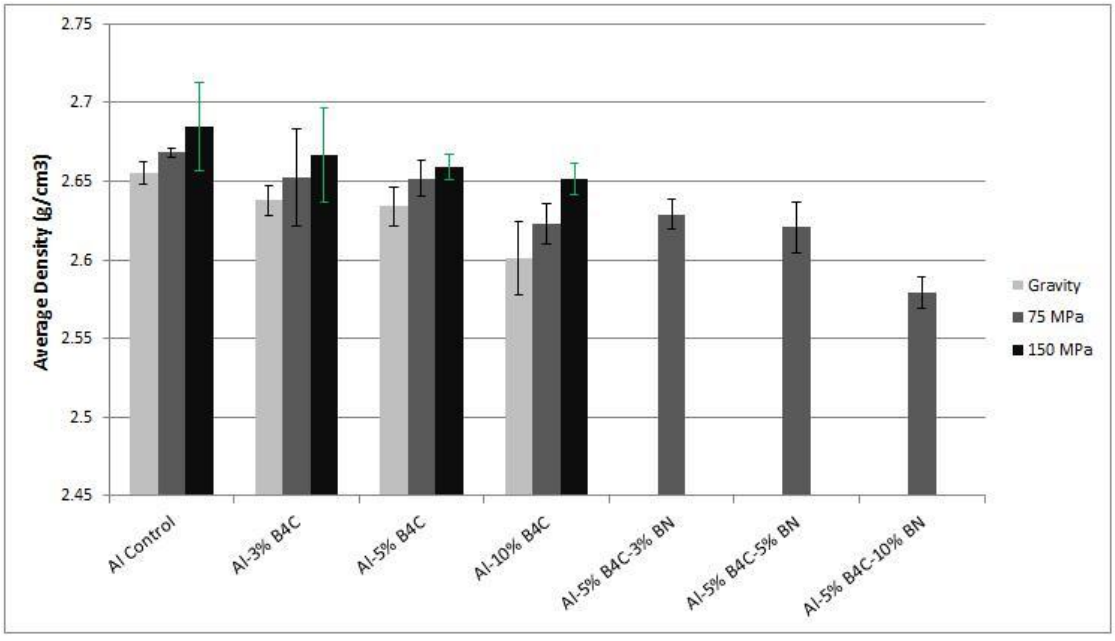

Figure 3.35. Variation in average density for different materials.

Figure 3.36. As cast specimens not-squeezed (left) and squeezed (right).

3.4.3. Mechanical Testing Results

Mechanical properties of the manufactured aluminium matrix composites were examined firstly by evaluating tensile strength of 5 specimen in each category and secondly by assessing hardness of materials.

Tensile test results of fractured specimens were listed in the Table 3.8, where ultimate tensile strength (UTS), elongation and yield strength (YS) are shown. For calculating yield strength values, 0.2% offset method was used. In order to figure out the variation in tensile strength by application of pressure in the time of squeeze casting, Stress-elongation graphs of all samples tested for pure aluminium are illustrated in Figure 3.37. As it is seen both UTS and YS are increased in consequence of applying pressure. Also elongation is increased by increase in the pressure, though this increase is negligible when 75 MPa pressure was applied. This is in agreement with the literature and the reason can be explained by effect of pressure as discussed in the Section 3.4.2.

Table 3.8. Average tensile properties of AMCs with different reinforcement contents and in presence of different squeezing pressures

Material	Pressure (MPa)	UTS (MPa) ± STD	Elongation (%) ±STD	YS (MPa) ±STD
AL Test	0	77.04±14.1	14.05±1.5	50.43±12.4
AL Test	75	94.56±7.2	14.4±1.9	73.21±5.2
AL Test	150	111.71±3.2	17.61±0.9	91.67±2.3
3 % B4C-AL	0	103.41±6.2	9.75±2.2	84.39±5
3 % B4C-AL	75	107.75±3.3	9.07±1.3	88.82±2.1
3 % B4C-AL	150	115.41±5.4	12.34±1	87.46±6.2
5 % B4C-AL	0	117.71±4.7	8.52±1.7	90.33±4.1
5 % B4C-AL	75	120.96±3.1	10.81±1.8	91.14±2.8
5 % B4C-AL	150	127.07±7.9	11.03±1.3	107.09±7.1
10 % B4C-AL	0	85.21±12.1	1.95±1.1	67.32±8.9
10 % B4C-AL	75	89.78±9.1	1.5±0.7	82.74±7.5
10 % B4C-AL	150	97.62±4.6	2.31±1.6	90.72±2.7
3 % BN-5 % B4C-AL	75	119.47±6.7	10.22±1.2	98.46±5
5 % BN-5 % B4C-AL	75	117.63±8.9	12.82±1	82.37±8.1
10 % BN-5 % B4C-AL	75	101.32±10.1	6.08±1.5	79.93±7.9

Also it can be seen from Table 3.8 and Figure 3.38 that increase in B_4C reinforcement contents, generally increases the UTS and YS values up to 5 % of boron carbide contents. At the same time elongation percentages of AMCs with higher volume fractions of B_4C are worsened. This can be justified with the fact that boron carbide particles absorb the stress applied on the aluminium matrix which means higher strength material will bear the stress. So the strength of AMC material will increase. Another justification is based on quench strengthening in which the large difference in thermal expansion or CTE between the matrix metal and the particulate results in the generation of dislocations on quenching from the recrystallization or solution treatment temperature. The dislocation density generated on quenching causes dislocation cumulation in matrix/reinforcement interface which prevent further dislocation motion and increases the strength. And as a final potential mechanism it can be said that, in the presence of grain

refiners, particles may act as nucleation sites for grains and grain sizes considerably finer than the grain size of unreinforced alloys might occur. This might contribute to the strength of the material formulated by the Hall-Petch equation which is discussed in the Section 2.3.4.

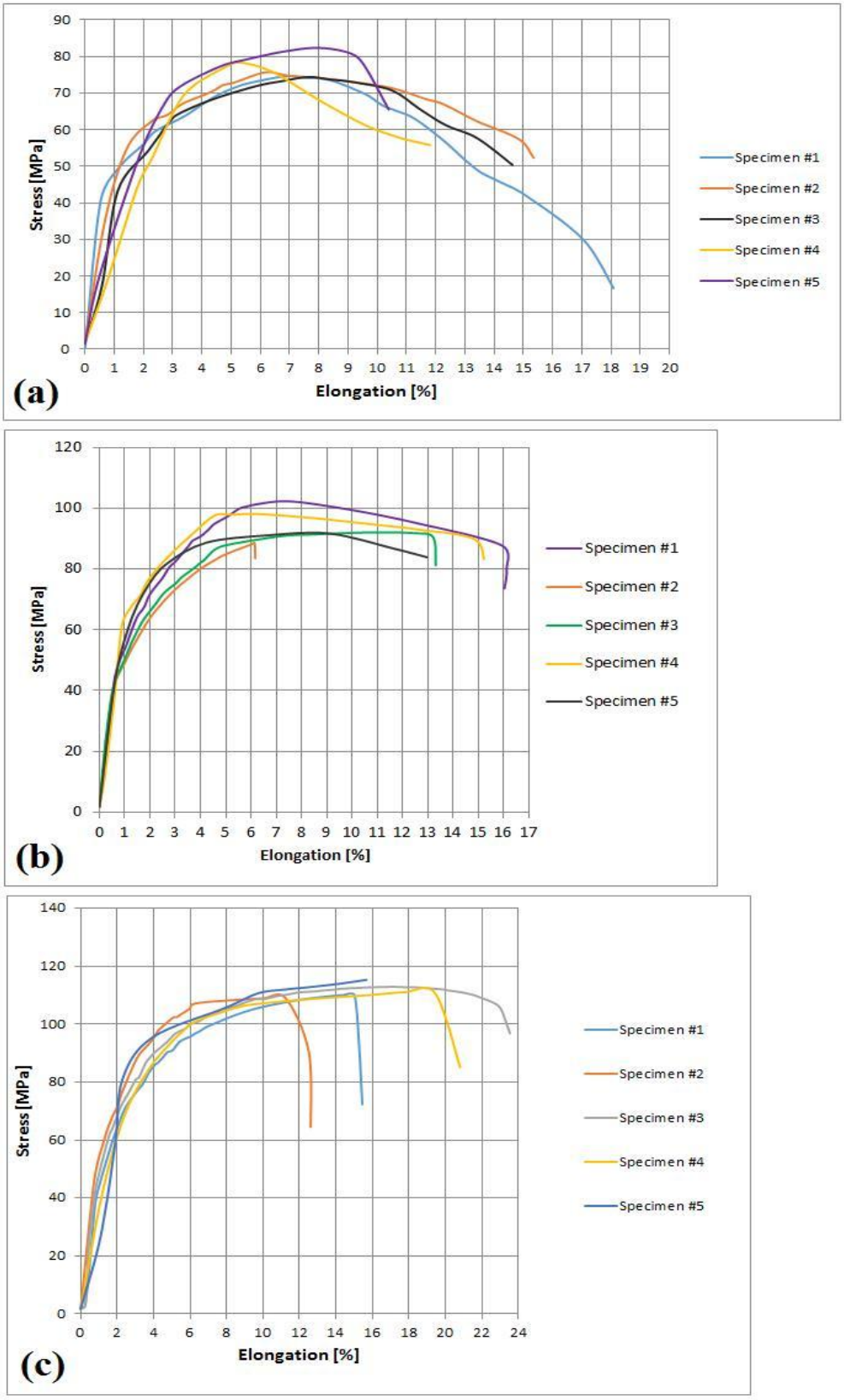

Figure 3.37. Tensile behavior of matrix material (Al) at (a) 0, (b) 75 and (c) 150 MPa squeezing pressure.

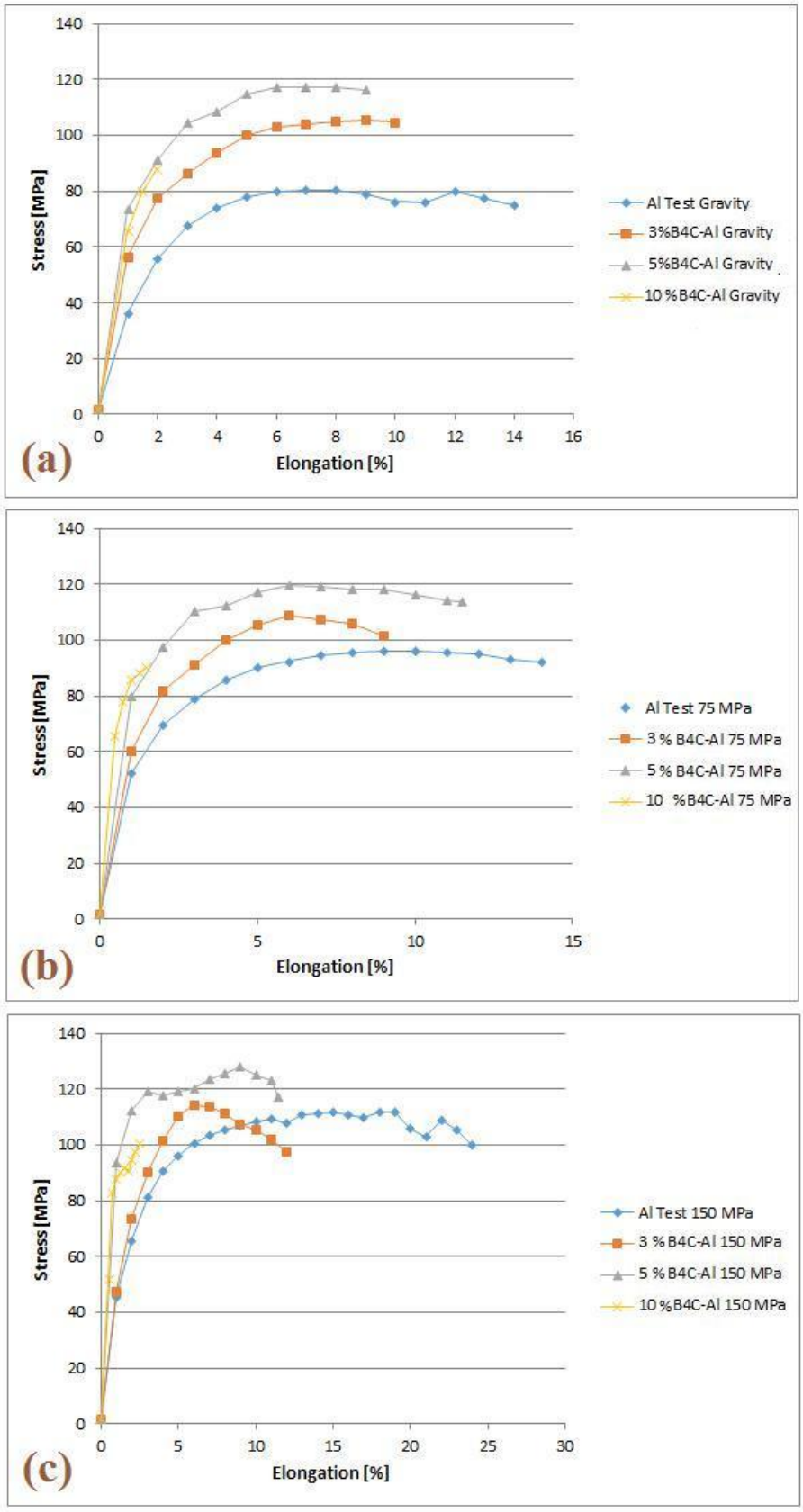

Figure 3.38. Tensile behavior of B_4C-Al MC (Al) at (a) 0, (b) 75 and (c) 150 MPa squeezing pressure.

It is also detectable in Figure 3.38 that further increase in the amount of B_4C particles from 5 % to 10 % has no improved effect on the tensile properties of the AMCs. Above this, specimens with 10 % of reinforcement materials show very low UTS, YS and also elongation values. This abnormal deterioration in the tensile strength can be due to the high porosities and agglomerated reinforcement particles in AMCs with 10 % of B_4C when the melt for squeeze casting was being prepared in phase 1-b. Moreover it can be said that to be able to distribute the high volume fractions of boron carbide into the aluminium melt there is a need for more advanced equipment and also fully vacuumed situation.

One aim of this study was to evaluate the effect of BN in hybrid BN-B_4C-Al composites. As it can be noted from Figure 3.39 and Table 3.8, increase in the amount of BN particles hardly has any major effect on the tensile strength of the composite material. However increase in the elongation can be seen, when the volume fraction of BN reinforcement is 5 %. Also stress-elongation graph of 5 % BN-5 % B_4C-Al hybrid composite shows promoted elastic behavior while retaining the strength comparing to 5 % B_4C-Al composite.

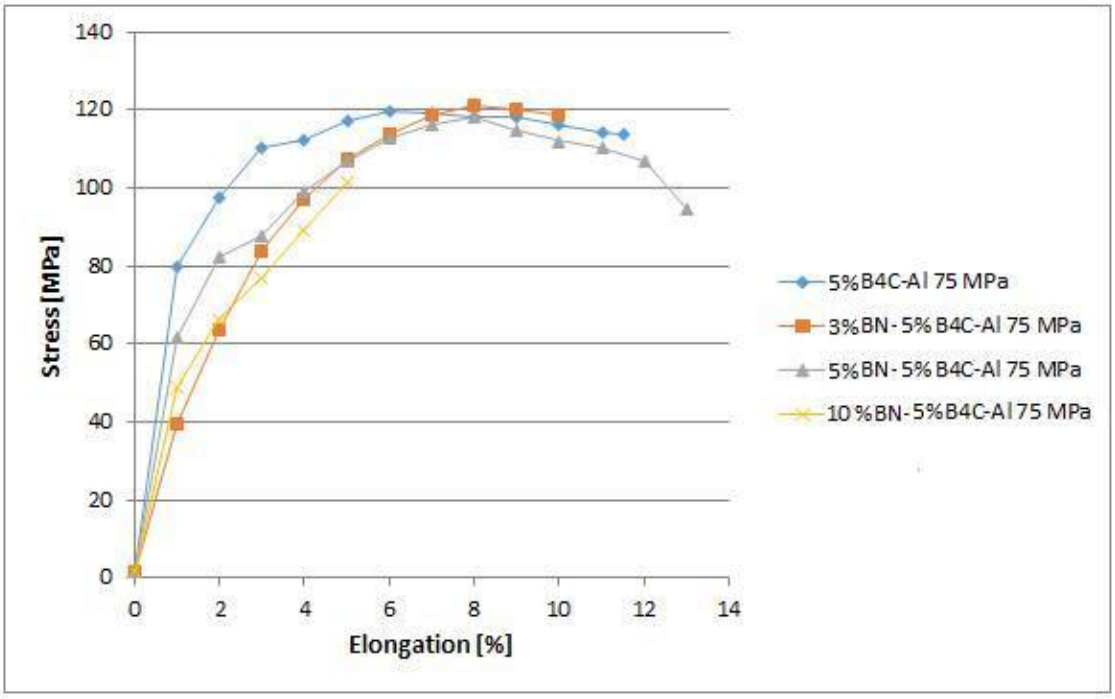

Figure 3.39. Tensile behavior of BN-B_4C-Al MCs at 75 MPa squeezing pressure.

Among composite materials tested in mentioned testing conditions and limitations, it can be stated that the optimum composite material is the material with aluminium matrix, 5 % volume fraction of B_4C particles and 5 % volume fraction of BN particles.

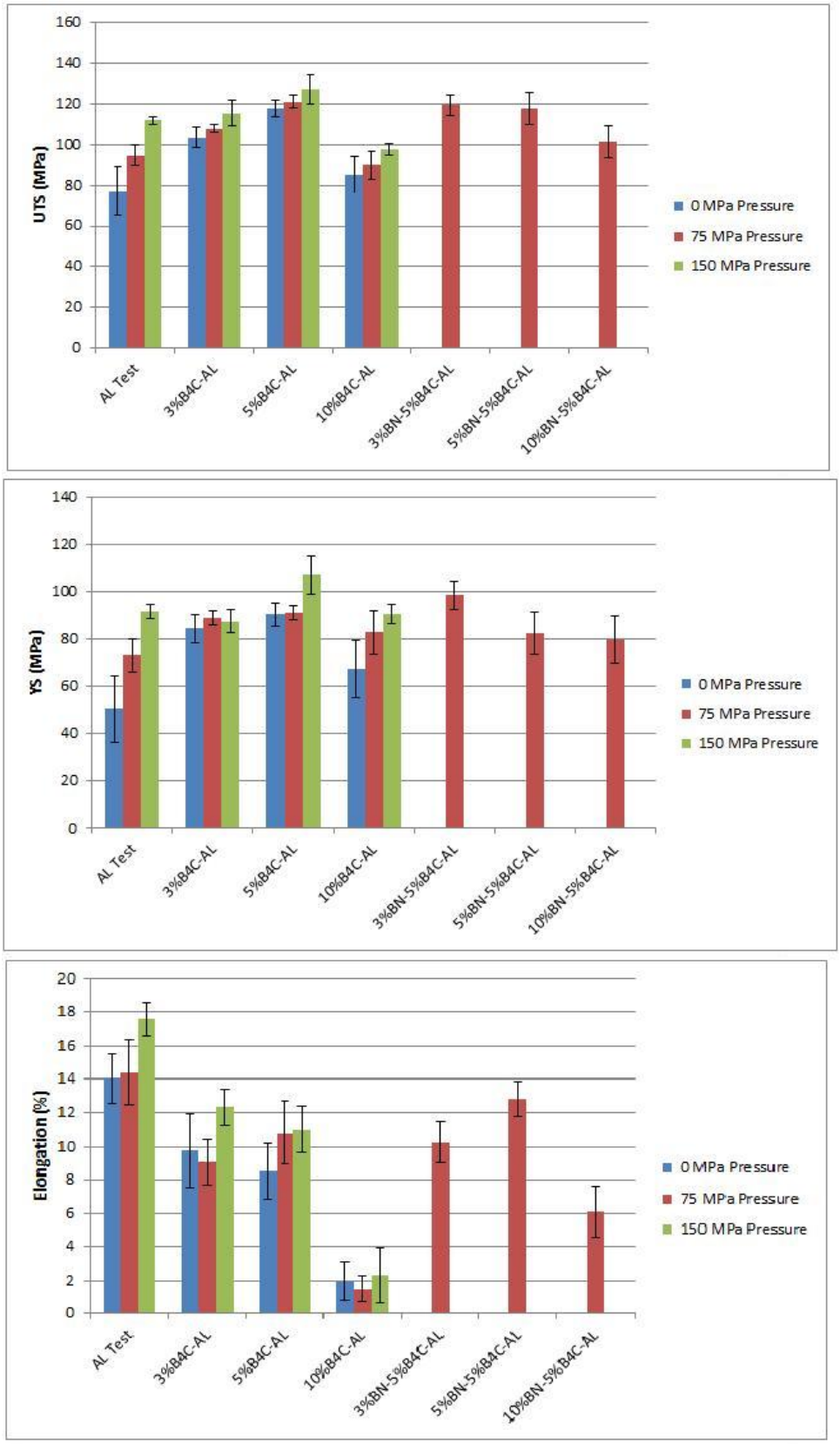

Figure 3.40. Illustration of average tensile properties of AMCs with different reinforcement contents and in presence of different squeezing pressures.

In the second step of mechanical testing, hardness of samples was evaluated which results are tabulated in Table 3.9 and Figure 3.41.

The results show that, as expected hardness values increase by increasing squeezing pressure. This increase is more sensible in case of Al test and Al-10 % B_4C samples. Also it is seen that more contents of boron carbide particles result in improved hardness values. Moreover it can be concluded from the results that addition of BN particles softens the structure of hybrid aluminium matrix composite. However by increasing BN contents from 5 % to 10 % there isn't any significant decrease in the hardness.

Table 3.9. Brinell hardness results for different materials

Specimen Name	**Pressure (MPa)**	**Measure 1**	**Measure 2**	**Measure 3**	**Average Hardness (BHN)**	**Standard Deviation**
Al Test	0	112.5	110.7	112.5	111.9	1.03
Al Test	75	112.2	116	115.6	114.6	2.08
Al Test	150	121.4	119.3	121.5	120.7	1.24
Al-3 % B_4C	0	160.6	164.3	161	161.9	2.03
Al-3 % B_4C	75	166.2	166.2	162	164.8	2.42
Al-3 % B_4C	150	168.8	164.6	168.4	167.2	2.31
Al-5 % B_4C	0	165	165.1	164.4	164.8	0.37
Al-5 % B_4C	75	167.7	164.4	165.2	165.7	1.72
Al-5 % B_4C	150	170.8	169.6	170.3	170.2	0.6
Al-10 % B_4C	0	180.1	176.5	174.2	176.9	2.97
Al-10 % B_4C	75	188.4	184.6	185.7	186.2	1.95
Al-10 % B_4C	150	189.5	187.1	191.7	189.4	2.3
Al-5 % B_4C-3 % BN	75	161.3	153.8	163.3	159.4	5
Al-5 % B_4C-5 % BN	75	150.6	164	147.2	153.9	8.88
Al-5 % B_4C-10 % BN	75	143.9	160.3	155.5	153.2	8.43

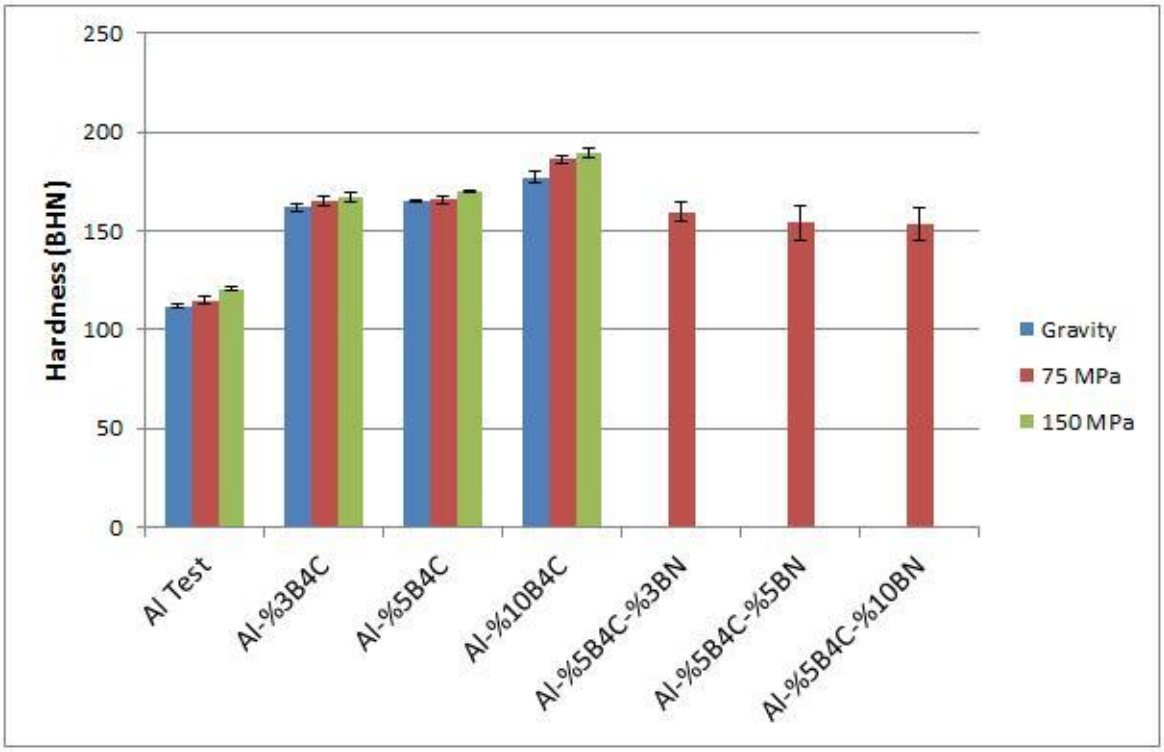

Figure 3.41. Brinell hardness average values for different materials.

3.4.4. Microstructure Evaluating Results

As discussed in the Section 3.3.8, the density increases with an increase in the amount of squeezing pressure which means that there should be less porosity in the material structure. As it can be seen in Figure 3.42 when 150 MPa of pressure is applied on pure aluminium, less porosities are detectable in the structure of material. These micro porosities can act as crack initiation sites during tensile testing and cause failure in the material.

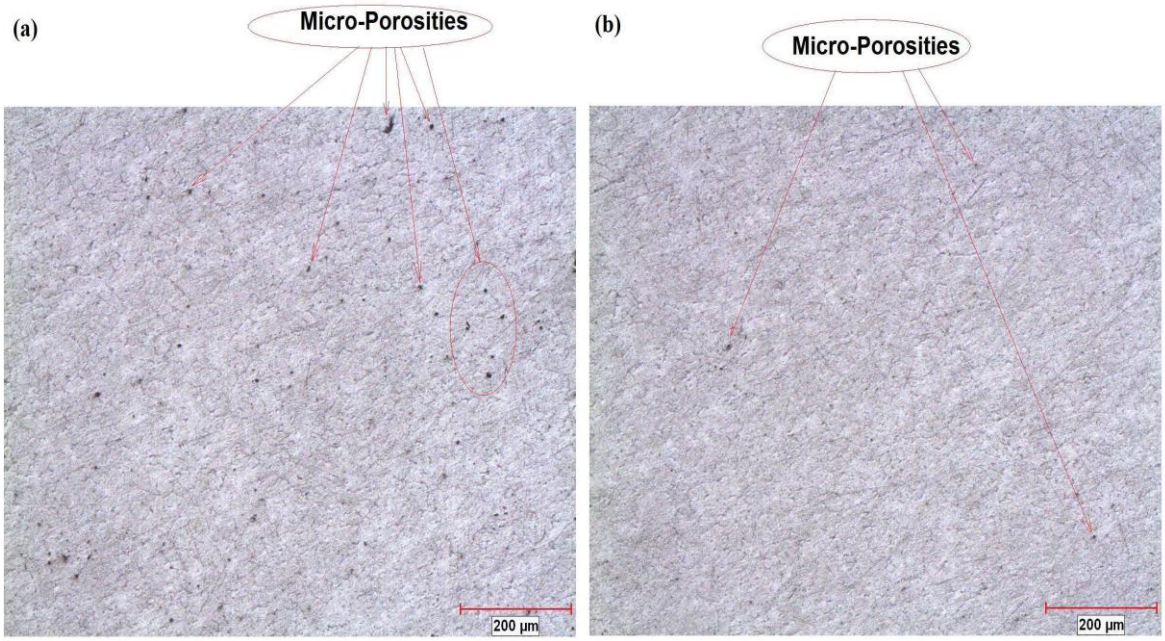

Figure 3.42. Porosities in (a) Al test control/Gravity and (b) Al test control/150 MPa samples.

As another concern, specimens were evaluated for particles distribution and found out that the distribution is not homogenous in all samples of 10 % B_4C-Al composites. In the other specimen categories, distribution homogeneity is acceptable. Homogenous distribution of reinforcement material in the matrix grain is an important measure which affects tensile strength and hardness of composite material however non-homogenous distribution will put the material exposed to defects and failures.

Regarding 10 % B_4C-Al samples, it was observed that in many areas there are agglomerations and porosities in the structure. Agglomeration itself creates a site which is likely to initiate porosities. These defects are significantly due to lack of controlled production situation and preventing gasses to enter the melt in the time of stirring, especially in the time of squeeze casting (Figure 3.44).

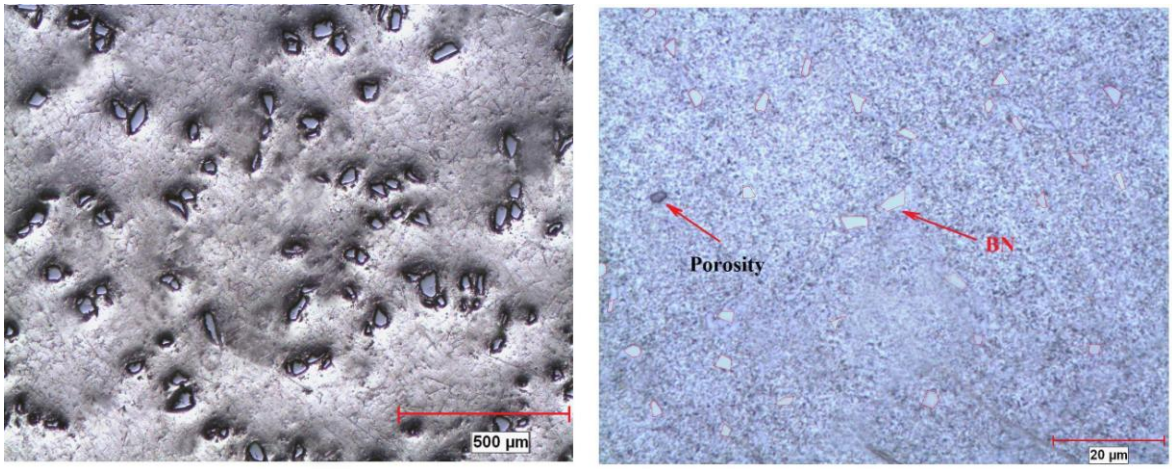

Figure 3.43. Homogenous distribution of reinforcement particles in the matrix material at (a) 5 % B_4C-Al/75 MPa and (b) 3 % BN-5 % B_4C-Al specimens.

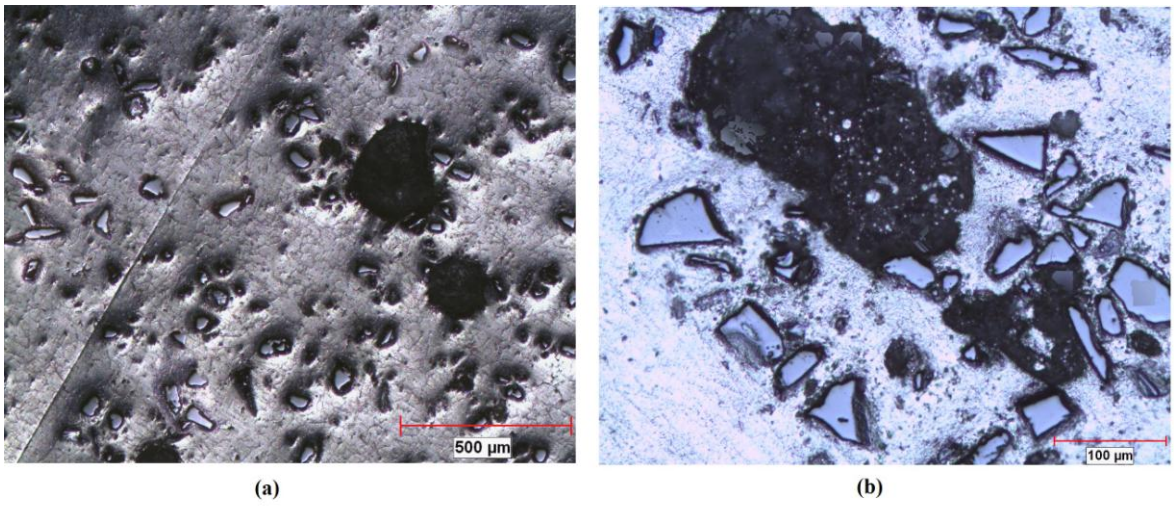

Figure 3.44. (a) Defected 10 % B_4C-Al/75 MPa sample and (b) effect of agglomeration on porosity initiation.

As discussed in the Section 2.3.4, effect of squeeze casting on the samples, was decrease in grain size, porosities and dendrite arm spacing (DAS). These changes in the microstructure are the cornerstone for improvement in hardness, tensile strength and density. Regarding porosity reduction in pressurized samples, density test was promising. By evaluating samples prepared for microstructure tests, it was seen that in some samples, porosities are decreased in squeeze cast samples. Void contents based on ASTM D2734 standard can be seen in Table 3.10.

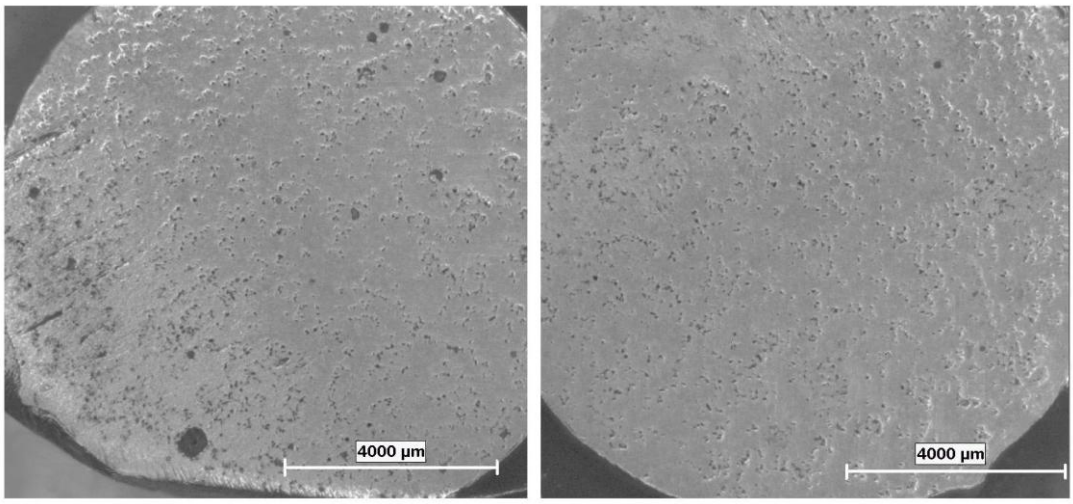

Figure 3.45. Porosities in (a) 5 % B_4C-Al/Gravity and (b) 5 % B_4C-Al/150 MPa samples.

Table 3.10. Void volume contents of samples

Specimen Name	Pressure (MPa)	Theoretic Void Contents (%)
Al Test	0	1.64
Al Test	75	1.17
Al Test	150	0.56
Al-3 % B_4C	0	2.09
Al-3 % B_4C	75	1.55
Al-3 % B_4C	150	1.02
Al-5 % B_4C	0	2.1
Al-5 % B_4C	75	1.43
Al-5 % B_4C	150	1.16
Al-10 % B_4C	0	2.97
Al-10 % B_4C	75	2.16
Al-10 % B_4C	150	1.08
Al-5 % B_4C-3 % BN	75	1.44
Al-5 % B_4C-5 % BN	75	1.20
Al-5 % B_4C-10 % BN	75	1.39

Moreover, as it was expected, pressure application caused grain refinement and increase the number of grain boundaries. It was seen that in case of pure aluminium grains can be refined from 740 μm to 178 μm (average) when pressurized from 0 to 150 MPa. As it can be seen in Figure 3.46 by increasing pressure from gravity to 150 MPa a visible refinement in the microstructure happens. As discussed before in the Section 2.3.4, one theory says refinement is effect of undercooling which takes place as the pressure is applied on the molten metal. This undercooling results in increase in nucleation rate which consequently refines the microstructure of material. The other theory which is likely the reason for this grain refinement is increase in the heat transfer coefficient which seems to be the dominant mechanism in this study considering the time and temperature of pressure application. Since the B_4C particles were large, grains and grain boundaries were not completely visible in the structure, but it is seen in some of the samples that boron carbide particles were located on the grain boundaries and also a portion was distributed inside the grains (Figure 3.47). With this in mind, one can conclude that another mechanism which causes the improvement in mechanical properties of boron carbide reinforced AMCs is the incapability of dislocations to pass through the grain boundaries due to the presence of particles. This means boron carbide particles act as dislocation movement barriers in the grain boundaries. The extended effect of reinforcement materials on strengthening the composites is discussed in the Section 2.1.4.4.

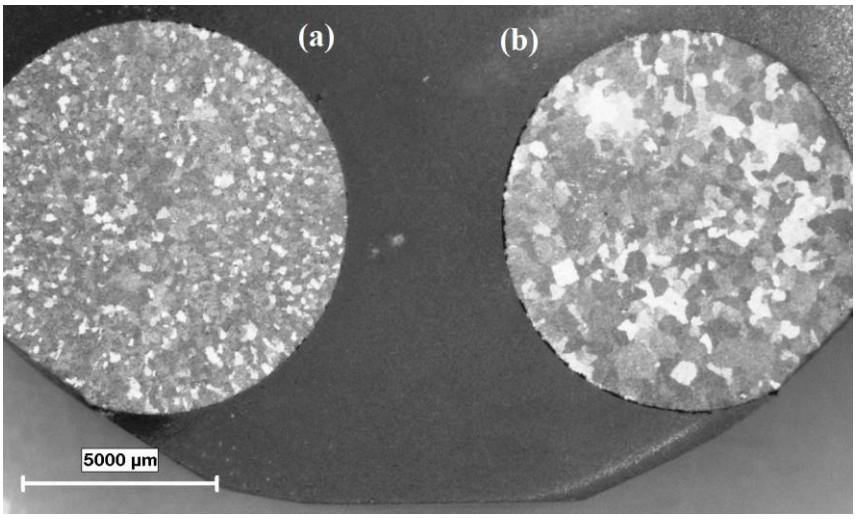

Figure 3.46. Grain refinement in squeeze cast specimen. (a) Al-Test control/150 MPa (d=178 μm) and (b) Al-Test Control/ Gravity (740 μm).

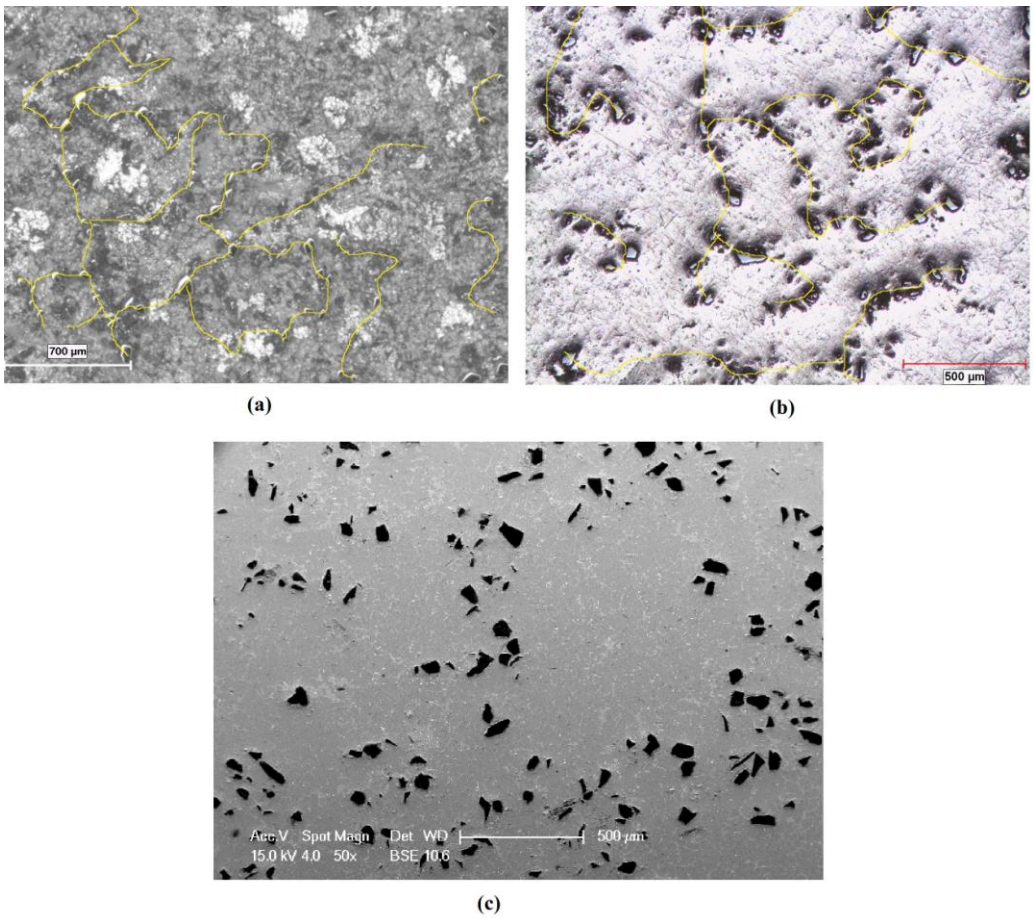

(a) (b)

(c)

Figure 3.47. Boron carbide particles aligned in the rows in 5 % B_4C-AL/150 MPa specimen (a) etched, (b) not etched and (c) SEM capture.

One other important issue in this work was to evaluate the effect of Ti addition to the AMC through adding K_2TiF_6 flux. Refering to the Section 2.4.3, when the mentioned Al-Ti-B_4C system is in accordance with thermodynamic conditions, there is always a reaction layer when the composite is manufactured with addition of K_2TiF_6. It is believed that this layer is in charge of increase in the wettability of the B_4C particles in the aluminium melt. This can be seen in Figure 3.48. The reason for using K_2TiF_6 flux is K and F remove the oxide layer from the aluminium melt surface and the contact between Al melt and B_4C, becomes possible.

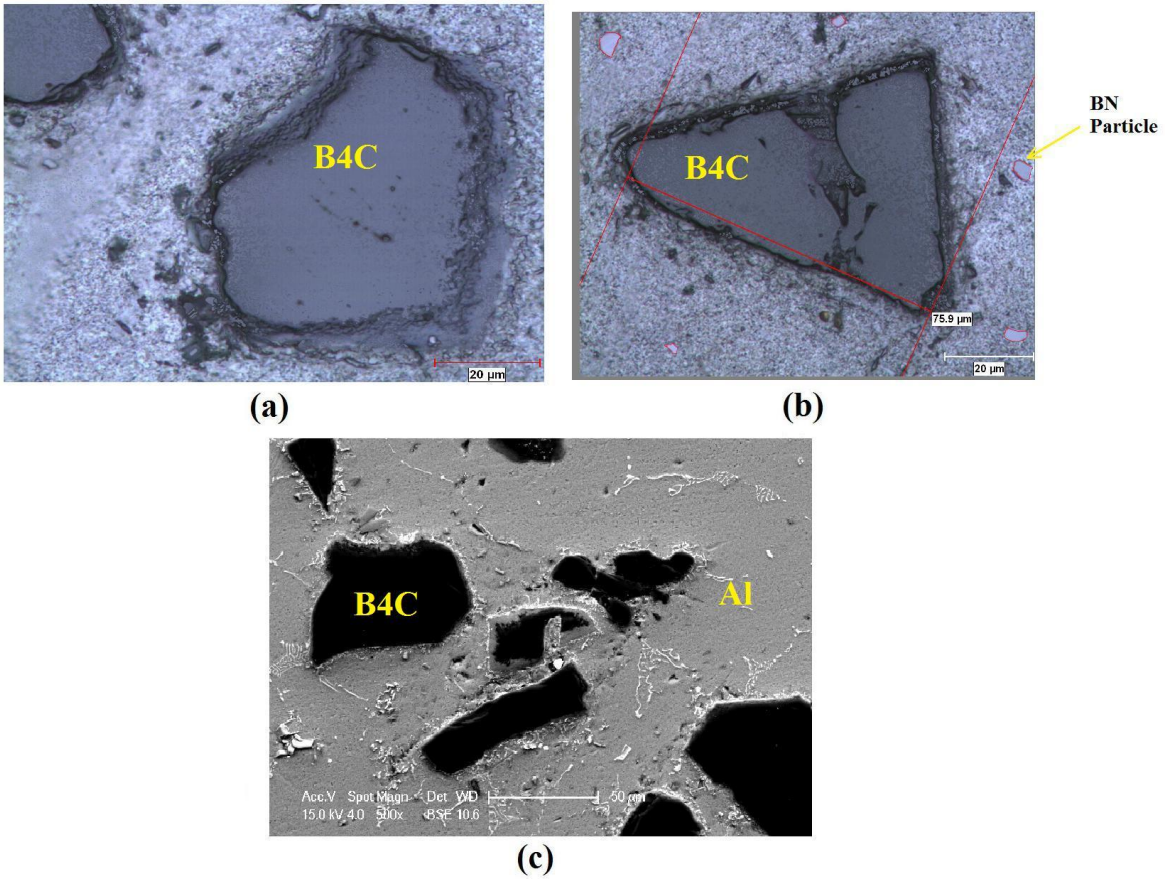

Figure 3.48. Proper wetting of reinforcement materials by aluminium melt in. (a) and (b) Optical microscope and (c) SEM.

Based on the discussion in the Section 2.4.3, theoretically a reaction layer containing TiC and TiB_2 is expected in Al-Ti-B_4C system. The analysis on the interface is in good agreement with this expectation. EDAX analysis has been done on the interface reaction layer in the scanning electron microscope and the results show that as expected, there are B, C and Ti elements in the reaction layer. So it can be concluded that K_2TiF_6 flux addition improved the wettability in the composite.

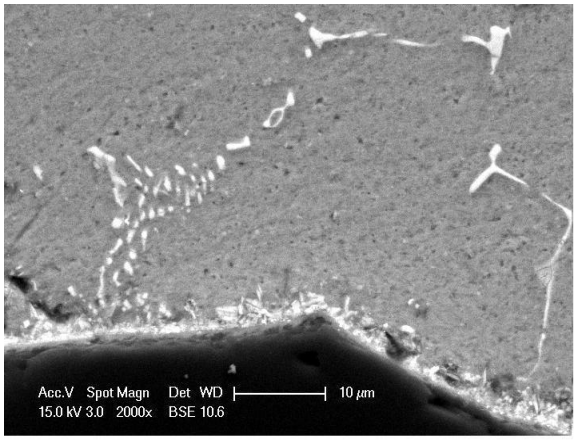

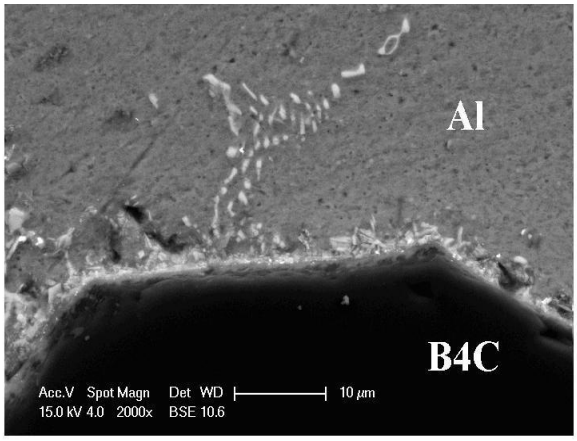

kV:15.00, Tilt: 0.70, Take-off:36.05, Tc:50.0
Detector Type :SUTW-Sapphire, Resolution :130.10, Lsec :26

EDAX ZAF Quantification, Standardless,
Element Normalized
SEC Table : Default

Element	Wt %	At %
Al K	68.57	79.41
Si K	2.6	2.78
Ti K	24.55	15.41
Fe K	4.27	2.3
Total	100	100

Figure 3.49. SEM-EDAX analysis of reaction layer in the interface of boron carbide particles and Al melt.

4. CONCLUSION

In the course of this research, aluminium matrix composite (AMC) reinforced with B_4C and hybrid AMC containing B_4C and BN were manufactured via stir casting and post processed by squeeze casting. Distribution of particles in the matrix structure was homogenous except some of the specimens with 10 % boron carbide. The processes of this study were conducted in two steps. In the first stage, the effect of various B_4C contents (3 % , 5 % and 10 %) under different squeezing pressures (0, 75 and 150 MPa) were studied on tensile strength, hardness characteristics, machinability, density and the microstructure of fabricated samples. In the second stage, Al-B_4C-BN hybrid AMC samples were manufactured with constant squeezing pressure (75 MPa) and constant B_4C volume fraction but with three different BN volume fractions (3 %, 5 % and 10 %) and effect of BN addition were evaluated.

It was found out that with increasing the amount of boron carbide particles in the AMC, there is an obvious deterioration in the chip length and consequently the machinability. Regarding effect of squeeze casting on machinability, it is found out that, in case of pure aluminium there is approximately 20 % decrease in the chip length by increasing pressure from gravity to 150 MPa, although there is a slight increase in chip length from zero to 75 MPa of pressure. Materials containing boron carbide particles showed same behavior with increasing the pressure but with lower rate. Also addition of BN particles contributed significantly to the machinability in the AMC.

This experiment could not draw a pattern for roughness variation by change in the squeeze pressure. However, there can be seen a decrease in the surface roughness by increasing pressure in the case of pure aluminium. Also it is concluded that except for pure aluminium, the increase in the cutting speed has positive effect on the surface roughness for AMCs. Regarding effect of boron nitride addition there was versatile behavior in roughness values, but it might be concluded that, in general, addition of boron nitride is decreasing surface roughness in the samples.

Moreover in all the cases increase in the applied pressure resulted in higher density values which is equal to lower porosities in the material structure. Also it was observed that squeeze cast parts can be manufactured near net shape with almost no need for post processing.

Tensile testing results presented that both UTS and YS are increased in consequence of applying pressure. Also elongation is increased by increasing the pressure, though this increase is negligible when 75 MPa pressure was applied. In addition, increase in the amount of boron carbide particles, had increased UTS and YS while decreasing the elongation gradually. This was true up to 5 % B4C and for specimens with higher ceramic contents (10 %) there was abnormal deterioration in both tensile strength and elongation which was due to high porosities and agglomerated reinforcement particles in some of the AMC samples. Furthermore increase in the amount of BN particles hardly has any major effect on the tensile strength of the composite material. However there can be seen increase in elongation when the volume fraction of BN reinforcement is 5 %. Regarding hardness evaluation, as expected, hardness values increases by increasing squeezing pressure. This increase is more sensible in case of Al control and Al-10 % B_4C samples. Also it is seen that more contents of boron carbide particles result in improved hardness values. Moreover it can be concluded from the results that addition of BN particles softens the structure of hybrid aluminium matrix composite. However by increasing BN contents from 5 % to 10 % there isn't any significant decrease in the hardness.

Furthermore, grain refinement in the microstructure of pressurized materials was visible and the micro-porosities in such samples were less. Also it can be reported that there are B, C and Ti elements in the reaction layer which is the main site responsible for the strength in AMCs. So it can be concluded that K_2TiF_6 flux addition improved the wettability in the composite by affecting the interface of reinforcement and the matrix material.

For the future work, particles with different nano and micro sizes can be employed and evaluated to see the effect of reinforcement size on both the properties and wettability in the AMC. Moreover production of AMCs with higher contents of B_4C and BN can be a potential future work which needs more integrated production system in vacuumed

condition. Also it is likely that addition of boron carbide contributes excessive grain refinement in the structure. It is reported that boron addition causes grain refinement in the material by forming AlB_2 [92] particles in the structure. On the other hand as discussed in the Section 2.4.3, when K_2TiF_6, is added to the composite, it reacts with boron carbide and titanium boride forms in the interface. Since TiB_2 is a grain refiner [114], this can be studied to see which phenomenon is the potential responsible for the grain refinement in B_4C-Al composites and in what shares. Also effect of novel grain refinements on the AMCs can be studied. Besides, it is very valuable to study deeply the wettability of boron carbide and boron nitride particles by examining different wetting agents such as $Mg(C_2H_3O_2)_2$ [115] or Na_3AlF_6 [116], since wettability is the main challenge in production of B_4C-Al and B_4C-BN-Al composites.

REFERENCES

1. Kainer, K. U., *Metal Matrix Composites. Custom-made Materials for Automotive and Aerospace Engineering*, WILEY-VCH Verlag GmbH & Co., KGaA, Weinheim, 2006.

2. KIm, Y. H., S. Lee, and Nack J. Kim, “Fracture Mechanisms of a 2124 Aluminium Matrix Composite Reinforced with SiC Whiskers”, *Metallurgical and Materials Transactions, A 1991, Vol23A*, pp.2589-2596, 1991.

3. Meyer, P., and A.M. Waas, "FEM Predictions of Damage In Continuous Fiber Ceramic Matrix Composites Under Transverse Tension Using the Crack Band Method", *Acta Materialia,, Volume 102, 1 January 2016*, pp.292-303, 2016.

4. Fulco, A. P. P., J. D. D. Melo, C. A. Paskocimas, S. N. Medeiros, F. L. A. Machado, and A. R. Rodrigues, "Magnetic Properties of Polymer Matrix Composites with Embedded Ferrite Particles", *NDT & E International, Volume 77, January 2016*, pp.42-48, 2016.

5. Chawla, N., K. K. Chawla, (2006). *Metal Matrix Composites*, Springer, New York, 2006.

6. Koli, D. K., G. Agnihotri, and R. Purohit, "Advanced Aluminium Matrix Composites: The Critical Need of Automotive and Aerospace Engineering Fields", *Materials Today Proceedings, Volume 2, Issues 4–5*, 2015.

7. European Aluminium Association, 2015, http://www.european-aluminium.eu/about-aluminium/facts-and-figures/, Accessed at September 2015.

8. Ilangovan, M., S. R. Boopathy, and V. Balasubramanian, "Microstructure and Tensile Properties of Friction Stir Welded Dissimilar AA6061–AA5086 Aluminium Alloy Joints", *Transactions of Nonferrous Metals Society of China, Volume 25, Issue 4, April 2015*, pp.1080-1090, 2015.

9. "The Differences Between Heat-Treatable and Non-Heat-Treatable Aluminium Alloys", 2014, http://www.esabna.com/us/en/education/blog/the-differences-between-heat-treatable-and-non-heat-treatable-aluminium-alloys.cfm, Accessed at December 2015.

10. Yue, T. M., and G. A. Chadwick, "Squeeze Casting of Light Alloys and Their Composites", *Journal of Materials Processing Technology, Volume 58, Issues 2–3, 15 March 1996*, pp.302-307, 1996 .

11. Chen, W. P., Y.Y. Li, G.W. Guo, D.T. Zhang, Y. Long, and T.L. Ngai, "Squeeze Casting of Al-Cu Alloys", *Journal of Central South University of Technology, September 2002, Volume 9, Issue 3,* pp.159-164, 2002.

12. Mahadevan, R., and R. Gopal, "Selectively Reinforced Squeeze Cast Pistons", *World Foundry Congress, 7th - 10th February, 2008,* pp.379-384, 2008.

13. Zhang, O., G. Chen, G. Wu, Z. Xiu, and B. Luan, "Property Characteristics of a AlNp/Al Composite Fabricated by Squeeze Casting Technology", *Materials Letters, Volume 57, Issue 8, February 2003*, pp.1453-1458 , 2003.

14. Kim, S. B., D. A. Koss, and D. A. Gerard, "High Cycle Fatigue of Squeeze Cast AL/SiCw Composites", *Materials Science and Engineering: A, Volume 277, Issues 1–2, 31 January 2000,* pp.123-133, 2000.

15. Pandey, A. B., E. Miracle, and L. Donaldson, *Metallic Matrices*, ASM Handbook, Vol. 21, ASM International, Metals Park, pp.396–402, 2001.

16. Baradeswaran, A., S. C. Vettivel, A. E. Perumal, N. Selvakumar, and R. F. Issac, "Experimental Investigation on Mechanical Behaviour, Modelling and Optimization of Wear Parameters of B_4C and Graphite Reinforced Aluminium Hybrid Composites", *Materials & Design, Volume 63, November 2014*, pp.620-632, 2014.

17. Saravanan, L., and T. Senthilvelan, "Investigations on the Hot Workability Characteristics and Deformation Mechanisms of Aluminium Alloy-Al_2O_3 Nanocomposite", *Materials & Design, Volume 79, 15 August 2015*, pp.6-14, 2015.

18. Takahashi, S., Y. Imai, A. Kan, Y. Hotta, and H. Ogawa, "Improvements in the Temperature-dependent Properties of Dielectric Composites by Utilizing MgO Whiskers as the Dielectric Filler in an iPP Matrix", *Journal of Alloys and Compounds, Volume 640, 15 August 2015*, pp.428-432, 2015.

19. Sharma, P., S. Sharma, and D. Khanduja, "Production and Some Properties of Si_3N_4 Reinforced Aluminium Alloy Composites", *Journal of Asian Ceramic Societies, Volume 3, Issue 3, September 2015*, pp.352-359 , 2015.

20. Johny James, S., K. Venkatesan, P. Kuppan, and R. Ramanujam, "Hybrid Aluminium Metal Matrix Composite Reinforced with SiC and TiB_2", *Procedia Engineering, Volume 97, 2014*, pp.1018-1026 , 2014.

21. Chen, K., Y. Hua, C. Xu, Q. Zhang, C. Qi, and Y. Jie, "Preparation of TiC/SiC Composites From Ti-enriched Slag by an Electrochemical Process in Molten Salts", *Ceramics International, Volume 41, Issue 9, Part A, November 2015*, pp.11428-11435, 2015.

22. Wang, Y., K. Lei, Y. Ruan, and W. Dong, "Microstructure and Wear Resistance of c-BN/Ni–Cr–Ti Composites Prepared by Spark Plasma Sintering", *International Journal of Refractory Metals and Hard Materials, Volume 54, January 2016*, pp.98-103, 2016.

23. Dieringa, H., and K.U. Kainer, *Particles, Fibers and Short Fibers for the Reinforcement of Metal Materials*, WILEY-VCH Verlag GmbH & Co. KGaA, Weinheim, 2006.

24. Timofeeva, E. V., A. N. Gavrilov, J. M. McCloskey, and Y. V. Tolmachev , "Thermal Conductivity and Particle Agglomeration in Alumina Nanofluids: Experiment and Theory", *Liquid Crystal Institute and Chemical Physics Interdisciplinary Program, Kent State University, Kent, Ohio 44242, USA*, 2007.

25. Huntz, A. M., L. Maréchal, B. Lesage, and R. Molins, "Thermal Expansion Coefficient of Alumina Films Developed by Oxidation of a FeCrAl Alloy Determined by a Deflection Technique*", Applied Surface Science, Volume 252, Issue 22, 15 September 2006*, pp.7781-7787, 2006.

26. Surappa, M. K., " Aluminium Matrix Composites: Challenges and Opportunities", *Sadhana, Vol. 28, Parts 1 & 2, February/April 2003*, pp.319–334, 2003.

27. Vijaya Ramnath, B., C. Elanchezhian, RM. Annamalai, S. Aravind, T. Sri Ananda Atreya, V. Vignesh, and C. Subramanian , "Aluminium Metal Matrix Composites - A Review", *Rev.Adv.Mater.Sci. (RAMS) No 1, Vol. 38, 2014*, pp.55-60, 2014.

28. Alman, D. E., *Properties of Metal Matrix Composites*, ASM Handbook, Vol.21, Ed. Miracle, D.B. and Donaldson, L., ASM International, pp.838-858, 2001.

29. Oluwatosin Bodunrin, M., K. K. Alaneme, and L. H. Chown, "Aluminium Matrix Hybrid Composites: A Review of Reinforcement Philosophies; Mechanical, Corrosion and Tribological Characteristics", *Journal of Materials Research and Technology, Volume 4, Issue 4, October–December 2015*, pp.434-445, 2015.

30. Kashyap, K. T., C. Ramachandra, C. Dutta, and B. Chatterji, "Role of Work Hardening Characteristics of Matrix Alloys in the Strengthening of Metal Matrix Composites", *Bull. Mater. Sci., Vol. 23, No. 1, February 2000*, pp.47–49, 2000.

31. Yang, W., R. Dong, Z. Yu, P. Wu, M. Hussain, and G. Wu, "Strengthening Behavior in High Content SiC Nanowires Reinforced Al Composite", *Materials Science and Engineering: A, Volume 648, 11 November 2015*, pp.41-46, 2015.

32. Emamy, S., E. Vaziri Yeganeh, A. Razaghian, and K. Tavighi, "Microstructures and Tensile Properties of Hot-extruded Al Matrix Composites Containing Different Amounts of Mg_2Si", *Materials Science and Engineering: A, Volume 586, 1 December 2013*, pp.190-196, 2013.

33. Jayashree, P. K., G. Shankar M.C , A. Kinia , S. Sharma, and R. Shetty, "Review on Effect of Silicon Carbide (SiC) on Stir Cast Aluminium Metal Matrix Composites", *International Journal of Current Engineering and Technology, Vol.3, No.3*, 2013.

34. Harichandran, R., and N. Selvakumar, "Effect of Nano/micro B_4C Particles on the Mechanical Properties of Aluminium Metal Matrix Composites Fabricated by Ultrasonic Cavitation-assisted Solidification Process", *Archives of Civil and Mechanical Engineering*, 2016.

35. Kennedy, A. R., and S. M. Wyatt, "The Effect of Processing on the Mechanical Properties and Interfacial Strength of Aluminium/TiC MMCs", *Composites Science and Technology, Volume 60, Issue 2, 1 February 2000*, pp.307-314, 2000.

36. Kurtoglu, A., *Aluminium Oxide and Titanium Diboride Reinforced Metal Matrix Composite and Its Mechanical Properties*, Master's Thesis, Middle East Technical University, 2004.

37. Miller, W. S., and F. J. Humphreys, "Strengthening Mechanisms in Particulate Metal Matrix Composites", *Acripta Metallurgica et Materialia, Vol. 25*, pp.33-38, 1991.

38. Ozben, T., E. Kilickap, and O. Cakır, "Investigation of Mechanical and Machinability Properties of SiC Particle Reinforced Al-MMC", *journal of materials processing technology 1 9 8*, pp.220–225, 2008.

39. Prabagaran, S., G. Chandramohan, and S. R. Devadasan, "Analysis on Machinability of Aluminium Metal Matrix Composites Reinforced With B_4C and Graphite Particles Under Specified Machining Conditions – A Critical Study on the Effect Of Surface

Roughness and Swarf Formation", *IJSR, Volume : 3,Issue : 4, April 2014*, pp.2277-8179, 2014.

40. Pandi, G., and S. Muthusamy, "A Review on Machining and Tribological Behaviors of Aluminium Hybrid Composites", *Procedia Engineering, Volume 38, 2012*, pp.1399-1408, 2012.

41. Najem, S. H., "Machinability of Al-2024 Reinforced with Al_2O_3 and/or B_4C", www.uobabylon.edu.iq/uobColeges/fileshare/articles/Machinability%20of%20Al-2024%20reinforced%20with%20Al2O3 % 20andor%20B_4C.pdf, Accessed at September 2015.

42. Song, W. Q., P. Krauklis , A. P. Mauritz, and S. Bandyopadhyay, "The Effect of Thermal Ageing on the Abrasive Behavior of Age-hardening Al/SiC and 6061 Al/SiC composites", *Wear 185(1995)*, pp.125-130, 1995.

43. Froes, F. H., "Advanced metals for Aerospace and Automotive Use", *Materials Science and Engineering, A 184 (1994)*, pp.119-133, 1994.

44. Macke, A., B. F. Schultz, and P. Rohatgi, "Metal Matrix Composites Offer the Automotive Industry an Opportunity to Reduce Vehicle Weight, Improve Performance", *Advanced Materials and Processes (2012)*, pp.12-23, 2012.

45. Devaraju, A., A. Kumar, and B. Kotiveerachari, "Influence of addition of Grp/Al_2O_3p with SiCp on Wear Properties of Aluminium Alloy 6061-T6 Hybrid Composites via Friction Stir Processing", *Transactions of Nonferrous Metals Society of China, Volume 23, Issue 5, May 2013*, pp.1275-1280, 2013.

46. Ravindran, P., K. Manisekar, S. Vinoth Kumar, and P. Rathika, "Investigation of Microstructure and Mechanical Properties of Aluminium Hybrid Nano-composites with the Additions of Solid Lubricant", *Materials & Design, Volume 51, October 2013*, pp.448-456, 2013.

47. Tjong, S. C., K. C. Lau, and S. Q. Wu, "Wear of Al-based Hybrid Composites Containing BN and SiC Particulates, *Metall Mater Trans A, 30 (9) (1999),* pp.2551–2555, 1999.

48. Garg, H. K., K. Verma, A. Manna, and R. Kumar, "Hybrid Metal Matrix Composites and Further Improvement in Their Machinability – A Review", *Int J Latest Res Sci Technol, 1 (1) (2012),* pp.36–44, 2012.

49. Srivatsan, T. S., I. A. Ibrahim, F. A. Mohamed, and E. J. Lavernia, "Processing Techniques for Particulate-reinforced Metal Aluminium Matrix Composites", *Journal of Materials Science November 1991, Volume 26, Issue 22*, pp.5965-5978, 1991.

50. Kevorkijan, M., Stabilisation and Rejection of Ceramic Particles from Molten Aluminium Alloy: Modelling and Experimental Testing", *Composites Science and Technology, Volume 59, Issue 16, 1 December 1999,* pp.2363-2374, 1999.

51. Yilmaz, H. S., *Characterization of Silicon Carbide Particulate Reinforces Squeeze Cast Aluminium 7075 Matrix Composite,* Master's Thesis, Middle East Technical University, 2004.

52. Calin, R., M. Pul, and Z. P. Pehlivanli, "The Effect of Reinforcement Volume Ratio on Porosity and Thermal Conductivity in Al-MgO Composites", *Mat. Res. vol.15 no.6 São Carlos Nov./Dec. 2012 Epub Oct 09*, 2012.

53. Yilmaz, M., *Production and Mechanical Behavior of Particulate Reinforced Aluminium Matrix Composites*, Ph.D Thesis, Boğaziçi university, 1997.

54. Nguyentat, T, "Diffusion Bonding - An Advanced Material Process for Aerospace Technology", http://www.vacets.org/vtic97/ttnguyen.htm, San Jose, USA, Accessed at September 2015.

55. Ghomashchi, M. R., and A. Vikhrov, "Squeeze Casting: An Overview", *Journal of Materials Processing Technology 101 (2000),* pp.1-9, 1998.

56. Iyer, A., " Squeeze Casting: The Future", http://issinstitute.org.au/wp-content/media/2011/05/ISS-FEL-REPORT-A-IYER-low-res.pdf , International Specialised skills Institute, 2011, Accessed at September 2015.

57. Natesh, G., Aluminium Die Casting: Lubrication Technology and Trends", http://www.chemtrend.com/, Accessed at September 2015.

58. Morgül, E., *Effects of Thermal Conditions on the Mechanical Properties of Squeeze Cast ZA-27 Alloy*, Master's Thesis, Boğaziçi University, 2007.

59. Lin, B., W. Zhang, Z. H. Lou, D. T. Zhang, and Y. Y. Li, "Comparative Study on Microstructures and Mechanical Properties of the Heat-treated Al–5.0Cu–0.6Mn–xFe Alloys Prepared by Gravity Die Casting and Squeeze Casting", *Materials & Design, Volume 59, July 2014,* pp.10-18, 2014.

61. Li, G. R., Y. T. Zhao, H. M. Wang, G. Chen, Q. X. Dai, and X. N. Cheng, "Fabrication and Properties of In Situ (Al_3Zr + Al_2O_3)p/A356 Composites Cast by Permanent Mould and Squeeze Casting, *Journal of Alloys and Compounds, Volume 471, Issues 1–2, 5 March 2009*, pp. 530-535, 2009.

62. Geng, L., S. Ochiai, H. X. Peng, L. Gao, J. Sun, and Z. Q. Sun, "Fabrication of Nanocrystalline ZrO_2 Particle Reinforced Aluminium Alloy Composite by Squeeze Casting Route", *Scripta Materialia, Volume 38, Issue 4, 13 January 1998*, pp.551-557, 1998.

63. Leng, J., G. Wu, Q. Zhou, Z. Dou, and X. Huang, Mechanical Properties of SiC/Gr/Al Composites Fabricated by Squeeze Casting Technology", *Scripta Materialia, Volume 59, Issue 6, September 2008,* pp.619-622, 2008.

64. Hwu, B. K., S. J. Lin, and M. T. Jahn, "Effects of Process Parameters on the Properties of Squeeze-cast SiCp-6061Al Metal Matrix Composite, *Materials Sciencea nd Engineering A 207 (1996)*, pp.135-141, 1996.

65. Mazahery, A., and M. Ostad Shabani, "Mechanical Properties of Squeeze-Cast A356 Composites Reinforced With B_4C Particulates", *Journal of Materials Engineering and Performance, (2012) 21*, pp.247–252, 2012.

66. Chen, W., Y. Liu, C. Yang, D. Zhu, and Y. Li, "(SiCp+Ti)/7075Al Hybrid Composites with High Strength and Large Plasticity Fabricated by Squeeze Casting", *Materials Science and Engineering: A, Volume 609, 15 July 2014*, pp.250-254, 2014.

67. Bhagat, R. B., "High Pressure Squeeze Casting of Stainless Steel Wire Reinforced Aluminium Matrix Composites", *Butterworth & Co (Publishers) Ltd Composites. Vol. 19. Number 5.* 1988.

68. Dhanashekar, M., and V. S. Senthil Kumar, "Squeeze Casting of Aluminium Metal Matrix Composites-An Overview", *Procedia Engineering, Volume 97, 2014*, pp.412-420, 2014.

69. Vijayaram, T. R., S. Sulaiman, A. M. S. Hamouda, and M. H. M. Ahmad, Fabrication of Fiber Reinforced Metal Matrix Composites by Squeeze Casting Technology", *Journal of Materials Processing Technology, Volume 178, Issues 1–3, 14 September 2006*, pp.34-38, 2006.

70. Skolianos, S. M., G. Kiourtsidis, and T. Xatzifotiou, "Effects of Applied Pressure on the Microstructure and Mechanical Properties of Squeeze-Cast AA6061 Alloy", *Journal of Materials Science and Engineering A231 (1997)*, pp.17-24, 1997.

71. Crouch, I. G., "Aluminium Squeeze Casting Technology", *a European Researches Viewpoint, Australian Conference on Materials for Industrial Development, Christchurch, New Zealand*, pp.24-26, 1987.

72. Sivaprakash, A., and S. Sathish, "Investigation of Microstructure and Mechanical Properties of Squeeze Cast LM6 Alloy with Varying Contents of $Al_2O_3$and Si_3N_4 - A Review", *Available online 01 February 2014, Special Issue-2*, 2014.

73. Baskaya, O., *The Mechanical Properties and Machinability of ZA-27 Casting Alloys*, Master's Thesis, Boğaziçi University, 2004.

74. Han, Z., X. Huang, A. A. Luo, A. K. Sachdev, and B. Liu, "A Quantitative Model for Describing Crystal Nucleation in Pressurized Solidification During Squeeze Casting", *Scripta Materialia, Volume 66, Issue 5, March 2012*, pp.215-218, 2012.

75. Masoumi, M., and H. Hu, "Influence of Applied Pressure on Microstructure and Tensile Properties of Squeeze Cast Magnesium Mg–Al–Ca Alloy", *Materials Science and Engineering: A, Volume 528, Issues 10–11, 25 April 2011*, pp.3589-3593, 2011.

76. Zhang, Y., G. Wu, W. Liu, L. Zhang, S. Pang, Y. Wang, and W. Ding, "Effects of Processing Parameters and Ca Content on Microstructure and Mechanical Properties of Squeeze Casting AZ91–Ca Alloys", *Materials Science and Engineering: A, Volume 595, 10 February 2014*, pp.109-117, 2014.

77. Maleki, A., B. Niroumand, and A. Shafyei, "Effects of Squeeze Casting Parameters on Density, Macrostructure and Hardness of LM13 Alloy", *Materials Science and Engineering: A, Volume 428, Issues 1–2, 25 July 2006*, pp.135-140, 2006.

78. Vijian, P., V. P. Arunachalam, "Experimental Study of Squeeze Casting of Gunmetal", *Journal of Materials Processing Technology, Volume 170, Issues 1–2, 14 December 2005*, pp.32-36, 2005.

79. Maleki, A., A. Shafyei, and B. Niroumand, "Effects of Squeeze Casting Parameters on the Microstructure of LM13 Alloy", *Journal of Materials Processing Technology 209*, pp.3790- 3797, 2009.

80. Önal, G., and F. Burat, "Boron Mining and Processing in Turkey", http://meeri.eu/Wydawnictwa/GSM2443/onal-burat.pdf , 2008, Accessed at September 2015.

81. Domnich, V., S. Reynaud, R. A. Haber, and M. Chowalla, "Boron Carbide: Structure, Properties, and Stability under Stress", *J. Am. Ceram. Soc., 94*, PP.3605–3628, 2011.

82. Thévenot, F., "Boron Carbide—A Comprehensive Review", *Journal of the European Ceramic Society, Volume 6, Issue 4, 1990*, pp.205-225, 1990.

83. Murray, P., *Low Temperature Synthesis of Boron Carbide Using a Polymer Precursor Powder Route*, Master's Thesis, University of Birmingham, 2011.

84. Halverson, D. C., A. J. Pyzik, and I. A. Aksay, "Boron Carbide Aluminium and Boron Carbide-reactive Metal Cermets", *US Patent no. 4605440*, 1985.

85. Chang, I. H., and C. L. Falticeanu, "Production of Boron Carbide Powder", *US patent no. US20150299421*, May 2014.

86. Trice, R. W., and J. W. Halloran, "Investigation of the Physical and Mechanical Properties of Hot-Pressed Boron Nitride/Oxide Ceramic Composites", *J. Am. Ceram. Soc., 82 [9]*, pp.2563–65, 1999.

87. Lontto, " Boron Carbide – B_4C", http://www.refractory-material.com/product/boron-carbide-B_4C/, Accessed at September 2015.

88. Ravi, B., B. Balu Naik, and J. Udaya Prakash, "Characterization of Aluminium Matrix Composites (AA6061/B_4C) Fabricated by Stir Casting Technique", *Materials Today: Proceedings, Volume 2, Issues 4–5, 2015*, pp.2984-2990, 2015.

89. Ibrahim, M. F., H. R. Ammar, A. M. Samuel, M. S. Soliman, and F. H. Samuel, "On the Impact Toughness of Al-15 vol. % B_4C Metal Matrix Composites", *Composites Part B: Engineering, Volume 79, 15 September 2015*, pp.83-94, 2015.

90. Lashgari, H.R, M. Emamy, A. Razaghian, and A. A. Najimi, The Effect of Strontium on the Microstructure, Porosity and Tensile Properties of A356–10 % B_4C Cast

Composite", *Materials Science and Engineering: A, Volume 517, Issues 1–2, 20 August 2009*, pp.170-179, 2009.

91. Baradeswaran, A., and A. Elaya Perumal, "Influence of B_4C on the Tribological and Mechanical Properties of Al 7075–B_4C Composites", *Composites Part B: Engineering, Volume 54, November 2013*, pp.146-152, 2013.

92. Nafisi, S., and R. Ghomashchi, "Boron-based Refiners: Advantages in Semi Solid Metal Casting of Al–Si Alloys", *Materials Science and Engineering: A, Volumes 452–453, 15 April 2007*, pp.437-444, 2007.

93. Toptan, F., A. Kilicarslan, A. Karaaslan, M. Cigdem, and I. Kerti, "Processing and Microstructural Characterization of AA 1070 and AA 6063 Matrix B_4C_p Reinforced Composites", *Materials & Design, Volume 31, Supplement 1, June 2010*, pp.S87-S91, 2010.

94. Lipp, A., K. A. Schwetz, and K. Hunold, "Hexagonal Boron Nitride: and Applications", *Journal of the European Ceramic Society 5 (1989)*, pp.3-9, 1989.

95. Wikipedia, "Boron Nitride", https://en.wikipedia.org/wiki/Boron_nitride ,, 2015.

96. Alavudeen, A., N. Venkateshwaran, and J. T. Winowlin Jappes, *Engineering Materials and Metallurgy*, Laxmi publications, New Delhi, 2006.

97. Ertuğ, B., "Powder Preparation, Properties and Industrial Applications of Hexagonal Boron Nitride, Sintering Applications", ISBN: 978-953-51-0974-7, InTech, DOI: 10.5772/53325. Available from: http://www.intechopen.com/books/sintering-applications/powder-preparation-properties-and-industrial-applications-of-hexagonal-boron-nitride , Accessed at September 2015.

98. Azom, "Properties and Information on Boron Nitride", http://www.azom.com/properties.aspx?ArticleID=78, Accessed at September 2015.

99. Technical Products, Inc., "Boron Nitride Material Specifications" , http://www.technicalproductsinc.com/bn_specs.html, Accessed at September 2015.

100. Eichler, J., and Ch. Lesniak, "Boron nitride (BN) and BN Composites for High-Temperature Applications", *Journal of the European Ceramic Society 28 (2008),* pp.1105–1109, 2008.

101. Zhang, J., R. Tu, and T. Goto, "Cubic Boron Nitride-containing Ceramic Matrix Composites for Cutting Tools", *In Advances in Ceramic Matrix Composites, edited by I.M. Low, Woodhead Publishing, 2014,* pp.570-586, 2014.

102. Jin, H. Y., H. Xu, G. J. Qiao, J. Q. Gao, and Z. H. Jin, "Study of Machinable Silicon Carbide–boron Nitride Ceramic Composites", *Materials Science and Engineering: A, Volumes 483–484, 15 June 2008,* pp.214-217, 2008.

103. Li, Y., G. Qiao, and Z. Jin, "Machinable Al2O3/BN Composite Ceramics with Strong Mechanical Properties", *Materials Research Bulletin, Volume 37, Issue 8, July 2002,* pp.1401-1409, 2002.

104. Behera, R., A. Datta, D. Chatterjee, and G. Sutradhar, "Role of SiCp on the Solidification Rate and Forgeability of Stir Cast LM6/SiCp MMCs", *International Journal of Scientific & Engineering Research, Volume 2, Issue 1,* 2011.

105. Buntan, R., D. Phuenchomphu, P. Sukmoung, K. Doomao, O. Anunapiwat, and T. Patcharawit , "Mechanical Properties of Stir-Mixed SiCp-Reinforced Aluminium Composites", *Journal of Metals, Materials and Minerals, Vol.21 No.*2, pp.73-83, 2011.

106. Stefanescu, D. M., *Science and Engineering of Casting Solidification*, Springer , 2009.

107. Kalaiselvan, K., I. Dinaharan, and N. Murugan, "Characterization of Friction Stir Welded Boron Carbide Particulate Reinforced AA6061 Aluminium Alloy Stir Cast Composite", *Materials & Design, Volume 55, March 2014,* pp.176-182, 2014.

108. Shorowordi, K. M., and T. Laoui, A. S. M. A. Haseeb, J. P. Celis, and L. Froyen, "Microstructure and Interface Characteristics of B_4C, SiC and Al_2O_3 Reinforced Al Matrix Composites: A Comparative Study", *Journal of Materials Processing Technology, Volume 142, Issue 3, 10 December 2003*, pp.738-743, 2003.

109. Hashim, J., L. Looney, and M. S. J. Hshmi, "Metal Matrix Composites: Prouction by the Stir Casting Method", *Journal of Materials Processing Technology 92-93*, pp.1-7, 1999.

110. Naidich, J. V., "The Wettability of Solids by Liquid Metals", *Elsevier, 1981, Volume 14*, pp.353-484, 1981.

111. Fuji, H., H. Nakae, and K. Okada, "Interfacial Reaction Wetting in the Boron Nitride/Molten Aluminium System", *Acta memll, maler. Vol. 41, No. 10*, pp.2963-2971, 1993.

112. Chena, C., L. Guob, J. Luoa, J. Haoa, Z. Guoa, and A. A. Volinsky, "Aluminium Powder Size and Microstructure Effects on Properties of Boron Nitride Reinforced Aluminium Matrix Composites Fabricated by Semi-solid Powder Metallurgy", *Materials Science & Engineering A 646 (2015)*, pp.306-314, 2015.

113. ASTM, "E8-04 Standard Test Methods for Tension Testing of Metallic Materials", *ASTM E8 Standard, www.astm.org*, 2013.

114. Sigworth, G., and M. Guzowski, "Grain Refiner for Aluminium Containing Silicon", *US patent No US5055256 A*, Oct 1991.

115. McCoy, L. R., "Method of Enhancing the Wettability of Boron Nitride for Use as An Electrochemical Cell Separator", *US patent no 4360578 A*, Nov 1982.

116. Mazaheri, Y., M. Meratian, R. Emadi, and A. R. Najarian, "Comparison of Microstructural and Mechanical Properties of Al–TiC, Al–B_4C and Al–TiC–B_4C

Composites Prepared by Casting Techniques", *Materials Science and Engineering: A, Volume 560, 10 January 2013*, pp.278-287, 2013.